LATE QUATERNARY CLIMATE VARIABILITY IN THE INDIAN MONSOON DOMAIN

Praveen Kumar Mishra

Fachbereich Geowissenschaften, Freie Universität, Berlin

December 2014

Late Quaternary climate variability in the Indian monsoon domain

(*Spät-quartäre klimavariabilität im Gebiet des Indischen monsun*)

Dissertation
zur Erlangung des akademischen Grades
Doktor der Naturwissenschaften (Dr. rer. nat.)

am Fachbereich Geowissenschaften
der Freien Universität Berlin

vorgelegt von

Praveen Kumar Mishra

Berlin, 2014

Als Dissertation angenommen vom Fachbereich Geowissenschaften der Freien Universität Berlin.

auf Grund der Gutachten
Erstgutachter: Dr. (Habil) Sushma Prasad
Zweitgutachter: Prof. Dr. Ulrich Cubasch

Datum der Verteidigung: den 07 Mai 2015, Berlin

Statement of Authorship

The thesis entitled “Late Quaternary climate variability in the Indian monsoon domain” has been submitted for the degree of Doctor in Natural Sciences. I hereby declare that:

- I have fully acknowledged and referenced the ideas and work of others, whether published or unpublished, in my thesis.
- This dissertation has not been submitted for the award of any other degree or diploma in any other institution.

Praveen Kumar Mishra

Berlin, 2014

Acknowledgements

I would like to express my deepest gratitude to my advisor, **PD Dr. Sushma Prasad**, for her excellent guidance, motivation, encouragement during my research. Additionally, I would like to acknowledge **Prof. Achim Brauer**, for permitting access to laboratory facilities and providing a positive working atmosphere during my stay in the section. I would also like to thank **Dr. Peter Dulski**, **Dr. Birgit Plessen**, **Dr. Georg Schettler** and **Mr. Rudolf Naumann** for training and permitting me to use their laboratories for sample analysis. Without their help and guidance, it would not have been possible to generate and interpret such a large data set.

My grateful thanks are due to other members of the research team, **Dr. Birgit Gaye**, **Dr. A. Anoop**, **Dr. Philip Menzel, Dr. Elisabeth Dietze, Dr. Stefan Polanski, Dr. Martin Wiesner**. My investigations would not been possible without the scientific knowledge and active participation of the Indian partners, especially **Prof. A.R. Yousuf, Dr. Arshid Jehangir** (Kashmir University**),** and **Prof. N. Basavaiah and Dr. K. Deendayalan** (Indian Institute of Geomagnetism, Mumbai**).** Thanks again to **Dr. A. Anoop** and **Dr. Philip Menzel** for their helpful and critical comments on this thesis.

In addition, I would like to extend special thanks to **Ms. Sylvia Pinkerneil** and **Ms. Christine Gerschke** for helping me in navigating though the complicated administrative matters. I owe additional thanks to **Dr. Birgit Plessen** and **Ms Pinkerneil** for their help in laboratory and the fieldwork. I would also like to acknowledge **Mr. Dieter Berger, Ms. Gabi Arnold** and **Mr. Brian Brademann** for their help during the laboratory work, and **Ms. Ursula Kegel** for assisting me during the grain size analysis. My sincere thanks to **Mr. Andreas Hendrich** for helping me with the beautification of figures and graphs for the manuscripts. I express my warm thanks to **Mr. Marcus Günzel** and **Mr. Matthias Köppl** for their help with computer related technical matters. I would also like to thank **Arun**, **Bernhard** and the **students of Potsdam University**, who provided their valuable help during sample processing.

My study would not have been possible without **Mr. Richard Niederreiter, Mr. Michael Köhler, and Mr. Daniel Niederreiter** who were responsible for raising the cores from the Tso Moriri Lake in difficult weather conditions.

I thank to all my friends from our **'Potsdam Gang'** for the unforgettable fun time in Potsdam's Balzac coffee house' and enjoyable discussions on various aspect of science, politics and culture. I warmly thank **Tarique** and **Chiranjit** for helping me with the editing of the thesis. Additionally, special thanks go to **Dharmu**, **JD bhai, Nishant**, **Rajak bhai**, **Sandeep**, **Somu, Varun**, and **Vinay** for their wonderful and unforgettable friendship, and their encouragement for doing research.

Finally, I express my sincere thanks to my father **Mr. R.K. Mishra**, my mother **Mrs. Shila Mishra**, and all my **family members**, for their constant encouragement and support in untold ways.

This Ph.D. study has been carried out as part of the research unit "**Himalaya: Modern and Past Climates (HIMPAC)**" (FOR 1380) which is funded by the "**DeutscheForschungsGemeinschaft**".

Praveen Kumar Mishra

Table of Contents

List of Figures

List of Tables

Abstract

The Indian subcontinent is characterised by a variety of climate zones ranging from the alpine climate in Himalaya, tropical climates in central India, to arid regions in the NW India. A variety of precipitation regimes (the SW and NE monsoon, and the winter westerlies) and glacial meltwater contribute to the regional hydrological balance – long term data on their variability is essential for infrastructural planning and securing food supplies in a global warming scenario.

The present work on the lake sediments from the NW Himalaya (Tso Moriri Lake) and the central India (Lonar Lake) involved reconstructing late Quaternary palaeoclimate in these two diverse climate regions. The Tso Moriri Lake is located in the climatically sensitive zone of NW Himalayas and is affected by both mid-latitude westerlies and Indian summer monsoon (ISM), whereas Lonar Lake situated in the core monsoon zone of India and receives moisture only from the Indian summer monsoon (ISM). The present work involved (i) testing of climate-sensitive proxies that are useful for climate reconstruction in high altitude regions; (ii) based on the identified proxies, reconstruction of late Quaternary palaeoclimate, and; (iii) regional comparison to identify spatio-temporal changes in precipitation regimes and, meltwater contributions (for the high altitude Tso Moriri Lake).

The present work indicates that the early Holocene intensification was visible in both NW Himalaya and central India, though the wettest phase ended earlier in the former (ca. 8.5 cal ka) as compared to the latter (ca. 6 cal ka). The central Indian record showed evidence of multiple abrupt events throughout the Holocene, as well as two periods of extended drought during the late Holocene. These “extremes” do not appear to be recorded in the high altitude Tso Moriri Lake. While chronological uncertainties could clarify some of the differences, one possible explanation for the apparent insensitivity of the NW Himalayan region to the “extremes” seen in peninsular India is probably due to the buffering effect of snowmelt, westerlies, and weaker ISM during the late Holocene.

Kurzfassung

Der Indische Subkontinent ist charakterisiert durch eine Vielzahl an Klimazonen, welche von alpinem Klima im Himalaya über tropisches Klima in Zentralindien bis zu ariden Regionen in NW-Indien reichen. Eine Vielzahl an Niederschlagsregimes (der SW- und NO-Monsun sowie die winterliche Westwinddrift) und glaziale Schmelzwasser tragen zum regionalen hydrologischen Gleichgewicht bei – eine langzeitliche Datengrundlage über dessen Variabilität ist notwendig für infrastrukturelle Planungen und die Sicherstellung der Nahrungsversorgung in einem Szenario globaler Erderwärmung.

Diese Arbeit über Seesedimente aus dem NW-Himalaya (Tso Moriri Lake) und dem zentralen Indien (Lonar Lake) beschäftigt sich mit der Rekonstruktion des spätquartären Paläoklimas in diesen beiden sehr verschiedenen Klimaregionen. Der Tso Moriri Lake befindet sich in der klimatisch sensitiven Zone des NW-Himalayas und wird sowohl von den Westwinden der mittleren Breiten als auch dem Indischen Sommermonsun (ISM) beeinflusst, während sich der Lonar Lake im Kernbereich der monsunal beeinflussten Zone Indiens befindet und demnach Feuchtigkeit nur vom Indischen Sommermonsun erhält. Diese Arbeit umfasst (i) die Untersuchung geeigneter klima-sensitiver Proxies für die Klimarekonstruktion in höher gelegenen Regionen, (ii) basierend auf den identifizierten Proxies die Rekonstruktion des spätquartären Paläoklimas und (iii) einen regionalen Vergleich zur Identifikation räumlich-zeitlicher Veränderungen in Niederschlagsregimes und Schmelzwasserspenden (für den Tso Moriri Lake in höherer Gebirgslage).

Die Ergebnisse in dieser Arbeit zeigen, dass die frühholozäne Intensivierung sowohl im NW-Himalaya als auch in Zentral-Indien sichtbar war, jedoch endete die feuchteste Phase in ersterem früher (etwa 8,5 cal ka) als in letzterem (etwa 6 cal ka). Die Daten über Zentral-Indien zeigen mehrere plötzliche Ereignisse während des Holozäns sowie zwei Perioden mit zeitlich ausgedehnten Trockenphasen während des späten Holozäns. Diese „Extreme“ zeigen sich nicht in den Daten des höher gelegenen Tso Moriri Lakes. Während chronologische Unsicherheiten einige der Abweichungen erklären könnten, ist eine weitere mögliche Erklärung für die offensichtliche Unsensitivität der NW-Himalaya Region gegenüber dieser “Extreme” auf dem halbinselförmigen Indischen Subkontinent ein Puffereffekt durch die Schneeschmelze, westwinddrift sowie ein schwächerer ISM während des späten Holozäns.

Chapter 1: Introduction

1.1. Introduction

A large part of the Indian subcontinent is under the influence of the Indian summer monsoon. Monsoon, derived from the Arabic word "*mausim*" (meaning season), is defined as the seasonal reversal of the wind systems caused by the annual variation of incoming solar radiation (Agnihotri et al., 2002; Gadgil, 2003). Monsoon may also be associated with dry (NE monsoon) or wet (SW monsoon or commonly known as ISM) weather. The NE monsoon brings limited rains to the southern parts of India and Sri Lanka (Fig. 1.1a and 1.1c). However, the ISM bringing in a significant amount of rainfall (Fig. 1.1a-b) is the driving force behind the agricultural productivity and hence the total economy of the country (agriculture contributed 14% of total GDP of India during 2013 to 2014, source: Ministry of Agriculture, India). ISM variability, therefore has a significant impact not only on the economy, but also on the largely rural fabric of the Indian subcontinent, home to ca. 23% of the world's population (World bank report-2013). The socioeconomic importance of ISM variability is clearly demonstrated by either recent floods in Mumbai (2005), Uttarakhand (2013), Kashmir (2014) (Singh et al., 2014), or the drought in NE India, Bihar and Jharkhand in 2013 (Indian Meteorological Department report, 2013). Historically, several famines and the mass mortality in the last millennium were also linked to the droughts in the Indian subcontinent (Deotare, 2006). The analyses of modern meteorological data indicated that (i) the frequency of extreme ISM events has increased in recent decades (Goswami et al., 2006); and (ii) there is spatial heterogeneity in the occurrence of extreme events (Rajendran and Kitoh, 2008; Ghosh et al., 2011). However, such studies on extreme events are based on the instrumental records covering only a few decades. Longer high-resolution palaeoclimate records are essential for understanding the monsoon variability on longer time scales.

Recent studies (Ponton et al., 2012; Anoop et al., 2013b; Menzel et al., 2014; Prasad et al., 2014) have shed light on the Holocene ISM variability in the core monsoon zone (Gadgil, 2003) of the central India. These records demonstrate extreme climate events (centennial scale intervals of weaker ISM) during the late Holocene. The limited palaeoclimate data from the Himalayas, which is under the influence of both the winter westerlies and ISM precipitation, also indicates climate variability during the late

Quaternary (Hedrick et al., 2011; Anoop et al., 2013a; Leipe et al., 2014a). The NW Indian lakes from Rajasthan and surrounding regions indicate an interval of enhanced westerly precipitation between 7.2 and 6 cal ka (Prasad and Enzel, 2006). The stalagmite data for the last millennium (Sinha et al., 2005) indicates decadal scale droughts in northeastern India and the probable westerly influence during the late Holocene (Berkelhammer et al., 2012). However, though the relative influence of these moisture pathways has shown considerable variations in intensity and spatial extent in the past (e.g., Herzschuh, 2006; Chen et al., 2008; Demske et al., 2009), the contribution of such fluctuations, and the extent of ISM contribution to local hydrology in the Himalayan region is not yet well documented.

In the following sections, I present an overview of the factors governing ISM variability (Section 1.1.1 and 1.1.2), and summarises the available palaeoclimate literature from the Indian subcontinent (Section 1.2.1) to lay the groundwork for my investigations on lake sediments from the Indian subcontinent.

1.1.1. The modern climate system

The modern climate system in the Indian subcontinent is mainly controlled by two major wind regimes. First, the Indian summer monsoon (ISM) and secondly, the mid-latitude westerlies. Additionally, some amount (ca. 20%) of rainfall is contributed by the NE monsoon in the southern part of the Indian subcontinent (Prasad and Enzel, 2006).

Monsoon is the seasonal reversal of the wind system caused by annual variation of the solar insolation. In 1686, Edmund Halley first proposed the mechanism of monsoon circulation visualizing it as a giant land-sea breeze triggered by the differential heating of the Indian subcontinent and oceanic regions, which reverses its direction twice a year (Kelkar, 2009). However, Simpson (1921) has criticized the giant land-sea breeze concept, and pointed out that there was no relation between the monsoon precipitation and the land-sea thermal contrast, as ISM is strongest in July and not in the hottest month (i.e. May), or that the hottest regions of north-west India get limited monsoon rain (Gadgil, 2003).

A second hypothesis links the origin of monsoon with the seasonal migration of the intertropical convergence zone (ITCZ) over the latitude of maximum insolation (Charney, 1969; Gadgil, 2003). During summer (June to September) due to the

maximum insolation at 23.5°N (Tropic of Cancer), the ITCZ shifts towards the low pressure area, resulting in surface winds bringing significant amounts of precipitation from the Indian Ocean (Arabian Sea and Bay of Bengal) to the continental parts of India (Fig. 1.1a-b). The Arabian Sea branch first strikes the Western Ghats of India, where its orography governs the spatial variability in the monsoon precipitation, resulting in windward slope of the mountain range receiving heavy precipitation, whereas the leeward side remains almost dry. After first encounter with the Western Ghats, monsoonal winds from the Arabian Sea continue their journey towards the low-pressure area over the Indian peninsula. The Bay of Bengal branch brings moisture to the NE India and further moves towards the Indo-Gangetic plain following the low pressure area extending from the Bay of Bengal to the northwestern part of India (Gadgil, 2003) (Fig. 1.1a-b). During winter (October to February) the ITCZ shift towards the low pressure area in the south (10°N) as a result, north easterly winds (NE monsoon) bring cold and relatively dry air into the large parts of the Indian subcontinent (Gadgil, 2007). NE monsoon is also termed as the retreating monsoon season or the post-monsoon season in which the zone of maximum rainfall migrates to the southern part of India (Fig. 1.1a and 1.1c).

Limited amount of precipitation is brought to the northern and northwestern parts of India by the mid-latitude cyclones steered by the westerlies. Along with the tropical cyclones, westerly winds move towards east and bring moisture from the Mediterranean Sea and the Atlantic Ocean (Benn and Owen, 1998; Kotlia et al., 2014). Upon reaching Asia, the westerlies bifurcate into two branches due to mechanical barrier of the Himalaya and the Tibetan Plateau (Pang et al., 2014) (Fig. 1.1a). During summer, the westerly jet stream over north India slowly weakens and disintegrates, causing the main westerly flow to move north into Central Asia. However, during winter the southern branches of the subtropical westerly jet stream reforms over the northern parts of the South Asia, bringing winter precipitation (Lockwood, 1974; Pant and Rupa Kumar, 1997).

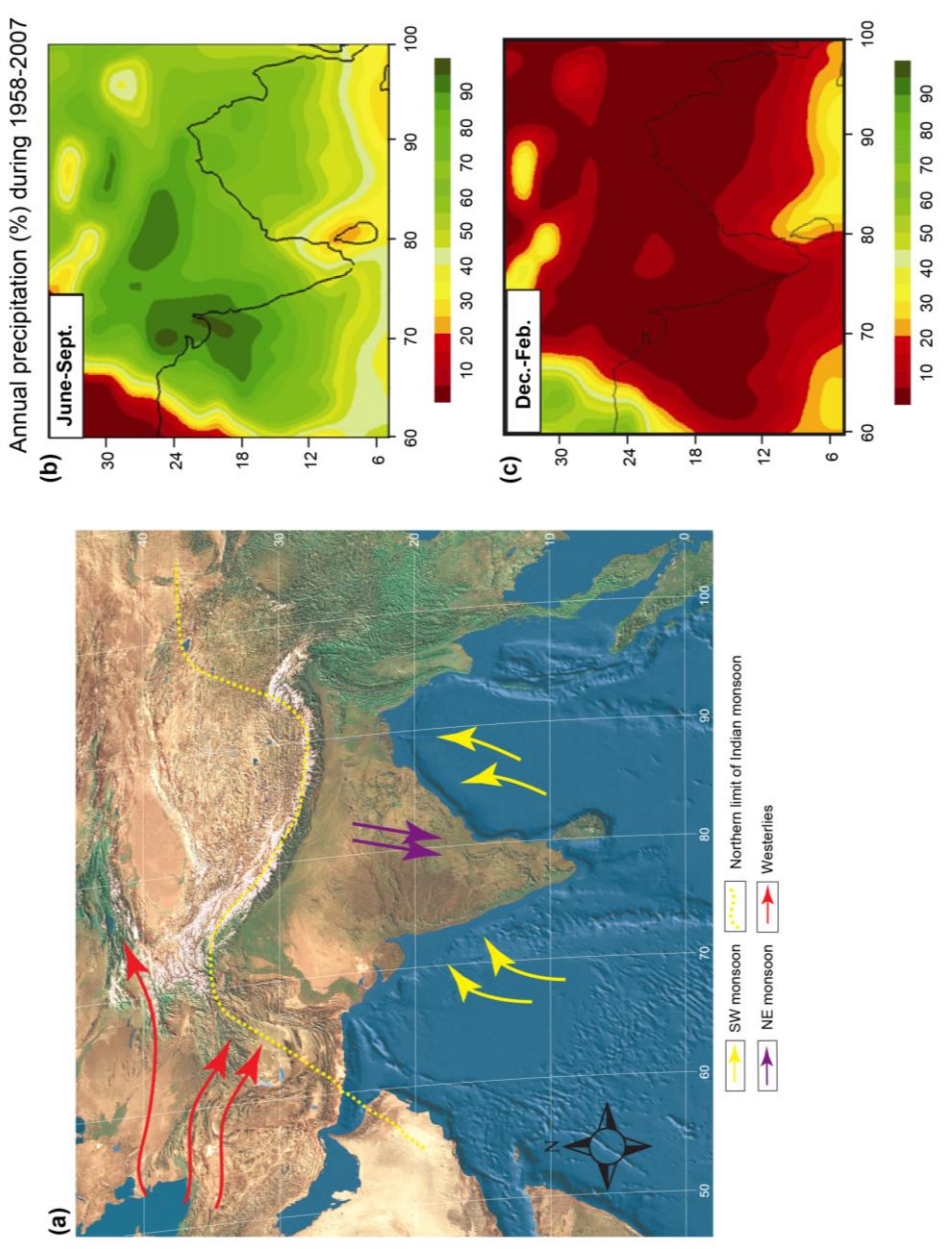

Fig. 1.1: (a) Large scale topographical map with dominant seasonal hemispherical airflows (modified after Prasad and Enzel, 2006; Rehfeld et al., 2012), (b-c) seasonal precipitation during 1958 to 2007.

1.1.2. Forcing factors and teleconnections

Multiarchive, multiproxy palaeoclimate reconstructions on different timescales (decadal to millennial) have indicated the role of various external (solar forcing) and internal (e.g. ocean-atmospheric teleconnections) factors influencing ISM variability on different time scales (e.g. Overpeck et al., 1996; Gupta et al., 2005; Menzel et al., 2014; Prasad et al., 2014). A brief description of these forcing factors is given below.

a) Forcing factors:

Climate forcing factors can be either external (e.g. solar variability) or internal (e.g. ocean circulation or land-sea thermal contrast) which operate at interannual (e.g. changes in atmospheric composition) to million year timescales (e.g. land-sea distribution).

There are two principal components of external forcing – one related to orbital forcing and second related to changes in solar irradiance. Milankovitch (1930) described different orbital forcings - these include Earth's movement around the Sun (eccentricity) and its own axis (obliquity and precession) (see also Beer et al., 2000). Both the obliquity and precession affect the hemispheric distribution of solar insolation over different time scales which in turn plays a key role in the global climatic change (e.g. Mayewski et al., 2004; Yuan et al., 2004). Another important feature of the external forcing is the solar irradiance produced by the Sun. Due to the advanced technology available now, direct measurement of solar activity is possible for recent times. However, for reconstruction of past solar activity, proxy indicators e.g. cosmogenic radionuclides (^{14}C and ^{10}Be) have been used (Wanner et al., 2008; Muscheler et al., 2014). The high-resolution palaeo-data from the ISM realm indicated that solar forcing is one of the critical factors controlling ISM precipitation on millennial time scales (Prell and Kutzbach, 1992; Neff et al., 2001; Agnihotri et al., 2002; Gupta et al., 2005, Hiremath et al., 2014).

Internal forcing factors for ISM variability include snow cover, changes in atmospheric composition, volcanic activity, and land-sea distribution. In connection with the external forcing, these factors are responsible for the climate variation at decadal to million year time scales. Snow cover has the ability to alter the surface albedo, thereby regulating the atmospheric temperature and its moisture content (Cohen and Entekhabi, 2001). Several models suggested that there is an inverse relationship between the

Eurasian snow cover and ISM (Dickson, 1984; Shukla 1987; Bamzai and Shukla, 1999). Increase in snow cover over Eurasia leads to a relatively colder temperature on land during summer because some fraction of solar energy is used for the melting snow and evaporating water rather than heating the surface leading to weaker ISM.

Changes in the atmospheric composition can be caused by both natural (volcanic gases, CO_2, methane) and anthropogenic (fossil fuels, industrial) processes. This is one of the significant factors that affects the global climate by varying (increasing or decreasing) the atmospheric temperature (Officer and Drake, 1983; Pickering and Owen, 1994). The small but constant rate of increasing CO_2 due to land-cover, and SST changes are responsible for a slight increase in global mean temperature since 8000 years (Wanner et al., 2008). However, since mid-20^{th} the increase in global temperature due to the greenhouse gases (GHGs) is dominantly caused by human influence (Stocker et al., 2013). Additionally, volcanic activity also has the ability to increase the mean global temperature due to addition of GHGs in the atmosphere (Pickering and Owen, 1994). In contrast, dominance of sulphur dioxide emission favours global cooling phenomenon (Officer and Drake, 1983).

Another important factor, which controls the Asian monsoon circulation on million year timescales is land-sea distribution. The uplift of the Tibetan Plateau due to collision of Indian-Asian plate, and the closing of Paratethys (<52 myr; Rowley, 1996), resulted in the initiation of monsoon circulation in the Asian subcontinent (Kutzbach et al., 1993; Ruddimann and Kutzbach, 1989). Additionally, the closing of oceanic gateways also affects the monsoon circulation (Wang et al., 2005). The weakening of the Asian monsoon due to decreased SSTs in the Indian Ocean is attributed to the shifting of the Australian plate, which resulted due to switching of the Indonesian throughflow from the warm south Pacific to cold north Pacific waters (Cane and Molnar, 2001; Wang et al., 2005).

b) Teleconnections:

The ISM is an active component of the global climate. It has the ability to interact with other modes of climate variability. Amongst them, the most important teleconnections linked to ISM variability are the El Niño Southern Oscillation (ENSO), Indian Ocean dipole (IOD), active/break cycles (tropical mid-latitude interactions), and the North

Atlantic Oscillation (NAO) (Krishnan et al., 2009; Menzel et al., 2014; Prasad et al., 2014).

The El-Niño/Southern Oscillation (ENSO) is a coupled system between easterly trade winds, westerly upper atmospheric winds, and equatorial thermocline system in the tropical Pacific Ocean (Sikka, 1980; Gadgil, 2003). The link between ENSO and ISM influences the interannual variability of summer monsoon rainfall over India. Earlier it was thought that in the Indian subcontinent the poor monsoon is associated with the El Niño years (Goswami, 2005; Gupta, 2010; Gadgil, 2014). However, this relationship has not been constant over a period of time – recent studies have shown monsoon precipitation can be normal even during intense El Niño events (e.g. in 1963 AD and 1997 AD), probably due to the influence of Indian Ocean Dipole (IOD) mode in Indian Ocean (Gadgil, 2014; Krishnaswamy et al., 2014). IOD is the anomalous state of the ocean-atmosphere system (Saji et al., 1999; Vinayachandran et al., 2007), in which there is an east-west temperature gradient in the Indian Ocean (Saji et al., 1999; Ashok et al., 2001; Krishnaswamy et al., 2014). A positive IOD is characterised by higher precipitation over the south Asia, whereas the negative IOD is linked to weaker monsoon (Krishnan et al., 2011).

The interaction between mid-latitude westerlies and the ISM winds leads to sub-seasonal or intraseasonal variations of the monsoon precipitation (Prasad and Enzel, 2006; Krishnan et al., 2009; Rajeevan et al., 2010). This variability is referred to as active/break cycle (Krishnamurti and Bhalme 1976; Sikka, 1980). In central India, during ‘active cycle’ the monsoonal rainfall increases whereas, during ‘break cycle’ weak rainfall is observed even in the peak monsoon period (Blanford, 1886). The phenomenon of ‘breaks’ has been more important because of its relationship with the interseasonal variability of monsoonal precipitation. During the break monsoon, the interaction between westerlies and the monsoon in northwestern and central India pushes the low pressure trough towards the foothills of the Himalaya, resulting in a decrease in rainfall all over India except the Himalaya region. During a normal monsoon season, frequent break cycles can affect crop production and lead to drought (Gadgil et al., 2003; Rajeevan et al., 2010).

Bond et al., (in 1997 and 2001) have documented a high correlation between solar output (production rates of the cosmogenic nuclides *i.e.* C^{14} and Be^{10}) and short-

term cold events (inferred from higher concentrations of ice-rafted debris in sediments) in the North Atlantic Ocean during the Holocene. The impact of these short-lived cooling events was globally felt (Gupta et al., 2003; Hong et al., 2003; Fleitmann et al., 2007; Feng and Hu, 2008; Marzin et al., 2013; Menzel et al., 2014). The North Atlantic cooling events may have influenced the ISM by indirectly influencing the Eurasian snow cover (Fleitmann et al., 2003). In the Indian subcontinent the millennial-scale monsoon variability is well correlated with North Atlantic warming/cooling events (Gupta et al., 2003; Hong et al., 2003; Fleitmann et al., 2007; Menzel et al., 2014). Additionally, the marine core from the Arabian Sea shows that the ISM variability during MWP (Medieval Warm Period) and LIA (Little Ice Age) was linked with the North Atlantic warm/cold events, respectively (Gupta et al., 2003).

1.2. State of the art

A large database of marine and terrestrial climate reconstructions on ISM variability is available from the South Asian region (Borgaonkar et al., 1996; Sinha et al., 2005; Gupta et al., 2005; Juyal et al., 2006; Demske et al., 2009; Mischke and Zhang, 2010; Rashid et al., 2011; Anoop et al., 2013a and 2013b; Döberschutz et al., 2013; Prasad et al., 2014; Sridhar et al., 2014). The high-resolution tree ring and speleothem data are valuable archives for the climate variability at centennial to decadal time scales. But the reconstruction of moisture availability on the basis of $\delta^{18}O$ (Sinha et al., 2005; Yadava and Ramesh, 2005; Tiwari et al., 2011) can be complicated by changes in storm tracks and moisture sources (Dayem et al., 2010).

On longer time scales, both marine and lake records can provide the information about past climate variability. The marine records from the Arabian Sea and Bay of Bengal indicate the climate variability on millennial to centennial time scales. Sediment cores from the Arabian Sea shows asynchronicity in their palaeo-records. The reconstructed ISM wind strength from the western Arabian Sea (based on the percentage of planktonic foraminifer *Globigerina bulloides*) is not always correlatable with continental monsoon precipitation (Prasad and Enzel, 2006).

High-resolution lake sediments have the potential to provide information about moisture availability and moisture sources on millennial to decadal time scales (Gasse et al., 1996; Demske et al., 2009; Mischke and Zhang, 2010; Anoop et al., 2013a;

Döberschutz et al., 2013; Leipe et al., 2014a; Prasad et al., 2014). Lake sediments contain a wide variety of physical, chemical and biological proxies that can be used for the palaeoclimate reconstruction. These proxies can provide the information about past environmental conditions that, in turn are related to the climate variability. However, each proxy has its own limitation and a different response time to the environmental forcing (Lotter, 2014). Therefore, the investigations of lake sediments using a multiproxy approach can provide several independent lines of evidence for environmental reconstruction. Various proxy investigations, such as mineralogy (detrital, authigenic evaporitic) and sedimentology can also provide the information on catchment geology, shoreline proximity, and energy of the transporting medium. Additionally, authigenic carbonates and pollen studies are also useful in reconstructing past hydrology identifying moisture sources and changing vegetation (Schoell, 1978; van Zeist and Woldring, 1978; Rashid et al., 2011) in the region.

1.2.1. Literature review: Palaeomonsoon studies

ISM variability in the south Asian continent during the Holocene epoch is evident from several marine (Overpeck et al., 1996; Gupta et al., 2003; Staubwasser et al., 2006; Rashid et al., 2011) and terrestrial records (Enzel et al., 1999; Phadtare, 2000; Kar et al., 2002; Sinha et al., 2005; Yadava and Ramesh, 2005; Herzschuh, 2006; Prasad and Enzel, 2006; Chen et al., 2008; An et al., 2011; Anoop et al., 2013b; Döberschütz et al., 2013; Leipe et al., 2014a; Prasad et al., 2014). These records show a complex interaction between the ISM and mid-latitude westerlies in northern India, which leads to hydrological changes on different time scales. However, due to the proxy limitation, and/or a complex process of moisture transport by the two branches of the ISM (Arabian Sea and the Bay of Bengal) and westerlies, differences in temporal resolution of the samples, and/or uncertainty in radiocarbon dates (Prasad and Enzel, 2006; Fleitmann et al., 2007; Wang et al., 2010; Mischke et al., 2013), the timing and extent of the monsoon precipitation during the Holocene from the Asian continent is not always synchronous with the nearby records (Fig. 1.2).

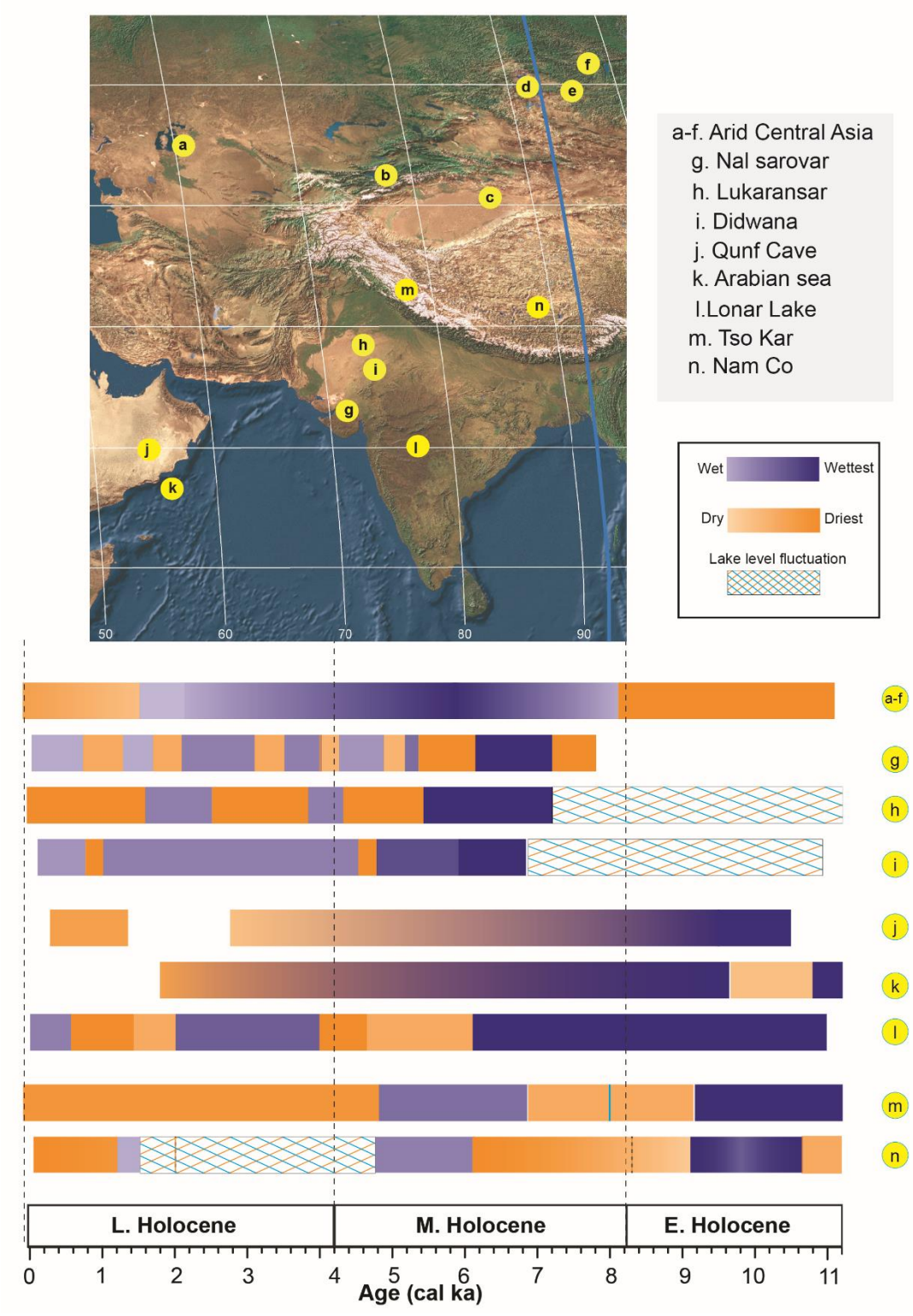

Fig. 1.2: Spatio-temporal patterns of effective-moisture change from ISM domain and central Asia during the Holocene: (a to f) Record from the central Asia (Chen et al., 2008); (g) Nal Sarovar (Prasad et al., 1997); (h) Lunkaransar (Enzel et al., 1999); (i) Didwana Lake (Wasson et al., 1984); (j) Qunf cave (Fleitmann et al., 2007); (k) Arabian Sea (Gupta et al., 2003); (l) Lonar Lake (Prasad et al., 2014); (m) Tso Kar Lake (Demske et al., 2009), and; (n) Nam Co Lake (Döberschutz et al., 2013)

The spatio-temporal variability of regional monsoon precipitation during the Holocene is discussed below. In the following section, I have used the subdivision of Holocene recommended by the working group of INTIMATE (Integration of ice-core, marine and terrestrial records) and ICS (International Commission on Stratigraphy) (Walker et al., 2012) – here the calendar ages are referred to as ka BP (1000 yr. before present). For the sake of consistency, I have used cal ka throughout for calendar ages.

(a) Early Holocene (11-8.2 cal ka)

The climate variability obtained from several palaeo-records on different time scales from the monsoon dominated regions indicate strengthened monsoon during the early Holocene (Van Campo and Gasse, 1993; Gupta et al., 2003; Hong et al., 2003; Fleitmann et al., 2007; Demske et al., 2009; Rashid et al., 2011; Anoop et al., 2013a; Döberschütz et al., 2013; Leipe et al., 2014a), whereas the proxy records from the westerlies domain (arid central Asia and NW India) shows relatively less moisture availability in the region (Fig. 1.2a-n) (Swain et al., 1983; Enzel et al., 1999; Herzschuh, 2006; Prasad and Enzel, 2006; Chen et al., 2008).

The multiproxy investigations on the lake sediments from the Lonar Lake in the core monsoon zone of India (Gadgil, 2003), provided the evidence of relatively wetter Holocene interval, during 11 to 6.2 cal ka (Prasad et al., 2014) then today (Fig. 1.2l). Similarly, in NW Himalaya and Tibetan Plateau, palaeoclimate reconstructions based on the geomorphological, geochemical and palynological studies indicated an early Holocene wet phase (Bookhagen et al., 2005; Herzschuh et al., 2006; Demske et al., 2009; Anoop et al., 2013a; Döberschutz et al., 2013; Leipe et al., 2014b). The records from the Arabian Sea (Gupta et al., 2005) and Oman stalagmites (Fleitmann et al., 2007) linked solar forcing with Holocene monsoon precipitation (Agnihotri et al., 2002; Gupta et al., 2003; Wang et al., 2010). However, most of the records from the south Asian region indicate early Holocene intensification (wet phase), the period of intensification is not always synchronous with the nearby records (Gasse et al., 1996; Herzschuh, 2006; Demske et al., 2009; Mischke and Zhang, 2010; Wang et al., 2010). This asynchronicity in the palaeo-records could be explaind by (i) dating uncertainties, (ii) climate sensitivity of the proxies, and (iii) interaction between different wind regimes (Gupta et al., 2003; Fleitmann et al., 2007; Demske et al., 2009; Mischke and Zhang, 2010; Wang et al., 2010; Döberschutz et al., 2013; Prasad et al., 2014) (Fig. 1.2j-n).

In contrast, the palaeo-record from the central Asia and NW India indicates relatively less moisture. Based on geochemistry, mineralogy, and sedimentology of the Didwana Lake sediments, Wasson et al., (1984) have suggested a moderately deep lake with fluctuating lake levels. This is in agreement with the investigations on the Lunkaransar Lake sediments (Fig. 1.2h) (Enzel et al., 1999) which also indicated moderately dry conditions during the early Holocene. Similarly, the palaeo-records from the arid central Asia also show relatively drier condition in the region (see Chen et al., 2008) (Fig. 1.2a-f).

(b) Mid-Holocene (8.2 to 4.2 cal ka)

During the mid-Holocene, the records from the central India and NW Himalaya show reduced moisture due to the weaker ISM precipitation (Demske et al., 2009; Rashid et al., 2011; Anoop et al., 2013a; Achyuthan et al., 2014; Prasad et al., 2014). However, in NW India, the centennial scale reconstruction from the sediments of Lunkaransar (ca. 7.2 to 6.0 cal ka) and Nal Sarovar Lakes (ca. 7.2 to 6.1 cal ka) inferred early to mid-Holocene wetter climate compared to the present day (Fig. 1.2g-h). This discrepancy is attributes to the influence of mid-latitude westerlies bringing in the winter rains during the mid-Holocene in NW India (Prasad and Enzel, 2006). Similarly, the out of phase relationship between the palaeo-records from the arid central Asia (ACA) and monsoonal Asia, indicated that the ACA was wettest during the mid-Holocene (Fig. 1.2a-f) (Herzschuh, 2006; Chen et al., 2008). The palaeo-records from the monsoon dominated regions showed that the strength of the ISM is related to northern hemisphere insolation maxima (Gupta et al., 2003; Herzschuh, 2006; Demske et al., 2009; Wünneman et al., 2010). However, the moisture variability in the westerly dominated regions was determined largely by North Atlantic Sea surface temperatures, and regional uplift and descent of air masses (Herzschuh, 2006; Chen et al., 2008; Lauterbach et al., 2014).

(c) Late Holocene (4.2 cal ka to recent)

The isotope investigations on the speleothem from the central India indicated the drier condition during 3.4 to 1.9 ka and 0.7 to 0.3 ka, Gupteswar (Yadava and Ramesh, 2005; Tiwari et al., 2009) and Dandak cave (Berkelhammer, 2010), respectively. Additionally, the lacustrine record, based on the isotopic composition of the authigenic carbonate from the Lonar Lake (central India) showed similar drying phase during 4.6 to 3.9 cal ka and 2 to 0.6 cal ka (Anoop et al., 2013b) (Fig. 1.2l). Similarly, the palaeo-records from the

Tibetan Plateau also showed the reduced moisture availability during the late Holocene compare to the early or mid-Holocene (Gasse et al., 1996; Demske et al., 2009; Mischke and Zhang, 2010; Döberschutz et al., 2013) (Fig. 1.2m-n). The cold event at lake Ximencuo (Mischke and Zhang, 2010) between 4.2 and 2.8 cal ka is coeval with other records from Garhwal Himalaya (Phadtare, 2000), Bangong Co and Sumxi Co (Gasse et al., 1996), and Guliya ice core (Yao et al., 1997).

During the late Holocene, the climate records from the Indian subcontinent show substantial changes on centennial to sub-centennial time scales (Fig. 1.2g-n). For example, based on the dendroclimatic records from the Himalayan region, a decreasing trend of atmospheric temperatures in the Himalayan region as compared to the increaing global temperatures is observed during the late 20thcentury (Esper et al., 2002; Tiwari et al., 2011). Additionally, the lack of LIA (Little Ice Age) from the western Himalaya as compared to the central Himalaya and the other sites from the Tibetan Plateau also indicated significant difference in the past climatic record (Tiwari et al., 2009; Mischke et al., 2013).

1.3. Motivation and Objectives

The importance of seasonal precipitation and meltwater to the social and economic well-being of Indian society cannot be overstated. My work largely focuses on the Tso Moriri Lake in the high altitude Indian Himalayas. Solving the riddle past hydrological changes, and the role of seasonal precipitation and meltwater on the large water resources stored in this 105 m deep lake can provide clues to understanding the impact of climate change on local hydrology. Additionally, I have also worked on the Lonar Lake in peninsular central India to decouple the regionality of seasonal precipitation during the Holocene.

My specific objectives were

- Establishing a link between modern lake sediment properties and environmental conditions to **identify climate sensitive proxies**.
- Using the identified proxies to **reconstruct ISM and westerlies** variability on millennial to decadal timescales.
- Identifying the **impact of seasonal precipitation and meltwater** to the local hydrological balance in the Tso Moriri Lake

To achieve these objectives my work is divided into the following three levels.

(a) Modern investigations: "*Present is the key to the past*", the famous quote, by James Hutton, emphasises the importance of modern environmental conditions as key to understanding past environmental changes. A crucial prerequisite for palaeo-reconstruction is the identification of sensitive proxies. The modern investigations on the high altitude NW Himalaya and the peninsular India involved (i) site selection; (ii) modern limnological investigations; and (iii) identifying climate sensitive proxies.

(i) *Site selection from climatically sensitive regions:* In view of the spatial heterogeneity in the modern climate and precipitation sources over India (Section 1.1), I have focussed on two lakes from different climate zones. The first site, the Tso Moriri Lake, lies in the transitional zone between westerlies and the ISM regime in the high altitude Himalayas. The water balance in the lake is maintained by meltwater from glaciers and seasonal precipitation (ca. 250 mm/y) (New et al., 2002) and relatively high evaporation (Srivastava et al., 2013). The second site is the Lonar Lake, which is situated in the core monsoon zone of India (Gadgil, 2003). The regional hydrology of the lake is sustained dominantly by ISM precipitation and limited ground water discharge (Anoop et al., 2013b; Menzel et al., 2014; Prasad et al., 2014).

(ii) *Identifying modern end members and limnological investigations:* Investigation of lake physico-chemical parameters (limnology), identification of water and sediment sources, understanding the major factors controlling the hydrochemistry and the isotopic composition of the feeder streams and the lake water.

(iii) *Proxy identification:* Geochemical, sedimentological, and mineralogical analyses of catchment and surface lake sediments to understand transport and sedimentation processes within the lake basin in order to identify environmentally sensitive proxies (isotopes, mineralogy, weathering indices).

(b) Reconstruction of the past hydrology (climate): Based on the identified proxies, the reconstruction of the past hydrological conditions, and identification of periods of extreme changes.

(c) Regional intercomparison to determine spatio-temporal variation of the past moisture sources, and infers probable forcing mechanisms.

1.4. Study area

1.4.1. Tso Moriri Lake, NW Himalaya

Tso Moriri (78°14'-78°25'E and 32°40'-33°02'N, >4500 m asl) is one of the largest lakes situated in the Changthang region of Ladakh region (Chandan et al., 2008). It extends 27 km in NS direction and 5-7 km in an EW direction (Fig. 1.3b). The lake lies within the rain shadow region of the NW Himalaya with cold-arid to semi-arid climate and an annual maximum temperature fluctuating between +30°C (in summer) and -40°C (during winter) (Mishra and HumbertDroz, 1998). Annual precipitation of the Tso Moriri region is very low, varies around ca. 250 mm (New et al., 2002). Modern data (1998-2007) indicates that the western part of the Himalaya (Indus catchment) receives 50% of the discharge from monsoonal rainfall during summer and the remaining 50% from snow melt (Bookhagen and Burbank, 2010).

Tso Moriri Lake has a watershed area of approximately 2,361 km^2 and a lake surface area of approximately 150 km^2 (Leipe et al., 2014b). The lake is closed (endorheic), fresh to brackish water (<5.85 g/l NaCl measured in mid-summer) and oligotrophic in nature (Chandan et al., 2008). The lake is fed by two major streams (Gyoma from the north and Phirse Phu from south) and several ephemeral streams, which contribute in the lake water budget.

The modern vegetation in the catchment of the lake is characterised by desert-steppe, alpine/high and alpine steppe plant communities (e.g. *Artemisia, Chenopodiaceae, Polygonum, Oxytropis, Poaceae, Cyperaceae)* (Hutchinson, 1937; Mishra and Humbert-Droz, 1998; Chandan et al., 2008; Leipe et al., 2014a, 2014b). The Kurzok village, situated along the northwestern shore of the lake, is one of the highest places of the world where agriculture is practiced (Hutchinson, 1937). The main cultivated crops are barley (*Hordeum*), wheat (*Triticum*), buckwheat (*Fagopyrum*) and millet (*Panicum*) (Bhattacharyya, 1991; Hartmann, 1999; Leipe et al., 2014b). The shallow part of the lake basin (up to 10 m of water depth) is characterised by the aquatic plant from *Potamogeton sp.* (*Potamogeton pectinatus*, *Potamogeton perfoiatus*), and *Ranunculus natans* (Chandan et al., 2008).

Geologically, the lake catchment is dominated by carbonate-bearing rocks in south and east-west extension of the lake basin (Fig. 1.3b) (Steck et al., 1998). The

northern part of the lake is surrounded by metamorphosed gneissic complex with characteristics ultra-high pressure (UHP) eclogite rocks, whereas the south-west part is covered by massive, unfoliated, coarse grained granitic body (Rupshu granite) (Fuchs et al., 1996).

1.4.2. Lonar Lake, central India

The Lonar (76°30'E and 19°58'N, ~480 m asl) is a crater lake formed by the meteoric impact at around 570 ka (Jourdan et al., 2011) (Fig. 1.3c). The lake is closed, hyposaline and alkaline in nature, with a mean diameter of ~1.2 km. The catchment is characterised by Deccan basalt, intertrappean palaeosols, and Quaternary deposits (Maloof et al., 2010; Basavaiah et al., 2013) (Fig. 1.3c). Climatically, the lake is situated in the core monsoon zone (Gadgil, 2003) of India, and receives moisture only from the SW monsoon (ISM). The average precipitation during the monsoon (June to September) ranges around ~680 mm, whereas the temperature during pre-monsoon period (March to June) varies around 31°C. During the monsoon and the post monsoon period the temperature ranges from 23 to 25°C (Anoop et al., 2013b).

The modern vegetation of the Lonar crater is dominated by tropical dry deciduous forest (Champion and Seth, 1968). Based on the abundance of different plant species the vegetation is roughly divided into three zones. The dry deciduous forest vegetation comprising, *Azadirachta indica* (local name: Neem), *Tectona grandis* (local name: Sagaun), *Cassia fistula* (local name: Amaltas), and *Wrightia tinctoria*, at the outer rim of the Lonar crater (Prasad et al., 2014). The shore region is exclusively dominated by *Prosopis juliflora* (local name: Babool), whereas the region between the outer rim of the crater and shore region is dominated by *Ficus benghalesis* (local name: Bargad), *Trewia nudiflora* (local name: Gutel), *Alangium salviifolium*, etc. (Prasad et al., 2014). In the NE part of the lake, swamp vegetation is dominant near to the mouth of Dhara stream, whereas in the distal part of the stream large area of alluvial fan is used for the crop plantation and cattle grazing (Fig. 1.3c). The lake is highly eutropic, which is indicated by the dominance of phytoplankton biomass in the lake epilimnion (Satyanaraya and Chaudhari, 2007). The common algal assemblage in the lake water is dominated by mainly cynophyceae followed by bacillariophyceae as well as euglenophyceae and chlorophyceae (Malu 2001; Satyanaraya and Chaudhari, 2007). The microscopic organisms (Zooplanktons) are dominated by rotifer species (Malu,

2001). The lake is also characterised by thermophilic, halophilic and alkalophilic bacteria with an important role in nutrient cycling and food web (Joshi et al., 2008).

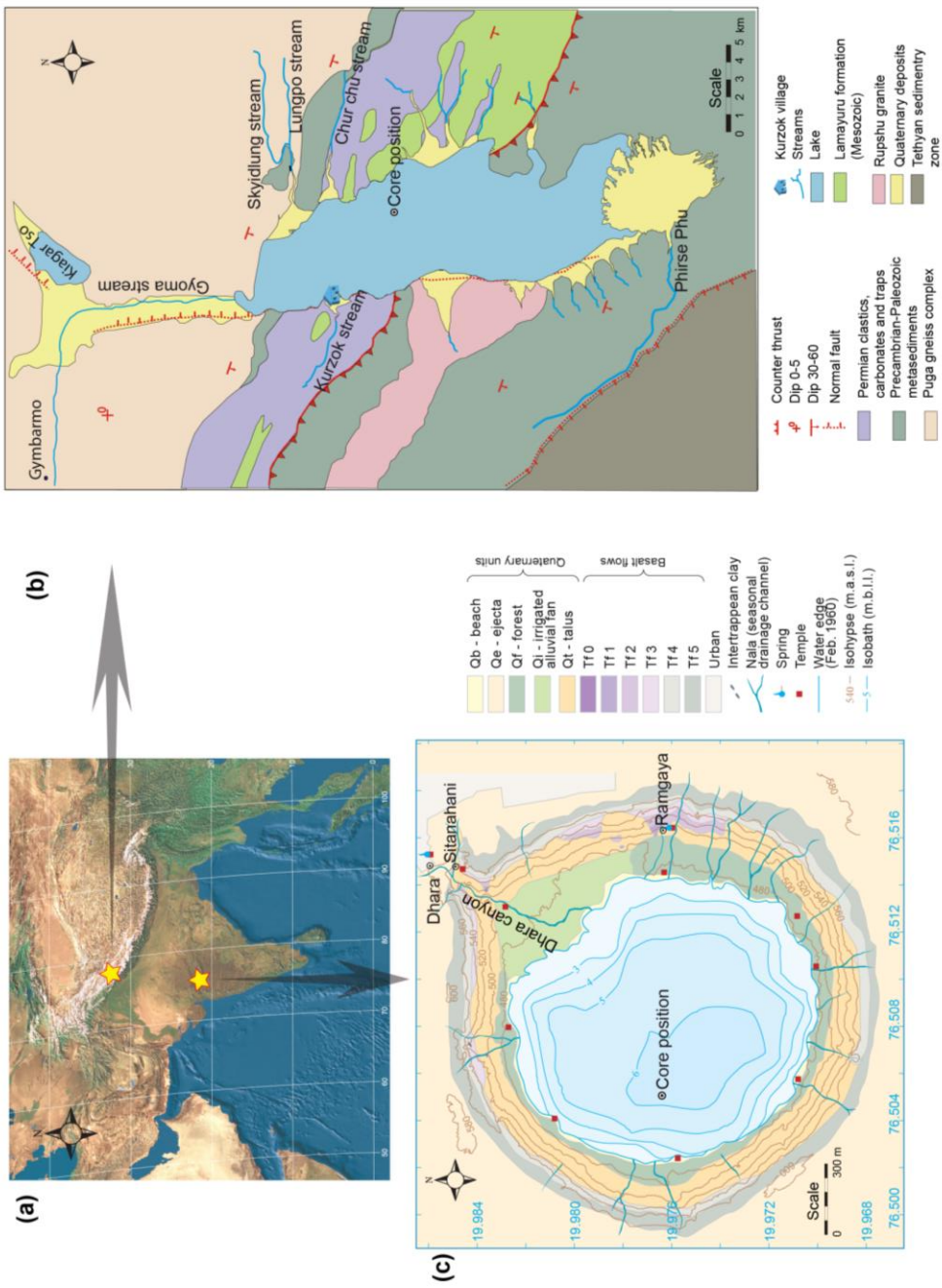

Fig. 1.3: (a) Topographical image of Indian subcontinent indicating the study area, and the geological map of (b) Tso Moriri Lake, NW Himalaya, and (c) Lonar Lake, central India

1.5. Organisation of thesis

The organisation of my thesis is based on the investigations on modern and core sediments from the Tso Moriri, NW Himalaya and the Lonar Lake, central India. With the former, I have identified environment (climate) sensitive proxies, which were used for palaeo-investigations on core sediments.

Chapter 2: **"Limnology and modern sedimentation patterns in high altitude Tso Moriri Lake, NW Himalaya – implications for proxy development"** This study deals with the geochemical and sedimentological investigations on catchment and surface lake sediments from the Tso Moriri Lake, NW Himalaya, and evaluates the potential of measured parameters for palaeoenvironmental (climate) reconstruction i.e. proxy identification.

Chapter 3: **"Reconstructed late Quaternary hydrological changes from Tso Moriri Lake, NW Himalaya"** provides high-resolution data from the Tso Moriri Lake, NW Himalayas The geochemical, mineralogical and sedimentological investigations on the core sediments reveal the climate forced hydrological variability *i.e.* ([Precipitation+Melt water=I]/[Evaporation=E] (I/E) balance and lake level changes since glacial period (~26 cal ka). This reconstruction was then compared with available literature from the ISM and westerly dominated regions to obtain the information on their spatial and temporal variability during the Holocene in the ISM realm.

Chapter 4: **"Carbonate isotopes from high altitude Tso Moriri Lake (NW Himalayas) provide clues to late glacial and Holocene moisture source and atmospheric circulation changes"-** high-resolution isotopic ($\delta^{18}O$ and $\delta^{13}C$) investigations on authigenic carbonates (calcite/aragonite) from the Tso Moriri Lake, NW Himalaya provide insights into the changing precipitation sources during selected time slices during the past 15.5 cal ka.

Chapter 5: **"Linking Holocene drying trends from Lonar Lake in monsoonal central India to North Atlantic cooling events-** this chapter deals with palaeoclimatic reconstruction on centennial scale from the Lonar Lake using biogeochemistry, mineralogy and grain size data. The centennial scale variability indicated the climate deterioration occurred at 6.2 – 5.2, 4.6 – 3.9, and 2.0 – 0.6 cal ka, linked with the North Atlantic cold events.

Chapter 2: Limnology and modern sedimentation patterns in high altitude Tso Moriri Lake, NW Himalaya – implications for proxy development

Praveen K Mishra[1], *A. Anoop*[2], *A. Jehangir*[3], *Sushma Prasad*[4], *P. Menzel*[5], *G. Schettler*[1], *R. Naumann*[1], *S. Weise*[6], *N. Andersen*[7], *A.R. Yousuf* [3], *B. Gaye*[5]

[1] Helmholtz Centre Potsdam, GFZ German Research Centre for Geosciences, Potsdam, Germany
[2] Department of Earth Sciences, Indian Institute of Science Education and Research, Kolkata, India
[3] Department of Environmental Science and Centre of Research for Development, University of Kashmir, India
[4] Institute for Earth- and Environmental Science, University of Potsdam, Karl-Liebknecht-Straße 24-25, 14476 Potsdam, Germany
[5] Universität Hamburg, Institute of Biogeochemistry and Marine Chemistry, Hamburg, Germany
[6] UFZ Centre for Environmental Research, Dept. Catchment Hydrology, Halle, Germany
[7] Kiel University, Leibniz Laboratory for Radiometric Dating and Stable Isotope Research, Kiel, Germany

Manuscript status: Published in Fundamental and Applied Limnology, DOI: http://dx.doi.org/10.1127/fal/2014/0664 (for full acess of this chapter please refer to given DOI).

Abstract

We report the results of our investigations on the catchment area, lake surface sediments, and hydrology of the high altitude alpine Tso Moriri Lake, NW Himalayas (India). Our results indicate that the lake is currently alkaline, and thermally stratified with an oxic bottom layer. Results from hydrochemistry and isotopic composition ($\delta^{18}O$ and δD) of inflowing streams and lake waters show that Tso Moriri Lake is an evaporative lake with contribution from both westerly source (snow melt) and Indian summer monsoon precipitation. Geochemical and mineralogical investigations on the catchment and lake surface sediments reveal the presence of authigenic aragonite in modern lake sediment. The lithogenic components reflect the inflow and sorting processes during transport into the lake, whereas the authigenic carbonate fraction can be linked to the changes in ([precipitation+meltwater]/evaporation) (I/E) balance within the lake. The spatial variability in grain size distribution within the lake surface sediments shows that the grain size data can be utilised as a proxy for transport energy and shoreline proximity in the lake basin. We have evaluated the applicability of commonly applied environmentally sensitive proxies (isotopes, mineralogy, weathering indices) for palaeoenvironmental reconstruction in the Tso Moriri Lake. Our results show that the commonly used weathering index (Rb/Sr) is not applicable due to Sr contribution from authigenic carbonates. The useful weathering indices in Tso Moriri Lake are the Si/Al and the Chemical Proxy of Alteration (CPA). Since the carbonates are formed by evaporative processes, their presence and isotopic values can be used as indicators of I/E changes in the lake.

Keywords: Geochemistry; Lake Sediments; Palaeoenvironmental proxies; Tso Moriri Lake; Weathering indices

Chapter 3: Reconstructed late Quaternary hydrological changes from Lake Tso Moriri, NW-Himalaya

Praveen K. Mishra*[1+]*, *A. Anoop[2], G. Schettler[1], Sushma Prasad[3], A. Jehangir[4], P. Menzel[5], R. Naumann[1], A. R. Yousuf [4], N. Basavaiah[6], K. Deenadayalan[6], M. G. Wiesner[5], B. Gaye[5]*

[1]Helmholtz Centre Potsdam GFZ German Research Centre for Geosciences, Potsdam, Germany
[2]Department of Earth Sciences, Indian Institute of Science Education and Research, 741252, Kolkata, India
[3]Institute for Earth- and Environmental Science, University of Potsdam, Karl-Liebknecht-Straße 24-25, 14476 Potsdam, Germany
[4]Limnology and Fisheries Laboratory, Centre of Research for Development, University of Kashmir, India
[5]Universität Hamburg, Institute of Biogeochemistry and Marine Chemistry, Hamburg, Germany
[6]Indian Institute of Geomagnetism, Navi Mumbai, India

Manuscript status: Published in Quaternary International. DOI: http://dx.doi.org/10.1016/j.quaint.2014.11.040

Abstract

We present the results of our investigations on the radiocarbon dated core sediments from the Lake Tso Moriri, NW-Himalaya aimed at reconstructing palaeohydrological changes in this climatically sensitive region. Based on the detailed geochemical, mineralogical and sedimentological analysis, we recognise several short-term fluctuations superimposed upon seven major palaeohydrological stages identified in this lake since ~26 cal ka. Stage I (>20.2 cal ka): shallow lake characterised by input of coarse-grained detrital sediments; Stage II (20.2-16.4 cal ka): lake deepening and intensification of this trend ca. 18 cal ka; Stage III (16.4 -11.2 cal ka): rising lake levels with a short-term wet phase (13.1-11.7 cal ka); Stage IV (11.2-8.5 cal ka): early Holocene hydrological maxima and highest lake levels inferred to have resulted from early Holocene Indian monsoon intensification, as records from central Asia indicate weaker westerlies during this interval; Stage V (8.5-5.5 cal ka): mid-Holocene climate deterioration; Stage VI (5.5-2.7 cal ka): progressive lowering of lake level; Stage VII (2.7-0 cal ka): onset of modern conditions. The reconstructed hydrological variability in Lake Tso Moriri is governed by temperature changes (meltwater inflow) and monsoon precipitation (increased runoff). A regional comparison shows considerable differences with other palaeo-records from peninsular India during late Holocene.

Keywords: Authigenic **c**arbonates; Holocene; Indian summer monsoon; Lake Sediments; Tso Moriri Lake; Westerlies.

3.1. Introduction

The modern climate in the Asian region is influenced by the Asian monsoon in the east (East Asian monsoon) and south Asia (Indian summer monsoon), the mid-latitude westerlies in central Asia, the orographic influence of the Tibetan Plateau, and the Siberian Anticyclone (Raymo and Ruddiman, 1992; Gong and Ho, 2002; Herzschuh, 2006; Anoop et al., 2013a). The relative influence of the moisture pathways (westerlies and the Asian monsoon) in these regions has shown considerable variations in intensity and spatial extent in the past (e.g., Herzschuh, 2006; Chen et al., 2008; Demske et al., 2009). The hydrological budget of the Himalayan lakes and rivers is controlled by both the snowmelt and monsoon rainfall contribution. Modern data (1998-2007) indicates that the western part of the Himalaya (Indus catchment) receives 50% of the discharge from monsoonal rainfall during summer and the remaining 50% from summer melting of snow precipitated during winter (Bookhagen and Burbank, 2010). However, the contribution of seasonal precipitation and snowmelt to the hydrological balance of lakes over longer time scales is not yet well documented. Additionally, prolonged droughts have been reported from central and NE India during the late Holocene (Prasad et al., 2014) though their impact, if any, in the NW-Himalayan region is unknown. These lacunae need to be urgently addressed as a major percentage of the Asian population is directly or indirectly dependent on the freshwater supplied from the Himalayan region.

In this study, we investigate core sediments from Lake Tso Moriri, NW-Himalaya, India (78°14’-78°25’E and 32°40’-33°02’N, >4500 m asl) as a palaeoenvironmental archive. Lakes in these high altitude regions respond to modest environmental changes (Herzschuh et al., 2009; Mischke and Zhang, 2010; Wünnemann et al., 2010), and are less influenced by the local human impact. Leipe et al., (2014a) have shown that higher *Artemisia* percentages in the pollen spectra and higher *Artemisia*/*Chenopodiaceae* (A/C) values in Lake Tso Moriri sediments are linked to increased moisture availability and have reconstructed a mean annual precipitation (MAP) curve for the Holocene. However, the relative role of seasonality of precipitation or meltwater to the Lake Tso Moriri hydrology is yet unknown. Our study is aimed at palaeohydrological reconstruction using geochemical, mineralogical, and sedimentological proxies from a composite core raised from the Lake Tso Moriri. We

compare our reconstruction with other records in the monsoon and westerly domains for a better understanding of the moisture sources (Fig. 3.1a).

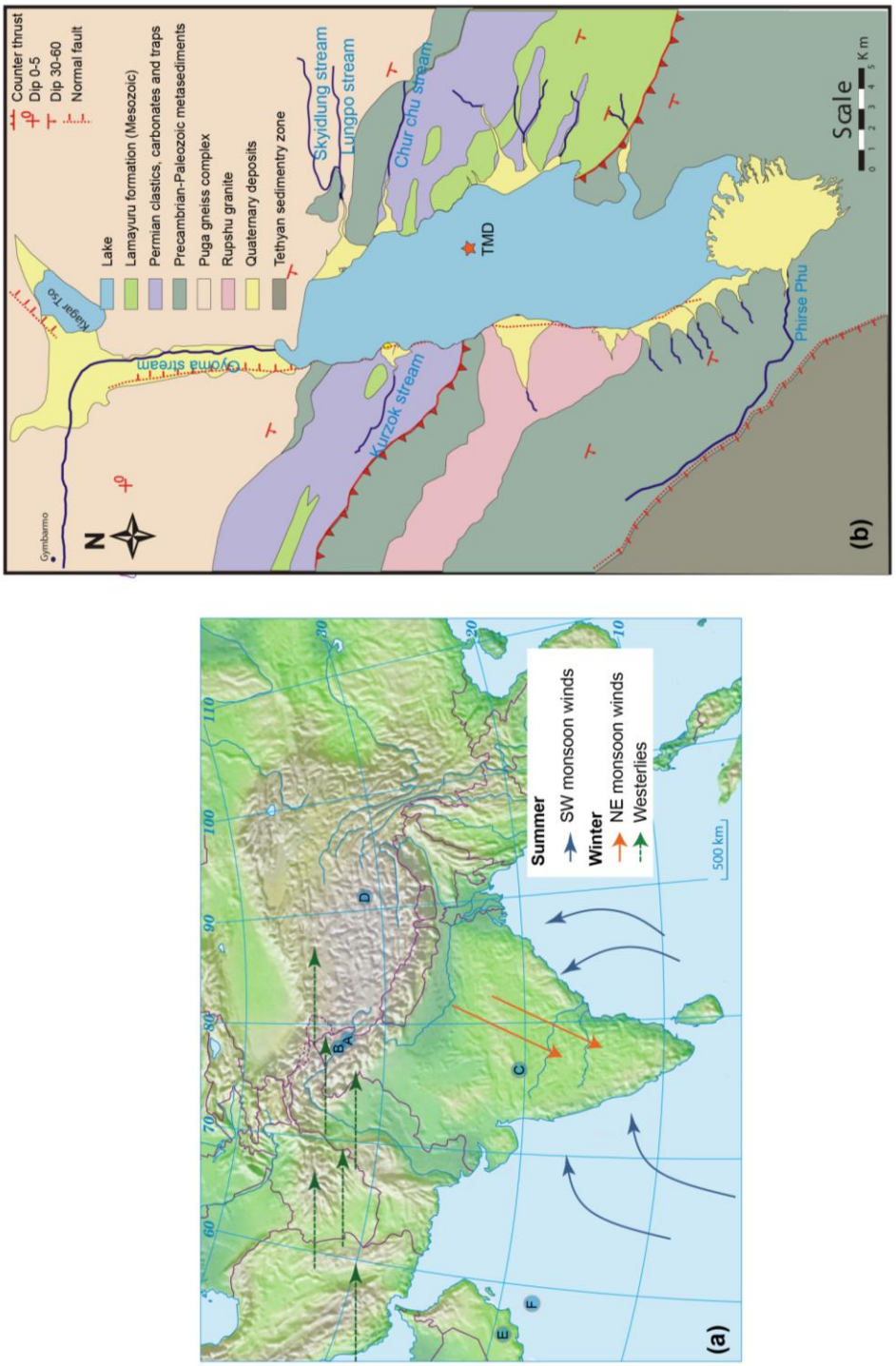

Fig. 3.1: Geographical setting of the Lake Tso Moriri: (a) Large scale morphological map with dominant seasonal hemispherical airflows (modified after Prasad and Enzel, 2006; Prasad et al., 2014) and different palaeoclimatic sites discussed in the text, (A) Tso Moriri (this study), (B) Tso Kar (Demske et al., 2009), (C) Lonar Lake (Anoop et al., 2013b; Prasad et al., 2014), (D) Nam Co Lake (Döberschütz et al., 2014), (E) Qunf cave, Oman (Fleitmann et al., 2003), (F) Arabian Sea (Gupta et al., 2003); (b) Geological map of Tso Moriri Lake catchment (modified after Fuchs and Linner, 1996; Steck et al., 1998; de Sigoyer et al., 2004). The star represents the location of the composite core (TMD).

3.2. Study area

3.2.1. Regional climate

Lake Tso Moriri lies within the rain shadow region of the NW-Himalaya with summer and winter temperature variations between 0° to +30°C and -40° to -10°C, respectively (Mishra and Humbert-Droz, 1998). Annual precipitation in the Tso Moriri region is ca. 250 mm (Leipe et al., 2014a). Modern climate data suggest that the Lake Tso Moriri is situated in a transitional zone affected by both the Indian summer monsoon and the mid-latitude westerlies (Bookhagen et al., 2005; Bookhagen and Burbank, 2010).

3.2.2. Geology

The Lake Tso Moriri is situated in the Tso Moriri crystalline complex (Steck et al., 1998; de Sigoyer et al., 2004), which is bounded by NW-SE trending belt (Zildat ophiolite mélange of Indus-Tsangpo suture zone) to the north (Berthelsen, 1953) and sedimentary rocks of the Tethyan Himalaya to the south (Singh et al., 2013). The northern boundary of the lake catchment is characterised by the Puga gneiss complex comprising of Quartzo-feldspathic augen gneiss as well as boudins of eclogites and discontinuous layers of metasedimentary schists (Steck et al., 1998). The northeastern part of the lake is dominated by the Lamayuru Formation (Mesozoic age), consisting of interbedded marls, limestone, dolomites, shales and sandstone (Steck et al., 1998) (Fig. 3.1b). The lower Proterozoic to Cambrian sediments of the Haimanta group with dominant carbonate lithology are exposed in the southern boundary of the catchment. To the south of the Kurzok village, the Haimanta group has been intruded by the unfoliated, coarse-grained Rupshu granite (Fig. 3.1b) (Fuchs and Linner, 1996).

The geomorphology in the Tso Moriri catchment is dominated by glacial and fluvial landforms; most common Quaternary sediments are characterised by alluvial and moraine deposits (Hedrick et al., 2011). Cosmogenic ^{10}Be dating of moraine deposits suggested that the glacial advance in Kurzok valley (~3.6±1.1 ka) is synchronous with the glacial advancement in northern Puga valley (4.2±2.2 ka) (Hedrick et al., 2011).

3.2.3. Hydrology

Tso Moriri is one of the largest lakes situated in the Changthang region of Ladakh (Chandan et al., 2006) with an N-S length of 27 km and E-W extent of 5-7 km. The lake has a watershed area of ca. 2,350 km^2 and a surface area of approximately 150 km^2. The

modern lake is closed (endorheic) and oligotrophic (Hutchinson, 1937; Chandan et al., 2006). Bathymetric mapping carried out during summer 2011, revealed a maximum lake water depth of 105 m. Interannual lake level fluctuations of 1-3 m have been observed during the last decade with high lake stands observed during June/July with contributions from both meltwater inflow and monsoon rainfall (Leipe et al., 2014b; Mishra et al., 2014). Lake Tso Moriri is fed by two major perennial streams, namely Gyoma in the north, and Phirse Phu in the south (Fig. 3.1b). Additionally, several ephemeral streams, prominent among them being the streams located in the eastern (Lungpo, Skyidlung, and Chur Chu stream), and northwestern (Kurzok) part of the basin, also contribute to the surface water inflow into the lake (Fig. 3.1b). The meltwater in eastern streams is contributed by Chamser Kangri (6600 m asl) and Lungser Kangri glaciers (6650 m asl), whereas Mentok I (6250 m asl) and II (6210 m asl) are the source of the meltwater for streams in the western part (Leipe et al., 2014b).

3.2.4. Modern vegetation

The modern vegetation in the vicinity of Lake Tso Moriri is characterised by desert-steppe and alpine/high, alpine steppe plant communities (Hutchinson, 1937; Mishra and Humbert-Droz, 1998; Chandan et al., 2008; Leipe et al., 2014a and 2014b), commonly comprising *Artemisia, Chenopodiaceae, Polygonum, Oxytropis, Poaceae, Cyperaceae* (Chandan et al., 2008; Dvorský et al., 2011). Kurzok village, situated along the northwestern shore of the lake, is one of the highest places of the world where agriculture is practised (Hutchinson, 1937). The main cultivated crops are barley (*Hordeum*), wheat (*Triticum*), buckwheat (*Fagopyrum*) and millet (*Panicum*) (Bhattacharyya, 1991; Hartmann, 1999; Leipe et al., 2014b). Chandan et al., (2008), have documented the presence of aquatic plants (*Potamogeton pectinatus, Potamogeton perfoiatus, and Ranunculus natans*) on the lake bottom down to 10 m depth.

3.3. Methodology

3.3.1. Coring and core correlation

During the field expedition in June/July 2011, we retrieved two long parallel sediment cores (Fig. 3.1b) in 2 m core sections, in 9 cm diameter liners. A 7.28 m long composite sediment profile was developed by correlating these two long parallel core sequences using visible macroscopic marker layers (e.g., mica and sand) and µ-XRF data from core scanning (Fig. 3.2a-b). Additionally, to better capture the water-saturated sediment

surface, several short (ca. 15-30 cm long) cores were also recovered from the lake basin using a gravity corer (Mishra et al., 2014).

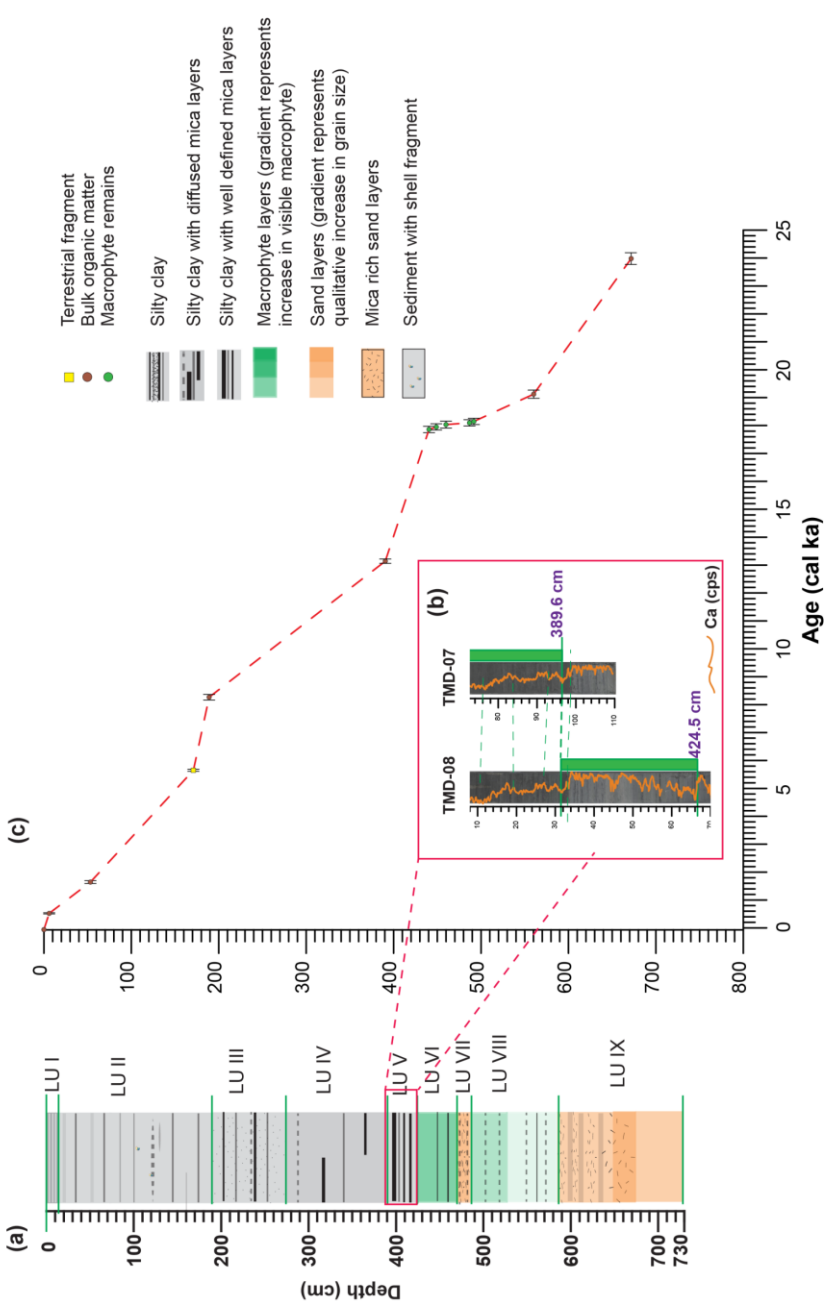

Fig.3. 2: (a) Lithology of the composite core; (b) Correlation using µ-XRF data (Ca, counts per second) and marker layers (dashed lines); (c) Age- depth model of the core.

3.3.2. Chronology

Due to limited amount of terrestrial organic fragments, analysis of bulk organic material or available submerged macrophytes was the only option for dating (Hou et al., 2012). The dating of the Lake Tso Moriri core sediment is based on AMS-^{14}C dates on seven bulk sediment samples, five macroscopic *Potamegeton* remains, and a terrestrial twig fragment (Table 3.1; Fig. 3.2c). The samples were dated in the Poznan AMS dating laboratory in Poland. Additionally, bulk sediment samples from the top (0-1 cm depth) of the composite core and leaves of *Potamogeton pectinatus* growing in the modern lake were radiocarbon dated to estimate the "reservoir effect" in the lake. Since the ^{14}C content in the modern atmosphere has been changed significantly by the admixture of large amounts of fossil fuel derived CO_2 (Hou et al., 2012), calibrated ^{14}C ages of the modern samples were calculated for the year of material formation/deposition (*i.e.* 2011 AD) and not for the ^{14}C concentration of the atmosphere in 1950 AD (Mischke et al., 2013). For the conversion of the older ^{14}C dates into calendar ages, we used the online-version of the OxCal 4.2 radiocarbon calibration program (Bronk Ramsey, 2008) using the INTCAL 13 calibration curve (Reimer et al., 2013) (Table 3.1).

3.3.3. Laboratory methods

Geochemical (quantitative and scanning X-ray fluorescence (XRF)), mineralogical, and sedimentological analysis were conducted on the core samples. The high-resolution X-ray fluorescence scans were done at 1 mm resolution. Furthermore, 95 samples (1 cm sample slices at 10-15 cm interval resolution until 415 cm, and 0.5 cm sample slices at 10 cm intervals in the lower part of the core) have been analysed for quantitative XRF, X-ray diffraction (XRD), and grain-size distribution.

Continuous down-core XRF scanning of the sediment cores was performed using the ITRAX core scanner. The sediment surface was carefully cleaned and covered with a thin ultra-clean film prior to analysis. In the case of the Lake Tso Moriri sediments, the scan was conducted using Cr-tube with a tube voltage of 30 kV, a current of 30 mA, and an exposure time of 10 seconds. The resulting data are semi-quantitative and provide relative down-core fluctuations in element composition as counts per second (cps).

The chemical composition of freeze-dried and powdered sediment samples was quantitatively determined by XRF (PANalytical AXIOS) advanced analytical system. The samples (0.35 g) were mixed with 6.65 g Fluxana and 0.5 g NH_4NO_3. The mixture

was gradually heated and melted on five different burners to prepare melted glass discs, which were used for the analysis. A Panalytical Axios Advanced wavelength-dispersive spectrometer and matrix correction programs were used to calculate concentrations.

Powder X-ray patterns were collected using a PANalytical Empyrean powder diffractometer with Cu Kα radiation, automatic divergent and anti-scatter slits and a PIXcel3D detector. The diffraction data were recorded from 5° to 85° 2θ via a continuous scan with a step-size of 0.013° and a scan time of 60 s per step. Semi-quantitative mineral contents of the samples were determined using the AUTOQUAN/BGMN software (Bergmann et al., 1998).

The grain-size distribution of lake and catchment sediments was determined using the Malvern Mastersizer 2000 analyser. Sample pre-treatment included the wet-oxidation of organic matter at room temperature. Ten ml H_2O_2 (30%) was added in two steps to approximately 0.3 g sample-aliquots in 50-ml centrifuge tubes (Sarstedt). The excess oxidising agent was removed by repeated washing with Millipore water (18.2 MΩcm), centrifugation (6000 rpm, 5 min), and suction of the supernatant. The solid residues were suspended in 20 ml Millipore water without chemical additions. Particle aggregates were disintegrated by hand shaking combined with a 15 min treatment in an ultrasonic bath. A homogenous suspension aliquot was transferred into the 'Small Volume Sample Dispersion Unit' of the instrument. The instrument measured the grain-size distribution of the suspended particles from 0.02 to 2000 µm for 100 grain-size classes. In the case of (coarse) sandy samples, the >200 µm particle fraction was separated by sieving prior to carrying out the Laser-Particle grain-size analyses. The content of coarse particles in the core sediment between 0 and 310 cm is generally low. The presence of a few coarse particles (>200 µm) in the suspension aliquots used for the Laser-Particle measurements of these samples cannot be representative for the entire sample. Therefore, we re-calculated primary analytical data of the grain-size distribution for the particle size fraction 0.02 to 200 µm. The average Relative Standard Deviations (RSDs) of five single measurements of the Volume-weighted-means (D[4,3]) was ~0.5%.

3.4. Results

3.4.1. Lithology

The Tso Moriri core sediments can be broadly divided into three dominant lithounits. The bottom (728.6-585 cm) of the composite core is sandy, and is overlain by silt mixed with variable amount of macroscopic macrophyte remains (585-425 cm). The remaining part of the core (425-0 cm) contains largely calcareous silty clay with variable degree of laminations. However, based on visual observations of degree and type of laminations, and macrophyte content a more detailed classification into nine lithounits (LU) has been made (Fig. 3.2a).

- LU-IX (728.6-585 cm): Dominated by sand with micaceous silt layer between 673 and 585 cm.
- LU-VIII (585-485.9 cm): Medium silt sized calcareous sediment, with macroscopic macrophyte fragments.
- LU-VII (485.9-471.3 cm): Micaceous sand.
- LU-VI (471.3-425 cm): Similar to LU VIII, but characterised by well-defined mica-rich lamination and abundance of macroscopic macrophyte fragments.
- LU-V (425-391.4 cm): Light grey medium size silt, with both indistinct and clearly visible mica-rich laminations (1-5 mm thick). Mica laminations are more prominent relative to LU IV.
- LU-IV (391.4-274.6 cm): Discontinuous lamination and disseminated mica in medium grained silt.
- LU-III (274.6-190.3 cm): This unit was dominated by silty clay with continuous black and light grey laminations (2-10 mm).
- LU-II (190.3-12.3 cm): Light to dark grey medium silt dominated sediment with discontinuous and diffuse black and light grey laminations. Occasionally shell fragments (<1 mm length) were found.
- LU-I (12.3-0 cm): Light brown silty sediment with alternating dark and light laminations. The thickness of the individual laminations varies between 2 and 8 mm.

3.4.2. Radiocarbon dating

The dates on bulk organic matter and macroscopic organic remains from Lake Tso Moriri sediments are shown in Table 3.1; Fig. 3.2c. The radiocarbon age (3319±35 yr) for the top sediment from the composite core (Table 3.1, sample TM 1) indicates that there is a significant "reservoir effect" in the Lake Tso Moriri. However, ^{14}C dating of the modern *Potamogeton* shows a radiocarbon age of 741±40 yr (Table 3.1, sample M1).

3.4.3. Geochemistry and mineralogy

Titanium (Ti) shows a positive correlation with Al, K and Fe (r = 0.80, 0.88, 0.82 respectively) for the entire continuous µ-XRF data set. However, Si is positively correlated with Ti (r= 0.83) only for sediments between 0-425 cm. Below this depth there is an inverse correlation between Ti and Si (r= -0.36) (Fig. 3.3a and 3.3b). Similarly, there is a strong inverse correlation between Ca and Ti (r= -0.83) between 0 and 425 cm depth which is absent in the lower part of the core (425-728.6 cm) (r= -0.045) (Fig. 3.3a and 3.3c). The CaO variability determined by discontinuous quantitative elemental data, and the carbonates (calcite and aragonite) based on mineralogical analysis, parallels the high-resolution scanned XRF profile of Ca (Figs. 3.3c, d and f) indicating that Ca is largely contributed by the carbonates.

The dominant mineral components, quartz, muscovite, and carbonates show large variability in the composite profile (Fig. 3.3f). In the lower part of the composite profile (>425 cm; >16.4 cal ka), quartz and muscovite dominate. The carbonates comprise aragonite, calcite, and small amounts of dolomite (~1-4%). Aragonite was not found in the lake's catchment and is an authigenic component (Mishra et al., 2014). Aragonite and calcite are dominant in sediments between ca. 425-310 cm (~16.4-11.2 cal ka) and ca. 197-0 cm (~8.5-0 cal ka). Between ca. 310-197 cm (~11.2-8.5 cal ka) the sediments are nearly non-calcareous. Along most of the composite core, calcite and aragonite co-vary (Fig. 3.3f) suggesting that most of the calcite is also of authigenic origin. There are a few sections at around 660 cm (ca. 23.5 cal ka), between 388 and 330 (13.1 to 11.7 cal ka), and 197-84.5 cm (ca. 8.5-2.7 cal ka), where aragonite is not detectable.

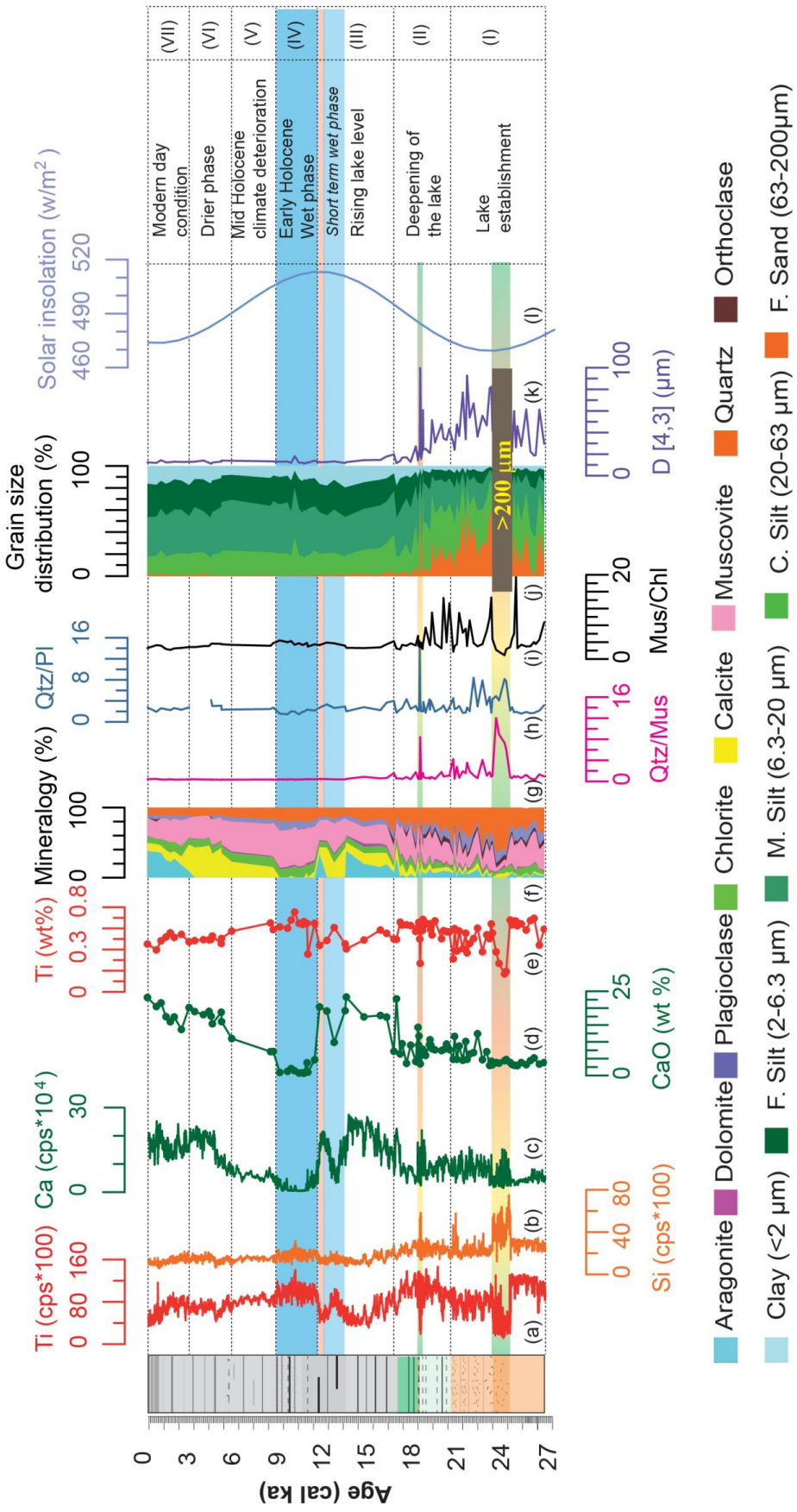

Fig. 3.3: Temporal variation in (a-f) geochemical and mineralogical data; (g-i) mineral ratios; (j) clay-, fine-, medium-, coarse-silt and fine-sand percentages in the < 200 µm fraction of the bulk sediment; (k) volume weighted mean D[4,3] of the grain-size distribution (< 200 µm fraction); (l) Summer solar insolation at 30°N (Berger and Loutre, 1991).

The deeper part of the composite core (>477 cm) shows large variability in the non-calcareous detrital component. The quartz/muscovite (Qtz/Ms) ratio in the sediments of the upper section of core (<477 cm) closely varies around 0.5. However, in the lower sediments (below 477 cm), Qtz/Ms is highly variable and can increase up to 12 (Fig. 3.3g). High Qtz/Ms ratios are typical for sediments from local granitic terrains (north and south-west) of the lake. Above ca. 477 cm, the quartz/plagioclase (Qtz/Plg) ratio varies around a base value of 2.8 but in deeper sediments ratios up to 8.4 occur (Fig. 3.3h). Similarly, the muscovite/chlorite ratio (Ms/Chl) shows distinct offsets above a base level (4.3) to 19.4 (Fig. 3.3i).

3.4.4. Grain-size distribution

Figure 3.3j, displays the grain-size data of the <200 µm fraction for 5 different grain-size classes that roughly correspond to the German classification of clay, fine-, medium-, coarse silt, and fine sand (Müller, 1967). The variation of the volume-weighted mean D[4,3] values in sediments below 425 cm (~37 µm), is much higher than in the upper part of core (average= 13 µm) (Fig. 3.3k).

3.5. Discussion

3.5.1. Chronology

A variety of potential sources of error in organic radiocarbon ages exist, the most important being (1) the "reservoir effect", caused by a disequilibrium between the atmosphere and the lake waters ^{14}C; and (2) inflow of "dead" DIC to lakes and that can result in old ^{14}C ages for lake waters (Björck and Wohlfarth, 2001; Wu et al., 2010; Mischke et al., 2013). Both (1) and (2) can result in "old ages" for modern aquatic organic material (sample M1 in Table 3.1); and (3) contamination of samples with reworked organic matter from the catchment (sample TM 1 in Table 3.1). The difference in ^{14}C ages for the living *Potamegaton* and modern sediment is likely due to a mixture of allochthonous and autochthonous organic carbon present in sediments. Assuming no change in the reservoir effect, we have used a reservoir correction of 3319 yr. for bulk samples, and 741 yr. for macroscopic *Potamegaton* remains in the core. The ^{14}C ages for the Lake Tso Moriri sediments after correction for reservoir effect are stratigraphically consistent (Fig. 3.2c). No reservoir correction has been carried out for the dated terrestrial twig (TM 4 in Table 3.1) that grows in equilibrium with the ambient atmospheric ^{14}C activity. The age-depth model of core is derived by linear interpolation

between the calibrated ages. The radiocarbon ages are available only down to a depth of 671 cm (top of the LU-IX). In view of the lithological similarity of the sediments below this depth (728.6-671 cm) with the upper section of LU-IX, an age extrapolation for the basal part was done using the sedimentation rate in the upper section of the LU-IX. The core top (0-1 cm) has been confirmed to be modern using ^{137}Cs dating method (Mishra et al., 2014)

We acknowledge that due to the variable detrital content, as evidenced in the lithological changes (section 4.1), the reworked organic content could have varied in the past and the "reservoir correction" may not have remained unchanged. Therefore, the age model proposed here can only be considered as accurate on millennial scale and not be used for detailed correlation of short-term (centennial or decadal) events.

3.5.2. Proxies for palaeoenvironmental changes

We examine changes in the authigenic (calcite and aragonite) and lithogenic components, variation in the grain-size distribution, and macrophyte data to infer changes in past lake level/hydrology. A brief summary of their significance is outlined below.

(a) Detrital input (mineralogy and grain size)

The chemical and mineralogical composition of the lithogenic (allochthonous) component of lake sediments documents the fluvial and surface run-off from the catchment (Konig et al., 2003; Limmer et al., 2012; Whitlock et al., 2012). Intense precipitation and seasonal melting of snow and ice can supply large amounts of detrital material and dissolved ions into lakes (Peng et al., 2005; Anoop et al., 2013a). The grain-size distribution of lake sediments varies depending on the proximity to the shoreline and the river inlet, changes in river discharge, and lake water depth (Magny et al., 2012; Anoop et al., 2013a). In the composite profile of Lake Tso Moriri sediments, the high positive correlation between Al, K, and Fe, with Ti for the entire continuous XRF data set indicates that Ti can be considered to be representative of the bulk siliciclastic input. Quartz, muscovite, dolomite, feldspars (orthoclase, albite), chlorite, and possibly some fraction of the calcite in the deeper sections (>585 cm; >20.2 cal ka) are of allochthonous origin (Whitlock et al., 2012). The presence of unweathered mica-rich laminations in lower sections of the core sediment (LU IX- below 585 cm) indicates short distance

transport towards the coring site (Fig. 3.3f). The chemical and mineralogical composition of the allochthonous detrital sediment can document variable contributions from local and remote sources (Limmer et al., 2012). In the case of the Lake Tso Moriri, which fills a basin that is surrounded by different geological units, mineralogical and geochemical fingerprints of the sediment can potentially help to identify the local source of the detrital deposition at the coring site (Fuchs and Linner, 1996; Steck et al., 1998; Morrill et al., 2006).

The mineral ratios Qtz/Plg, Qtz/Ms, and Ms/Chl show variability in the lower part of the core (>477 cm, >18 cal ka) and display only minor variations in the fine sediments deposited after 18 cal ka (Fig. 3.3g-i). The high variability in the mineral ratios in the older section can be linked to (i) the limited fractionation during the fluvial transport into the lake; and (ii) distinct variability in the grain-size distribution of the core sediments (Fig. 3.3j-k). This is consistent with the coarser grain-size distribution in the section where the mineralogical variability is highest, suggesting deposition in a shallow lacustrine environment (Magny, 2004; Magny, et al., 2012; Mishra et al., 2014). Subsequently (<18 cal ka), the sediments tend to be finer and the authigenic carbonate shows the largest variability.

(b) Authigenic carbonates

The strong inverse correlation between Ca and Ti (r= -0.83) between 0 and 425 cm depth indicates authigenic origin of the carbonates. However, the relative lack of correlation in the deeper sections between Ca and Ti (r= -0.045) implies some contribution from detrital calcite. Precipitation of calcite and aragonite requires an increase in Ca^{2+} and CO_3^{2-} in lake waters to achieve supersaturation for carbonate mineral precipitation (Stumm and Morgan, 1981). Our data on stream inflow show that these ions are brought in into the lake by meltwater fed streams (Mishra et al., 2014). Subsequently, the enrichment of these ions proceeds by evaporation. Beside evaporative enrichment, photosynthetic uptake of CO_2 increases the concentration of CO_3^{2-} by shifting the CO_3^{2-}-HCO_3^- equilibrium towards CO_3^{2-} and yields to precipitation of low-Mg $CaCO_3$ that increases the Mg/Ca ratio of the lake water (White, 2013). In the modern oligotrophic Tso Moriri Lake, (Hutchinson, 1937; Chandan et al., 2006) biogenic uptake of CO_2 is less important and evaporative enrichment can be considered as a forcing factor for carbonate precipitation.

Calcite is the first carbonate mineral to precipitate in the course of evaporative enrichment in response to high temperature (Eugster and Hardie, 1978). Precipitation of calcite results in a relative enrichment of Mg^{2+} versus Ca^{2+} in the lake water - enrichment of Mg in the lake inhibits the crystallisation of the calcite within the lake (Mucci and Morse, 1983). With progressive evaporation, aragonite begins to precipitate in response to an increase in the Mg/Ca ratio (Morse et al., 1997). Stein et al., (1997) document aragonite precipitation for Mg/Ca ≥ 4; Lippmann (1973) and Möller and Kubanek (1976) report onset of its precipitation for Mg/Ca > 3.5 and > 1.5. Beside evaporative enrichment, authigenic carbonates needs the influx of Ca^{2+} and CO_3^{2-} from the catchment. The largely coincident increase in calcite and aragonite from 20.2 cal ka to present documents steady influx of dissolved Ca and carbonate under a strong summer evaporative regime.

3.5.3. Palaeohydrological reconstruction using a multiproxy approach

We hypothesise that a coincident increase in detrital influx and changes in authigenic carbonate precipitation is related to monsoon strength, warming and associated meltwater release, that are recorded as hydrological changes within the sediments.

Between 23.5-20.2 cal ka, detrital input was high (Fig. 3.3a), and coarse sandy-silt sediments with highly variable mineralogy (indicated by Qtz/Ms, Qtz/Plg, Ms/Chl) were deposited indicating a shallow lake. The relatively low values for authigenic carbonates (calcite + aragonite) prior to 16.4 cal ka (average ~11%) are likely related to the regional colder temperatures (Thompson et al., 1997) during this period that inhibited calcite precipitation (Haberzettl et al., 2005; Haberzettl et al., 2007), and/or reduced chemical weathering and inflow (and hence ions) into the lake. We also note the appearance of few macrophytes remains (*P. pectinatu*s) ca. 20.2 cal ka accompanied by an increase in pelagic sedimentation suggesting increasing water depth. This trend intensifies after ca. 18 cal ka and continues until 16.4 cal ka during which macrophytes flourished, detrital input begins to decrease, and sediments become finer in response to increased distance from the shoreline and greater water depths (Peng et al., 2005). *Potamogeton pectinatu*s prefers shallow, still, clear water and can grow up to a maximum water depth of 10 m (Kantrud, 1990) indicating that an increase in lake level relative to the preceding stage resulted in conditions favourable for the growth of

macrophytes. We propose that between ca. 20.2-16.4 cal ka, a shallow lake was established but the detrital input was still significant (Fig. 3.3a and 3.3f).

The period between ca. 16.4-11.2 cal ka is characterised by a high carbonate content (average sum of calcite and aragonite is ~36%), fine-grained sediments, absence of macrophytes, and relatively low siliciclastic component in the sediments (Fig. 3.3a and 3.3f) – all these characteristics point towards a rise in lake level, but the evaporative conditions persist. This apparent contradiction is linked to increasing summer insolation resulting in an increased meltwater inflow, coincident with higher summer evaporation (Fig. 3.3l). This is consistent with modern environment where the water chemistry data clearly shows that, unlike inflowing meltwater streams, the Mg/Ca ratio is high (>10) in lake waters and is suitable for authigenic aragonite precipitation (Mishra et al., 2014). Modern study of the lake sediments show aragonite percentages of up to 65% (Mishra et al., 2014). A short interval of decline in the authigenic calcite content, absence of aragonite, accompanied by an increased detrital influx (Fig. 3.3a and 3.3f) is seen between ca. 13.1-11.7 cal ka - this interval documents a freshening of the lake that could have been caused by a combination of stronger monsoon (first intensification) and increased meltwater inflow. There is a retreat to previous ([precipitation+meltwater=I]/evaporation=E) (I/E) following this short wet event.

The period between ca. 11.2-8.5 cal ka is characterised by a decline in precipitation of authigenic carbonates and higher detrital input resulting from increased meltwater inflow and runoff (Fig. 3.3a and 3.3f). We propose that this period corresponds to intensified Indian summer monsoon, synchronous with an increase in meltwater inflow that resulted in freshening of the lake (highest I/E in the studied interval) and increased influx of siliciclastics during the early Holocene warming. Summer rains would have decreased the evaporation efficiency resulting in lower lake water salinity. Subsequently, the period between 8.5-5.5 cal ka was characterised by the re-appearance of authigenic calcite which resulted from a decrease in freshwater (monsoon?) inflow and a shift in hydrological balance to lower I/E (Fig. 3.3f).

After ca. 5.5 cal ka there is a further reduction in detrital input coincident with an increase in calcite precipitation that reaches a stable maxima around 3.7 cal ka (Fig. 3.3a and 3.3f) that persists until 2.7 cal ka when aragonite re-appears. This indicates a decreased but largely stable inflow between 5.5-2.7 cal ka, in combination with high

evaporation, caused an increase in Mg/Ca favouring aragonite precipitation. From 2.7 cal ka to present, the conditions largely remain similar to today.

Summarising, the authigenic carbonates provide qualitative information on the I/E ratio in the lake. This, in combination with sedimentological and mineralogical data enables identification of the following hydrological stages in the study area. Stage I: period of lake establishment (ca. 728-585 cm; >20.2 cal ka) – increased coarse-grained detrital input with high mineralogical variability indicating a shallow lake level. Relatively low values for authigenic carbonates are linked to the cooler conditions during the glacial period; Stage II: deepening of the lake (ca. 585-425 cm; 20.2-16.4 cal ka) – characterised by climate amelioration and the growth of macrophytes; Stage III: rising lake level caused by increased meltwater input in an evaporative regime resulting in an increase in carbonate precipitation (ca. 425-310 cm; 16.4-11.2 cal ka); Stage IV: high lake levels during the early Holocene wet phase (ca. 310-197 cm; 11.2-8.5 cal ka) – characterised by absence of aragonite and low authigenic calcite. The high fine-grained, detrital content and low mineralogical variability likely relates to increased surficial erosion and pelagic sedimentation in a deep lake. The high input of detrital matter is likely caused by surficial erosion during an intensified summer monsoon; Stage V: mid Holocene climate deterioration (ca. 197-168 cm; 8.5-5.5 cal ka) – gradual weakening of summer monsoon with reduced detrital influx and decreasing I/E; Stage VI: (168-84.5 cm; 5.5-2.7 cal ka) -lower, but stable I/E with reduced surficial erosion and calcite maxima; Stage VII: onset of present day conditions (ca. 84.5-0 cm; 2.7-0 cal ka) – marked by a further decrease in lake level (lower I/E) indicated by the onset of aragonite precipitation that continues until today.

3.5.4. Regional comparison of hydrological changes (westerlies derived snow melt vs Indian monsoon)

In the following, we compare the reconstructed hydrological changes (I/E) from Lake Tso Moriri with other continental and marine records from the westerlies and Indian monsoon domains.

The Tso Moriri sediments before 20.2 cal ka are characterised by high detrital input and low authigenic carbonate precipitation indicating colder climate and deposition in a shallow lake. Only a few climate records are available from the Indian summer monsoon and mid-latitude westerly domains for this interval. These records indicate

cooler and drier climatic conditions are related to a weakened summer monsoon during insolation minima (An et al., 1991; Berger and Loutre, 1991; Herzschuh, 2006; Rashid et al., 2011).

The period between ca. 20.2-16.4 cal ka in Lake Tso Moriri shows climate amelioration with conditions favourable for shallow lacustrine sedimentation coincident with increasing insolation (Fig. 3.3l). Following the termination of the glacial maxima, the warming resulting from a steadily increasing insolation was sufficient to trigger an enhanced meltwater inflow into the lake (Zhang and Mischke, 2009). The climate amelioration inferred from our record is in line with several reconstructed palaeo-records from the Tibetan Plateau (e.g., Herzschuh, 2006; Zhang and Mischke, 2009).

In Lake Tso Moriri, the period between ca. 16.4-11.2 cal ka is marked by increased meltwater inflow, though evaporation remains dominant factor influencing the I/E. This interval of drier climate in Lake Tso Moriri is in agreement with palaeoclimate data from the NW-Himalaya, Tibetan Plateau (Herzschuh, 2006; Demske et al., 2009) and the Bay of Bengal (Rashid et al., 2011). However, within this interval there is a short-term wetter phase during ~13.1-11.7 cal ka marked by increased detrital influx and absence of aragonite. Many records from the monsoonal central Asia demonstrate that the first strong intensification of the Asian monsoon circulation took place at the beginning of the interval broadly coincident with the Bølling/Allerød warm period (Zhou et al., 1999; Herzschuh, 2006). In view of the limited dates and reservoir correction uncertainties associated with our record, a detailed regional correlation of short-term events is not possible at this stage (see also section 3.5.1). However, we note that the succession of events (older to younger): wetter (13.1-11.7) - drier (11.7-11.2 cal ka) – early Holocene wet phase (11.2-8.5 cal ka) could be correlatable with Bølling/Allerød (wetter)–Younger Dryas (drier)-early Holocene (wetter) periods.

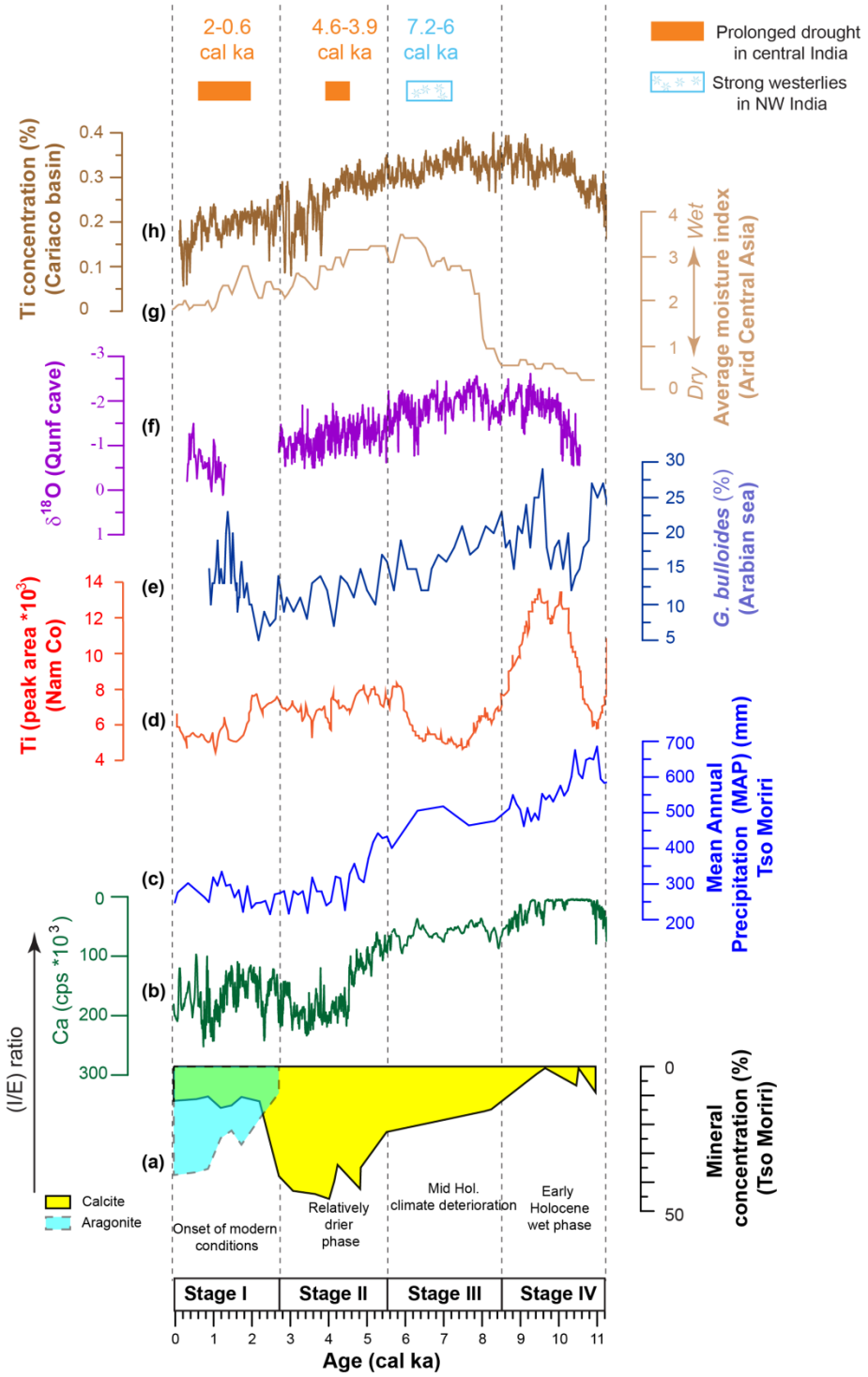

Fig. 3.4: Regional comparison of Tso Moriri climate data with other palaeoclimatic records: (a) Authigenic mineral % (aragonite and calcite) of Tso Moriri core profile, (our study); (b) µ-XRF profile of calcium (in cps) of core sediment (our study); (c) Tso Moriri mean annual precipitation (MAP), inferred from pollen data (based on our chronology), (Leipe et al., 2014a); (d) Nam Co Lake, Tibet (Döberschütz et al., 2014); (e) Concentration of G. bulloides from Arabian Sea (Gupta et al., 2003); (f) $\delta^{18}O$ records from Qunf cave, Oman (Fleitmann et al., 2003); (g) Average moisture index inferred from several palaeo-records from arid central Asia (Chen et al., 2008); (h) Cariaco Basin, Ti record indicating changing terrestrial runoff (Haug et al., 2001).

The onset of the wettest interval in the Tso Moriri record at ca. 11.2 cal ka coincides with the summer monsoon intensification resulting from the northward shift of the intertropical convergence zone (Haug et al., 2001) (Fig. 3.4h) that resulted in increased runoff and the higher detrital influx into the lake. The monsoon precipitation also changed the I/E balance, resulting in reduced authigenic carbonate precipitation. This shift towards intensified monsoon is synchronous with the vegetation shift (increase in *Artemisia*/Chenopodiaceae ratio) and increased moisture in the catchment of Lake Tso Moriri and Lake Tso Kar (Demske et al., 2009; Leipe et al., 2014a) (Fig. 3.4c). This timing of onset of the wet phase in Lake Tso Moriri is also largely comparable with the palaeoclimate records from the Tibetan Plateau (Van Campo and Gasse, 1993; Herzschuh et al., 2006; Mischke and Zhang, 2010; Dietze et al., 2013; Döberschütz et al., 2014) (Fig. 3.4d). The early Holocene monsoon intensification is also in agreement with central India (Prasad et al., 2014), the Arabian Sea (Sirocko et al., 1993; Fleitmann et al., 2003; Gupta et al., 2003) (Fig. 3.4e and f), the Indus catchment (Limmer et al., 2012), and the Bay of Bengal records (Govil and Naidu, 2011; Rashid et al., 2011). The increase in precipitation ca. 11.2 cal ka in Lake Tso Moriri coincides with the summer insolation maximum at 30°N (Fig. 3.3l). Our data provides further evidence that changes in solar insolation, that caused the northward shift of the intertropical convergence zone, have been the primary trigger for the early Holocene monsoon intensification. We exclude the possibility of intensified westerlies during the early Holocene as the records from westerlies influenced arid central Asia (Fig. 3.4g) (Chen et al., 2008) indicate that the lakes in the westerly influenced regions were dry or were very shallow before 8 cal ka.

In Lake Tso Moriri, the period after 8.5 cal ka was characterised by an increase in calcite precipitation indicating decreasing I/E, coincident with decreasing solar insolation and the southward movement of the intertropical convergence zone (Haug et al., 2001). The gradual weakening of the summer monsoon precipitation in Lake Tso Moriri beginning ca. 8.5 cal ka is in phase with available regional data (Van Campo and Gasse, 1993; Van Campo et al., 1996; Demske et al., 2009; Dietze et al., 2013). However, in the period after 8 cal ka, the intensified westerlies influence in arid central Asia (Chen et al., 2008) does not appear to have made a strong impact in the NW-Himalayas (Fig. 3.4g). Also, stronger westerlies between 7.2-6 cal ka in NW India (Enzel et al., 1999; Prasad and Enzel, 2006), and between 6-4 cal ka in the regions north (central Asia) of Tso

Moriri (Wang et al., 2010), did not have a strong impact in the Tso Moriri region indicating spatio-temporal variability in precipitation seasonality (Fig. 3.4). Interestingly, the short-term events reported from peninsular India e.g., the 4.2 ka event from NW and central India (Anoop et al., 2013b; Dixit et al., 2014), or the impact of prolonged Indian summer monsoon droughts, seen in the central India (Prasad et al., 2014), was not felt in the Himalayan region probably because of (i) the southward shift of the intertropical convergence zone had already limited the impact of monsoon weakening on the regional hydrology; and/or (ii) the attenuating impact of westerlies and continuing meltwater inflow.

The decrease in I/E in the Lake Tso Moriri is correlatable with the other records from the Tibetan Plateau (Mischke and Zhang, 2010; Dietze et al., 2013), NW-Himalaya (Demske et al., 2009; Leipe et al., 2014a), NW India (Enzel et al., 1999; Prasad and Enzel, 2006) and central India (Anoop et al., 2013b). In Lake Tso Moriri, the final lower I/E value characterised by the presence of aragonite sets in ca. ~2.7 cal ka and is synchronous with the glacier advancement in the Kurzok valley (~3.6±1.1 ka) (Hedrick et al., 2011), indicating strongly reduced meltwater input (I/E) in the lake.

3.6. Conclusions

- The geochemical, mineralogical and sedimentological investigations on Lake Tso Moriri core reveal orbital forcing on hydrology (I/E) since ~26 cal ka.
- Evaporative enrichment was a forcing factor for authigenic carbonate (aragonite and calcite) precipitation within the lake and can be used to infer past hydrological variability (I/E) in the region.
- We have identified the following stages in Lake Tso Moriri - Stage I: period of lake establishment (>20.2 cal ka); Stage II: deepening of the lake (20.2-16.4 cal ka); Stage III: rising lake levels (16.4-11.2 cal ka); Stage IV: early Holocene wet phase (11.2-8.5 cal ka); Stage V: mid Holocene climate deterioration (8.5-5.5 cal ka); Stage VI: relatively lower but stable I/E, detrital input decreases indicates reduced surficial erosion (5.5-2.7 cal ka); Stage VII: onset of modern conditions (2.7-0 cal ka).

  The reconstructed hydrological changes in Lake Tso Moriri are largely insolation forced and are correlatable with regional records during the early Holocene. However, they show significant differences with other records from peninsular

India during the late Holocene, most likely related to different forcing mechanisms governing regional hydrology.

- Except during the early Holocene when the Indian summer monsoon played a major role in higher I/E, the hydrological budget of Lake Tso Moriri has largely been controlled by meltwater inflow.

3.7. Acknowledgements

This project is being funded by the DeutscheForschungsGemeinschaft under the coordinated programm “Himalaya: Modern and Past Climates” (HIMPAC, FOR 1380). The Tso Moriri coring and field expeditions have also received financial and logistic support from the Deutsches GFZ Potsdam, the Kashmir University, and the Indian Institute of Geomagnetism. We are grateful to S. Pinkerneil, B. Shehzad, C. Leipe, B. Wünnemann for their help during the field work. The hard work invested by R. Niederreiter, D. Niederreiter and M. Köhler for raising the core is gratefully acknowledged. Special thanks to E. Dietze for the useful discussion and suggestions during the manuscript writing. We also thank to B. Zimmerman and Mrs U. Kegel for assistance in the laboratory. The scanning XRF data was provided by Dr. P. Dulski. The help extended by the Jammu & Kashmir Wildlife Department during the coring programme, especially by the Chief Wildlife Warden and Regional Wildlife Warden, Leh and their field staffs at Tso Moriri Lake is gratefully acknowledged.

Table

Table 3.1: Radiocarbon dates for the samples from Tso Moriri composite profile (TMD). Calibaration was performed using online version of OxCal 4.2 calibaration program (Bronk Ramsey, 2008; Reimer et al., 2013) (M1: Modern plant from the lake; TM 4: Terrestrial plant fragment)

^{14}C sample name	**Sample code**	**Bulk/Organic material (OM)**	**Composite depth (cm)**	**^{14}C age (yr)**	**Reservoir corrected age ^{14}C age (yr)**	**Calibrated reservoir corrected ^{14}C age (cal a)**
Modern plant	M1	Modern plant	n.a.*	741±40	n.a*	n.a*
TM-10	TM 1	Bulk	0	3319±35	0	-61
TMD-1 (0-1)	TM 2	Bulk	6	3800±35	481±35	521±21
TMD1 (47.5-47.8)	TM 3	Bulk	53.2	5050±40	1731±40	1643±51
TMD-3 (30.5)	TM 4	Twig**	171	4920±35	4920±35	5648±37
TMD-3 (48-49)	TM 5	Bulk	189	10780±100	7461±100	8266±98
TMD-8 (32.3-32.6)	TM 6	Bulk	390.5	14590±80	11271±80	13141±77
TMD-9(31.4)	TM 7	OM	440.5	15420±80	14679±80	17860±113
TMD-9(39.8)	TM 8	OM	448.9	15490±80	14749±80	17947±115
TMD-10 (12.8-13.4)	TM 9	OM	459.9	15560±90	14819±90	18034±123
TMD-10 (40)	TM 10	OM	486.8	15620±80	14879±80	18097±113
TMD-10 (45)	TM 11	OM	491.8	15670±80	14929±80	18148±114
TMD-11 (75.7-76)	TM 12	Bulk	560.2	19160±110	15841±110	19123±146
TMD-15(5-6)	TM 13	Bulk	671.7	23250±170	19931±170	23981±211

*n.a. Not applicable

**Reservoir correction is not required for twig of terrestrial origin

Chapter 4: Carbonate isotopes from high altitude Tso Moriri Lake (NW Himalayas) provide clues to late glacial and Holocene moisture source and atmospheric circulation changes

***Praveen K. Mishra*[1]**, *Sushma Prasad* [2], *A. Anoop*[3], *B. Plessen*[1], *A. Jehangir*[4], *B. Gaye*[5], *Philip Menzel* [5], *S. M. Weise* [6], *A.R. Yousuf* [4]

[1] *Helmholtz Centre Potsdam GFZ German Research Centre for Geosciences, Potsdam, Germany*
[2]*Institute for Earth- and Environmental Science, University of Potsdam, Karl-Liebknecht-Straße 24-25, 14476 Potsdam, Germany*
[3]*Indian Institute of Science Education and Research, Kolkata, India*
[4]*Limnology and Fisheries Laboratory, Centre of Research for Development, University of Kashmir, India*
[5]*Universität Hamburg, Institute of Biogeochemistry and Marine Chemistry, Hamburg, Germany*
[6]*UFZ Helmholtz Centre for Environmental Research, Dept. Catchment Hydrology, Halle, Germany*

Manuscript status: Published in Palaeogeography, Palaeoclimatology, Palaeoecology. DOI: http://dx.doi.org/10.1016/j.palaeo.2015.02.031

Abstract

High resolution isotopic ($\delta^{18}O$ and $\delta^{13}C$) investigations on endogenic carbonates (calcite/aragonite) from Tso Moriri Lake, NW Himalaya show dramatic fluctuations during the late glacial and the early Holocene, and a persistent enrichment trend during the late Holocene. Changes in this lake are largely governed by the [input (meltwater+monsoon precipitation)/evaporation] (I/E) ratio, also reflected in changes in the carbonate mineralogy with aragonite being formed during periods of lowest I/E. Using new isotopic data on endogenic carbonates in combination with the available data on geochemistry, mineralogy, and reconstructed mean annual precipitation, we demonstrate that the late glacial and early Holocene carbonate $\delta^{18}O$ variability resulted from fluctuating Indian summer monsoon (ISM) precipitation in NW Himalaya. This region experienced increasing ISM precipitation between ca. 13.1-11.7 cal ka and highest ISM precipitation during the early Holocene (11.2-8.5 cal ka). However, during the late Holocene, evaporation was the dominant control on the carbonate $\delta^{18}O$. Regional comparison of reconstructed hydrological changes from Tso Moriri Lake with other archives from the Asian summer monsoon and westerlies domain shows that the intensified westerly influence that resulted in higher lake levels (after 8 cal ka) in central Asia was not strongly felt in NW Himalaya.

Key words: Carbonates; Holocene; Indian summer monsoon; Isotopes, Tso Moriri Lake

4.1. Introduction

The Indian summer monsoon (ISM) is an important branch of the Asian monsoon and today governs the livelihood of more than a billion people over a variety of timescales. Long palaeo-reconstructions for ISM are available only from the marine sediments (Schulz et al., 1998; Govil and Naidu, 2011) and do not always coincide with the reconstructed continental hydrological maxima, which show significant spatiotemporal variability related to precipitation seasonality and evaporation (e.g., Prasad and Enzel, 2006). The situation is particularly complicated in the Himalayan region where some of the largest reservoirs of freshwater are stored. The precipitation in this region is provided by both the winter westerlies and ISM (Benn and Owen, 1998; Anoop et al., 2013a; Leipe et al., 2014a). Though the relative influence of these moisture pathways has shown considerable variations in intensity and spatial extent in the past (e.g., Herzschuh, 2006; Chen et al., 2008; Demske et al., 2009; Mishra et al., 2015), the contribution of such fluctuations in the Himalayan region is not yet well documented.

Here we focus on the high altitude, pristine Tso Moriri Lake in the NW Himalaya (Fig. 4.1). The lake is little influenced by the anthropogenic activity making it a key site to understand past hydrological and climate variability. In this study we explore the possibility of using the isotopic data from the endogenic carbonates found in the upper 4.15 m (ca. 15.5 cal ka) of a 7.28 m long core, in combination with previously available sedimentological, mineralogical (Mishra et al., 2015) and pollen data (Leipe et al., 2014a), to infer late glacial and Holocene changes in ISM precipitation in this high altitude cold desert.

4.2. Study area

Tso Moriri is one of the largest high altitude lakes situated in the eastern part of Ladakh region (78°14'-78°25'E and 32°40'-33°02'N, 4600 m.a.s.l) with a N-S extension of 27 km and E-W extension of 5-7 km. The catchment area (~2,350 km^2) of the Tso Moriri Lake is dominated by mainly schist, gneisses and boudins of eclogite bearing Puga gneiss complex, Proterozoic to Cambrian metasediments, intrusive granitic body (Rupshu granite) and marine Tethys sediments (Fuchs et al., 1996; Steck et al., 1998; Steck, 2003; de Sigoyer et al., 2004; Singh et al., 2013) (Fig. 4.1). Annual precipitation in the Tso Moriri region is <250 mm (http://indiawaterportal.org/met_data/).

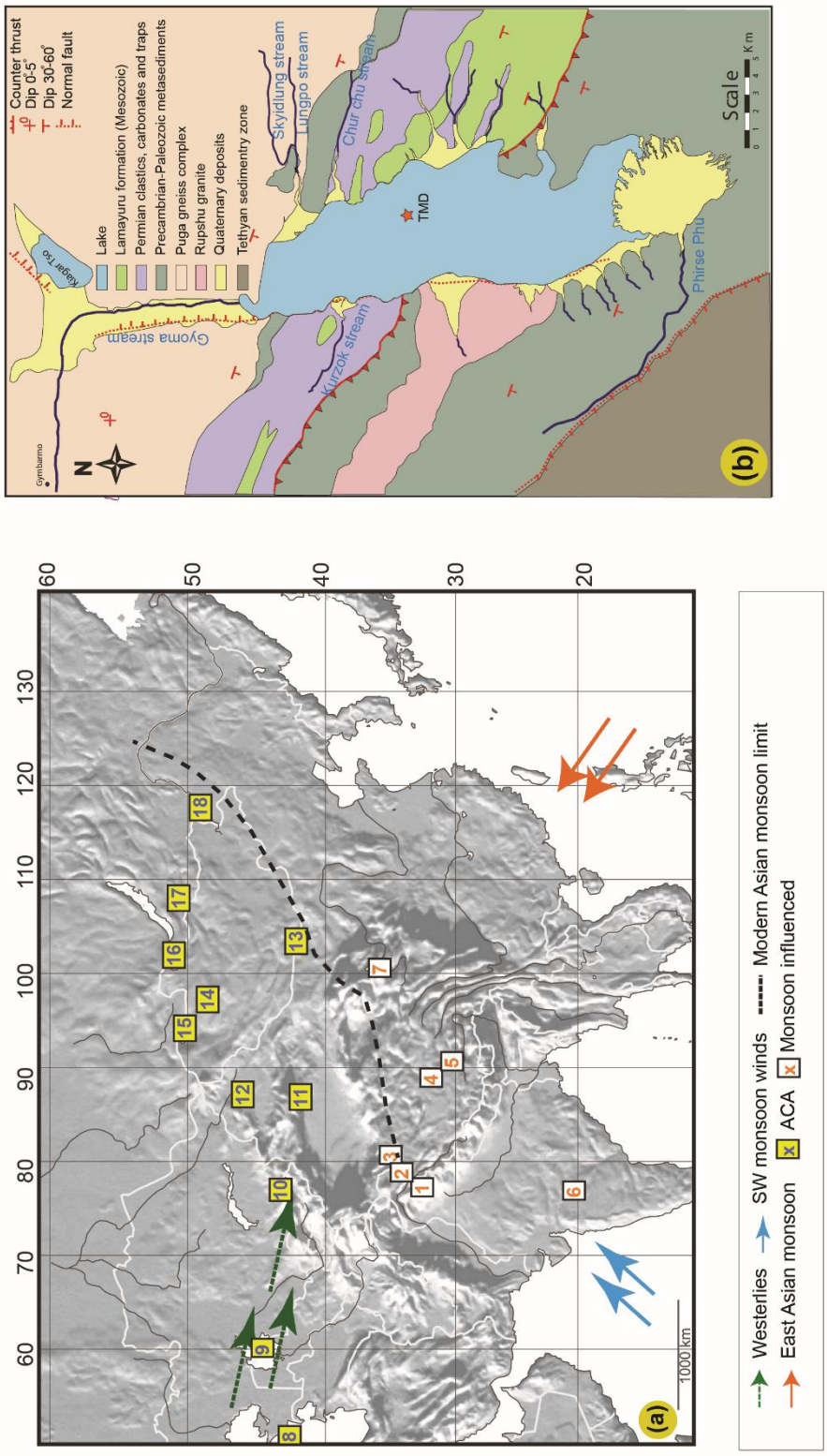

Fig. 4.1: (a) Overview map showing the sites selected in this study from arid central Asia (ACA) (yellow squares) and monsoonal Asia (white squares), and the dominant wind regimes. Dashed line indicates the modern monsoon limit (Chen et al., 2008). Sites influenced by both westerlies and ISM are (1) Tso Moriri (this study); (2) Sumxi Co; (3) Bangong Co; (4) Nam Co; (5) Selin Co. Lonar Lake (6) is influenced only by the ISM. Quinghai Lake (7) is influenced both by the East Asian Monsoon (EASM) and the westerlies. ACA sites used to develop the ACA index (Chen et al., 2008) shown in Figure 5 are numbered as (8) Caspian Sea; (9) Aral Sea; (10) Issyk Kul; (11) Bosten Lake; (12) Wulun Lake; (13) Juyan Lake; (14) Telmen Lake; (15) Bayan Nuur; (16) Hovsgol Nuur; (17) Gun Nuur; (18) Hulun Nuur. (b) Geological map of Tso Moriri Lake with the location of the long (TMD) core.

4.2.1. Hydrology and hydrochemistry

The maximum lake water depth is ca. 105 m. The lake is fed by a number of small glacier streams with the major streams Gyoma in the north, Phirse Phu stream in the south and the Korzong Chu in the west. Because the lake presently has no permanent outlet the lake level is governed by the balance between evaporation and inflow from precipitation, as well as long and short-term changes in melt water discharge from snow and glaciers during the summer months (De Terra and Hutchinson, 1934; Srivastava et al., 2013). Modern investigations using ICESat/GLAS (The Ice Cloud and Land Elevation Satellite carrying the Geoscience Laser Altimeter System) reveal that Tso Moriri Lake level was falling at the rate of 0.119 m/y during 2003-2009 AD (Srivastava et al., 2013) due to higher evaporation (Lesher, 2011). A large alluvial fan to the south limits the lake level (Leipe et al., 2014b), and a former outlet in the south has been reported by Gujja et al., (2003) and Panigrahy et al., (2012). This, combined with the facts that Tso Moriri is not a saline lake and a higher palaeoshoreline exists ca. 7 m above the present lake level (Leipe et al., 2014b), suggests that the past lake level could have been affected either through overflow or groundwater loss.

In the study area (Fig. 4.2), the westerlies derived snow has $\delta^{18}O$ and δD values of -16‰ and -120‰ respectively. The melt water streams show average $\delta^{18}O$ and δD values of -16.6‰ and -122‰, similar to the snow, indicating derivation from snow melt. In summer the $\delta^{18}O$ and δD of lake waters is ca. -3‰ and -49‰. Similar trends (Fig. 4.2) are also seen in other high altitude Tibetan lakes in this region (Bangong Co, Sumxi Co, and Longmu Lake) indicating significant evaporative enrichment in response to the atmospheric dryness (Gasse et al., 1991; Fontes et al., 1993; Fontes et al., 1996). The isotopically enriched rainwater samples from the study area follow the global meteoric water line (GMWL), whereas snow and lake water display highly depleted values (Fig. 4.2).

Hydrochemistry of feeder springs (Mishra et al., 2014) shows that the lithology of the catchment area controls the water ionic and isotopic composition, whereas evaporation processes control the lake water chemistry. Although the inflowing waters are low in Mg/Ca (<1), the lake waters in summer show average Mg/Ca value of 10 (Mishra et al., 2014) which is conducive to the precipitation of endogenic aragonite.

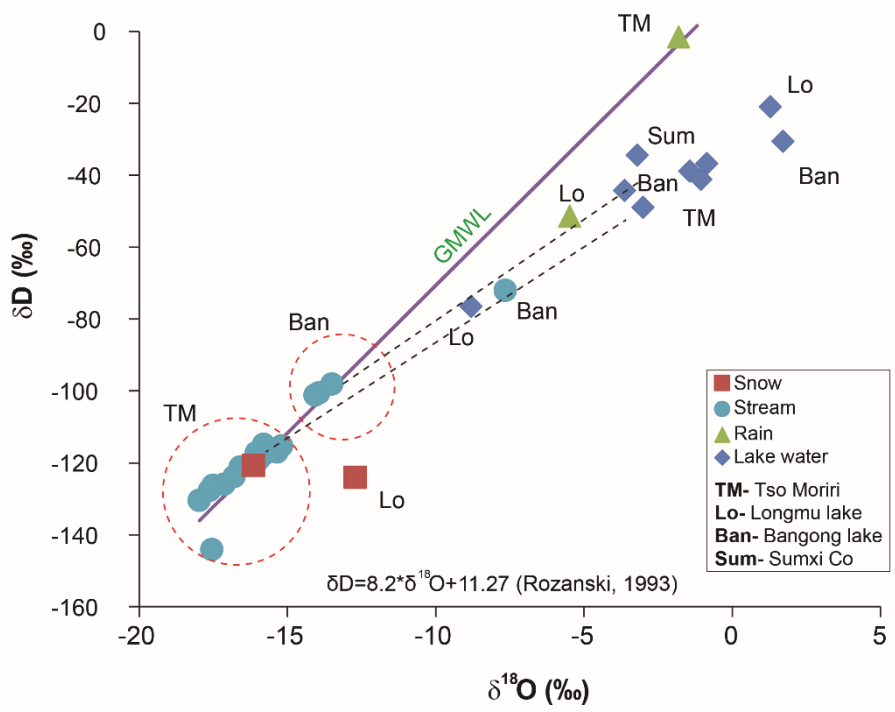

Fig. 4.2: Compiled hydroisotopic data from Tso Moriri (Mishra et al., 2014); Longmu Lake (Fontes et al., 1993); Bangong Lake (Fontes et al., 1996); Sumxi Co Lake (Gasse et al., 1991). The lake waters show evaporitic enrichment in response to the atmospheric dryness. The snow and rain data are from isolated events.

4.2.2. Core description and chronology

A ca. 7.28 m long core (TMD) was raised from the Tso Moriri Lake at a water depth of 105 m and radiocarbon dated (Mishra et al., 2015). A summary of these results is presented here. The bottom (7.28-4.71 m) part of the core is sandy with intervening occasional visible macrophyte remains, and is overlain by clayey sediment (4.71-4.25 m) rich in visible macrophyte fragments deposited in a shallow lake (Mishra et al., 2015). The remaining part of the core (4.25-0 m) contains largely calcareous clay with variable degree of lamination deposited in a deep lake. Absent or limited endogenic carbonates between 3.10-1.97 m (11.2-8.5 cal ka, Figure 4.3) indicates lowest salinity and highest I/E. For this study we have focused only on the upper 4.15 m of the core that contains endogenic carbonates (Fig. 4.3) identified using a combination of XRD, selected thin sections, and inter relationships between geochemical parameters (Mishra et al., 2015). Investigations on modern sediments indicate since the carbonates are formed by evaporative processes, their occurrence and isotopic values can be used as indicators of I/E changes in the lake (Mishra et al., 2014).

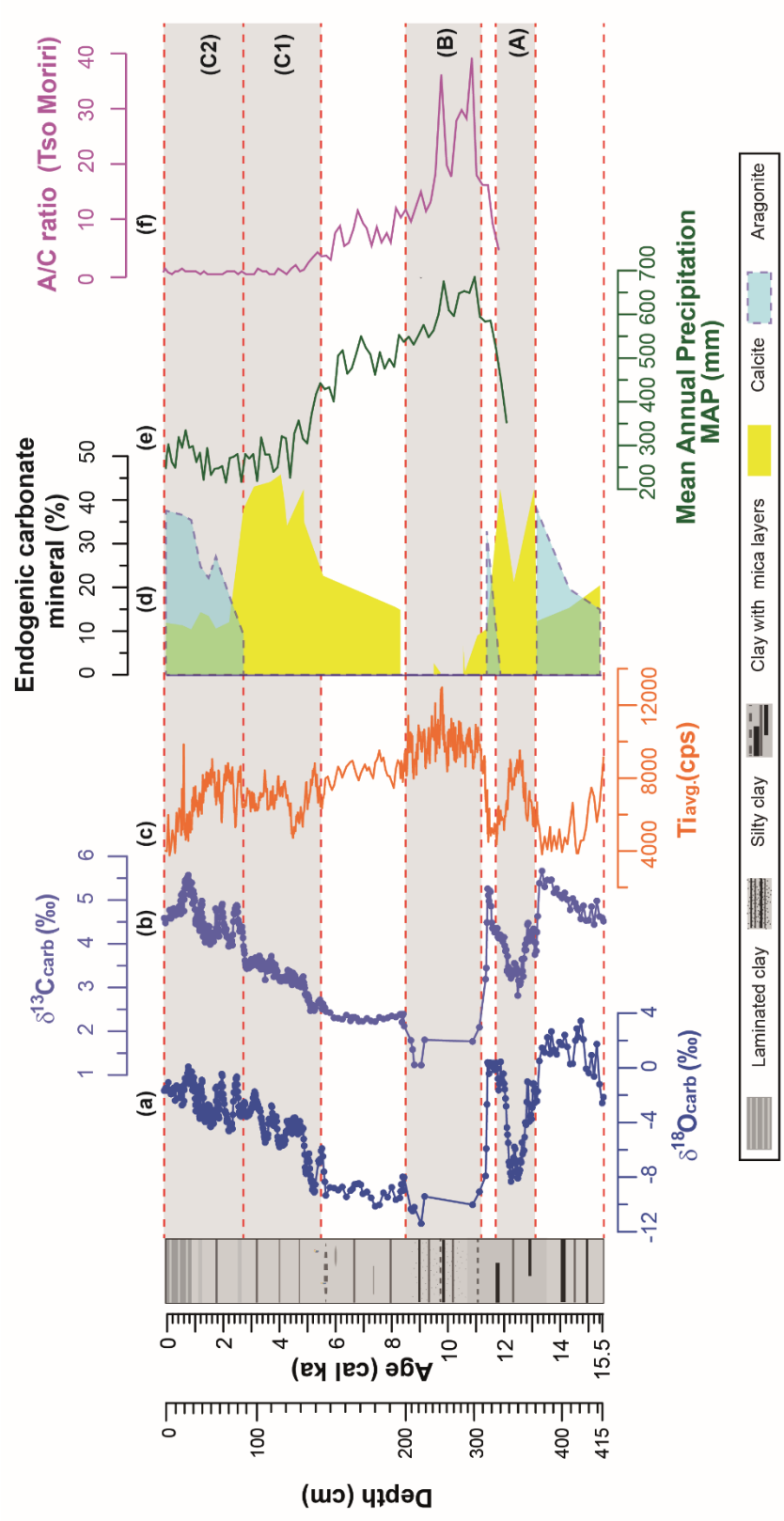

Fig. 4.3: Carbonate isotope (this study) (panels a, b), geochemical (c), mineralogical (d) (Mishra et al., 2015), reconstructed MAP (e), and pollen (f) data (Leipe et al., 2014a) from the Tso Moriri core. Artemisia/Chenopodiaceae (A/C) values in arid and semi-arid environments are linked to increased moisture availability (Leipe et al., 2014a). Progressive decrease in I/E results in the formation of evaporative calcite followed by aragonite (panel d) in response to an increase in Mg/Ca of lake waters. Green areas indicate where both calcite and aragonite are present. $\delta^{18}O$ shows enrichment (depletion) during intervals with lower (higher) I/E. The horizontal grey bars indicate prominent intervals (A, B, C1 and C2) of isotopic changes in the Tso Moriri core.

The core chronology is based on radiocarbon dating of reservoir corrected bulk organic matter and macrophyte plant remains, and terrestrial fragments (Mishra et al., 2015). The radiocarbon dates were converted into calendar age using INTCAL 13 calibration curve (Reimer et al., 2013) and linear interpolation was used to determine dates of intervening samples. The core top (0-1) has been confirmed to be modern using ^{137}Cs dating method (Mishra et al., 2014).

Due to the variable detrital content (Mishra et al., 2015) the reworked organic content could have varied in the past and the "reservoir correction" may not have remained unchanged. Therefore, the age model used here can only be considered as accurate on millennial scale and not be used for detailed correlation of short-term events.

4.2.3. Core mineralogy and pollen data

The positive correlation between Al, K and Fe with Ti (r = 0.80, 0.88, 0.82 respectively) for the entire (7.28 m) continuous µ-XRF data set of TMD (Mishra et al., 2015) indicates that Ti can be considered to be representative of the bulk siliciclastic input. In the upper 4.15 m of the core there is a strong inverse correlation between Ca and Ti (r=-0.83) that, in combination with the mineralogical data, indicates an endogenic origin for the carbonates. In an evaporative lake, calcite is the first carbonate mineral to precipitate in the course of evaporative enrichment (Eugster and Hardie, 1978). With progressive evaporation, aragonite begins to precipitate in response to an increase in the Mg/Ca ratio (Morse et al., 1997) indicating reduced input (I) (inflow+precipitation) and increased evaporation (E) i.e. (I/E).

Leipe et al., (2014a) have shown that higher *Artemisia* percentages in the pollen spectra and higher *Artemisia*/*Chenopodiaceae* (A/C) values in arid and semi-arid environments are linked to increased moisture availability. Based on this a mean annual precipitation (MAP) curve for the Holocene from the Tso Moriri Lake has been reconstructed by Leipe et al., (2014a) using the relationship between the A/C ratio and mean annual precipitation derived from the dataset from New et al., (2002) (Fig. 4.3).

4.3. Methodology

4.3.1. Analytical methods

The core was sub-sampled in the laboratory at a continuous interval of 0.5 cm until a depth of 3.25 m (average sampling resolution ca. 20 years between 0-11.6 cal ka) and subsequently at an interval of 1cm until 4.15 m (average sampling resolution ca. 50 years between 11.6-15.5 cal ka).

The stable isotope ($\delta^{13}C_{carb}$ and $\delta^{18}O_{carb}$) compositions of bulk carbonates (calcite and/or aragonite) were determined in continuous flow mode using a Finningan GasBenchII with a carbonate option coupled to a DELTAplusXL mass spectrometer at the GeoForschungsZentrum Potsdam. From each sample, depending on carbonate content, 200 to 1000 mg was loaded into 10-mL Labco Exetainer vials. After automatically flushing with He, the carbonate samples were reacted with phosphoric acid (100%) at 75˚C for 60 min, following the analytical procedure described by Spötl and Vennemann (2003). The isotope compositions were given relative to the VPDB standard in the conventional delta notation, and were calibrated against two international reference standards (NBS19 and NBS18). The standard deviation (1 sigma) for reference analyses was ±0.06‰ for $\delta^{13}C$ and ±0.08‰ for $\delta^{18}O$.

4.4. Results

4.4.1. Late glacial and Holocene changes in carbonate isotopic composition and siliciclastic influx

The stable isotope composition of bulk carbonates of the core sediment ranges from +2.1 to +5.7‰ (average ca. +3.9‰) for $\delta^{13}C_{carb}$, and -10.1 to +3.4‰ (average ca. -3.6‰) for $\delta^{18}O_{carb}$. The $\delta^{13}C_{carb}$ and $\delta^{18}O_{carb}$ show a strong correlation (r=0.89) for the investigated upper 4.15 m of the core where endogenic carbonates are present.

Plots (Figs. 4.3 and 4.4) of the isotope ($\delta^{13}C_{carb}$ and $\delta^{18}O_{carb}$) data together with the siliciclastic (Ti, indicator of inflow, Mishra et al., 2015), endogenic carbonate (indicator of lower I/E, Mishra et al., 2015), and pollen (A/C) reveal interesting patterns. While the broader phases of lake evolution inferred from endogenic mineral data (increasing carbonates and appearance of aragonite indicating progressively lower I/E and vice versa) are also reflected in isotopic enrichment, the isotopic data shows high amplitude changes (up to 10‰ for $\delta^{18}O$, and 5‰ for $\delta^{13}C$) that are abrupt during the late glacial and early Holocene but gradual during the late Holocene (Fig. 4.3). Highest

siliciclastic (Ti) influx is seen between 13.1-11.7 cal ka and early Holocene (11.2-8.5 cal ka). Generally, the trends in isotopic variability and siliciclastic influx are opposite with depleted $\delta^{18}O_{carb}$ intervals being characterised by higher Ti (Fig. 4.4). Interestingly, while the re-appearance of endogenic calcite ca. 8.8 cal ka indicates reduced I/E, this change is not unambiguously reflected in the $\delta^{18}O$. The reconstructed MAP (Leipe et al., 2014a), after an initial peak between 11.5-9 cal ka, shows a rather gradual reduction until 5.5 cal ka but low values thereafter (Fig. 4.3).

We identify the following prominent intervals (Figs. 4.3 and 4.4) of isotopic changes in the Tso Moriri core.

Interval A (13.1-11.7 cal ka): is characterised by endogenic calcite, absence of aragonite, and high siliciclastic influx. Though data points are limited, the $\delta^{18}O_{carb}$ is lower (-7‰) than the preceding interval. $\delta^{18}O_{carb}$ and $\delta^{13}C_{carb}$ show a high (0.91) correlation (Fig. 4.4).

Interval B (11.2-8.5 cal ka): is characterised by very low or absent endogenic carbonates, and high siliciclastic influx. Limited $\delta^{18}O_{carb}$ isotopic data show significantly depleted (upto 10‰) values compared to the preceding interval.

Interval C (5.5-0 cal ka): clearly differs from intervals A and B as the isotopic enrichment trend is gradual, coupled with decreasing siliciclastic influx, and increasing calcite percentages (interval C1) followed by the re-appearance of endogenic aragonite at ca. 2.7 cal ka (interval C2). Here too a strong correlation (0.89) between $\delta^{18}O_{carb}$ and $\delta^{13}C_{carb}$ is seen.

4.5. Discussion

4.5.1. Possible factors influencing the isotopic composition of the lacustrine carbonates

Contamination by detrital carbonates is a major concern in lakes with carbonate rich catchments, especially in the Tso Moriri region where carbonate rocks are exposed in the southern and eastern parts. However, our investigations on isotopic composition of catchment rocks (Mishra et al., 2014) clearly indicate that these, unlike the core sediments, show lower isotopic values (+1.6 to +0.1‰ for $\delta^{13}C_{carb}$ and -3.8 to -7.7‰ for $\delta^{18}O_{carb}$) as compared to the investigated core top (+4.6‰ for $\delta^{13}C_{carb}$ and -1.7‰ for $\delta^{18}O_{carb}$) indicating that the possibility of detrital carbonate contamination is low. In the investigated core sediments the strong correlation (0.89) between $\delta^{13}C_{carb}$ and $\delta^{18}O_{carb}$ suggests an evaporative origin in a closed basin (Talbot, 1990; Fontes et al., 1996; Leng

and Marshall, 2004). Additionally, the intervals (A and B) of most depleted isotopic values during the late glacial and early Holocene also coincide with reduced/absent carbonates (Fig. 4.3) further excluding any possibility of contamination by detrital carbonate.

Leipe et al., (2014b) have raised the possibility of outflow/overflow from the Lake Tso Moriri in Holocene and even recent times. The latter has not been confirmed by the authors' (AJ and ARY) observations in this region. As discussed in Section 2.1, either sporadic lake overflow and/or loss by groundwater leakage during the entire interval under consideration are likely. However, we note that the high correlation (0.89) between $\delta^{18}O$ and $\delta^{13}C$ records of endogenic carbonates (see section 4.1 above) clearly indicates that the loss did not affect the isotopic record.

4.5.2. Interpretation of isotopic signal from endogenic carbonates

The $\delta^{18}O$ and $\delta^{13}C$ records of endogenic carbonates can potentially provide palaeoenvironmental information about biological and hydrological changes (Stuiver, 1975; Leng and Marshall, 2004). The carbon isotopic composition of lacustrine carbonates is controlled by (i) variations in $^{13}C/^{12}C$ values of the dissolved inorganic carbon; (ii) CO_2 exchange between the atmosphere and the lake water (Whiticar et al., 1986; Talbot, 1990; Valero- Garcés et al., 1999); (iii) photosynthesis, which selectively removes ^{12}C, resulting in enrichment of ^{13}C in the dissolved inorganic carbonate. Since Tso Moriri is an oligotrophic lake (<2% total organic carbon for the upper investigated 4.15 m of core), we conclude that the role of phytoplankton productivity in influencing the isotopic composition of the $\delta^{13}C_{TDIC}$ is minimal.

The $\delta^{18}O$ of lake water (and endogenic carbonates formed therein) in closed lakes is controlled by the isotopic composition of inflowing water and precipitation (temperature-dependent $\delta^{18}O$ values in precipitation and continental effects related to moisture source history), altitude, and hydrological effects including evaporative enrichment (Talbot, 1990; Leng and Marshall, 2004; Yu et al., 1997; Hren et al., 2009). The $\delta^{18}O$ of aragonite is about 0.6‰ more positive than the $\delta^{18}O$ of calcite formed under same conditions (Land, 1980; Leng and Marshall, 2004).

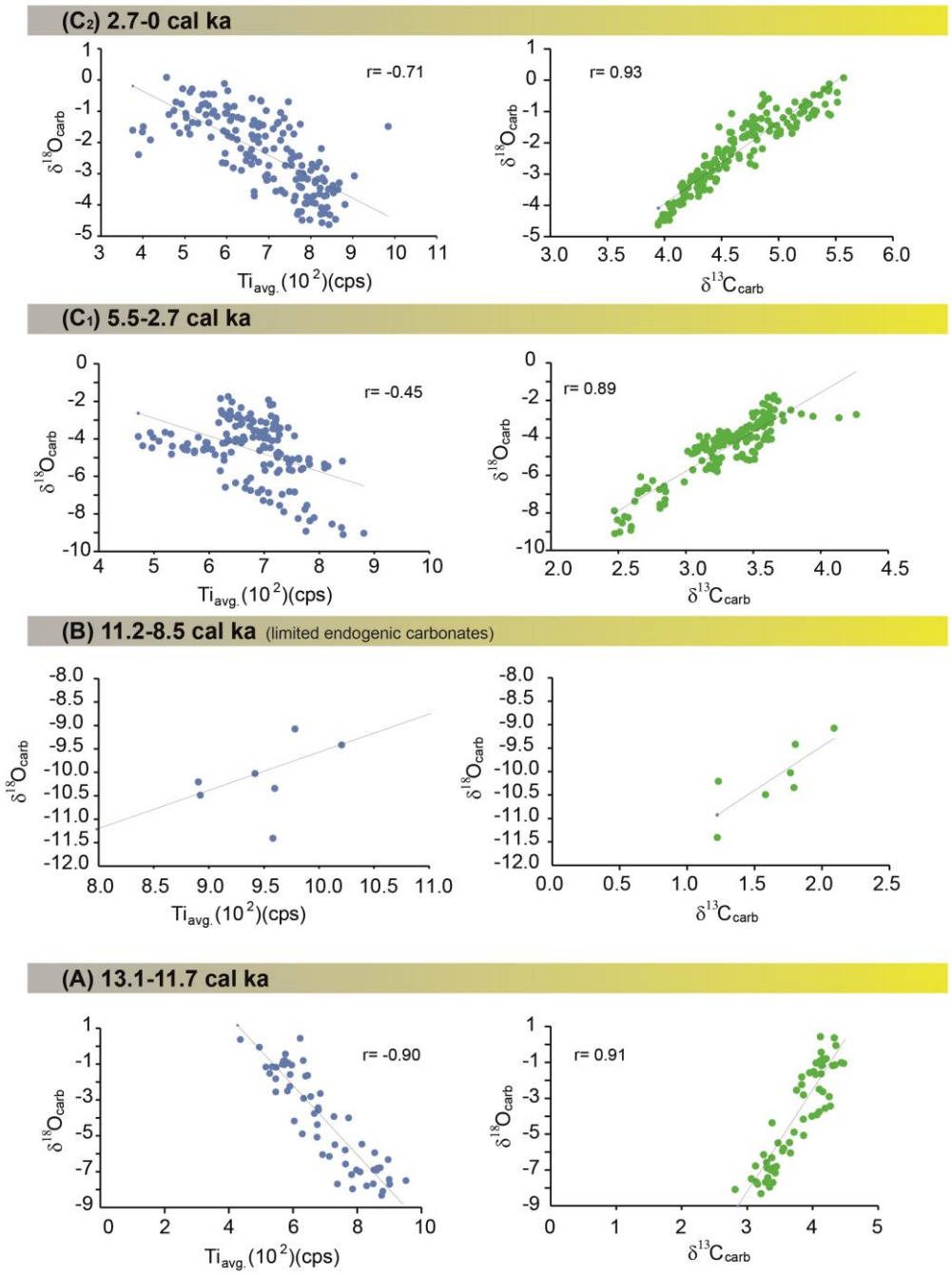

Fig. 4.4: Plots of $\delta^{18}O$ (a) and $\delta^{13}C$ (b) for carbonates from Tso Moriri core show correlation in interval A, C1 and C2 indicating evaporative origin. The intervals A, C1 and C2 also show inverse covariance between $\delta^{18}O$ and Ti (c) indicating that stronger ISM (depleted $\delta^{18}O$) is also accompanied by increased surficial erosion (higher Ti). Carbonates (d) were largely absent in interval B resulting in limited data.

The amplitude (upto 12‰ for $\delta^{18}O$ and 5‰ for $\delta^{13}C$) of isotopic changes in Tso Moriri core sediments during the past 15.5 cal ka could be due to (i) changes in temperature; (ii) different sources of precipitation; and/or (iii) changing I/E (Fontes et al., 1996; Wei and Gasse, 1999; Leng and Marshall, 2004).

In the high altitude Himalayan region, the temperature effect cannot be completely

excluded over the time scales under discussion. Indeed, temperature has been considered to be the major source of isotopic variability in the Dunde Ice Cap in the Qilian Shan and the Guliya glacier in the West Kunlun Mountains (Thompson et al., 1997). However, temperature changes cannot singly explain the magnitude of changes in the Tso Moriri record. General circulation model (GCM) simulations (Kutzbach and Guetter, 1986) indicate a warming of ca. 3-5^{o}C between 15-9 ka in the Tibetan Plateau. Assuming an average $\delta^{18}O$ -ground temperature coefficient of ca. 0.6‰/^{o}C (Van der Straaten and Mook, 1983), this warming coincides with an isotopic shift of about +2 to +3‰ in precipitation (Wei and Gasse, 1999) which would also be amplified by higher evaporation during warmer periods. On the contrary, in the Tso Moriri record, a depletion of ca. 8 to 10‰ is seen in this interval.

Since the temperature and mineralogical effects are minor (temperature-dependent aragonite–water and calcite–water fractionations are similar (0.24‰/°C; Epstein et al., 1953), changes in isotopic composition could have been singly or jointly caused by changing sources, and/or hydrological balance (I/E). On the times scales under consideration, monsoon strengthening should also be considered in the changing isotopic composition of meteoric water.

4.5.3. Late glacial and Holocene changes in source water

A comparison of the isotopic composition of the snow, stream melt water, modern ISM precipitation, and the lake waters clearly indicates that the glacial melt is the dominant source of water in the modern Tso Moriri Lake and is subjected to evaporative enrichment (Fig. 4.2, and Mishra et al., 2014). Several studies have shown that in the monsoonal domain, δ-values of precipitation are correlated with the amount of summer monsoon precipitation which is strongly depleted in heavy isotopes (Wei and Gasse, 1999; Li et al., 2009; Joswiak et al., 2010). An additional indirect effect of stronger (weaker) summer monsoon precipitation will also be the reduction (increase) in summer evaporation efficiency that will further augment (reduce) the depletion of $\delta^{18}O$ in carbonates.

To investigate the possibility of intensified westerlies during intervals A and B, we have checked the records from westerlies influenced arid central Asia (ACA) (Fig. 4.5) (Chen et al., 2008). Many lakes, including Bosten Lake, Bayan Nuur, Juyan Lake, Gun Nuur and Hulun Nuur, were dry or were very shallow during the early Holocene

before 8 ka. Large deep lakes, such as the Aral Sea, Issyk-Kul, and Lake Van showed low lake levels (references in Chen et al., 2008). In view of this, we rule out increased westerly precipitation as a factor in the $\delta^{18}O$ depletion during intervals A and B.

Based on our own data and the available literature, we assume that (i) endogenic carbonates form in lake surface waters close to isotopic equilibrium with summer temperatures and water composition (Leng and Marshall, 2004) – this assumption is reasonable as, even accounting for the small enrichment resulting from the presence of aragonite, the measured number ($\delta^{18}O$ =-1.7‰ for the top 0.5cm of the Tso Moriri core) is close to the calculated (following Anderson and Craig, 1983) value of the endogenic calcite $\delta^{18}O$ value (-2.01‰); (ii) surficial erosion is highest during periods of intensified monsoon in the poorly vegetated areas of higher Himalayas and Tibet (Fontes et al., 1996; Anoop et al., 2013a; Doberschütz et al., 2014); (iii) intensified monsoon precipitation in north India is associated with greater $\delta^{18}O$ depletion (Joswiak et al., 2010).

Thus, the $\delta^{18}O$ depletion observed in intervals A and B could have been caused by either reduced evaporation (of isotopically depleted meltwater from pre-existing glaciers/snow) or increased (isotopically depleted) ISM contribution to the lake. Both the scenarios are consistent with positive hydrological balance, and reduced/absent endogenic carbonates (Fig. 4.3). However, during both these shifts, isotopic depletion is accompanied by an abrupt increase in siliciclastic contribution (Ti) into the lake (Fig. 4.4) indicating increased surficial erosion. Interval B (11.2-8.5 cal ka) was also marked by highest summer insolation (Berger and Loutre, 1991) which should have led to increased evaporation (more endogenic carbonates) and enriched $\delta^{18}O$ values. On the contrary endogenic carbonates are low/absent, and $\delta^{18}O$ shows the lowest values, MAP is high (Leipe et al., 2014a) signifying that interval B represents highest I/E during the past 15.5 cal ka as intensified ISM would have also reduced the summer evaporation efficiency. Since the westerlies influence was weak prior to 8 cal ka (Chen et al., 2008), we rule out increased westerly precipitation in the $\delta^{18}O$ depletion during intervals A and B. On the contrary, other archives from the ISM and/or east Asian summer monsoon (EASM) influenced regions show early Holocene increase in moisture availability (Fig. 4.5) supporting our hypothesis of additional intensified ISM resulting in depleted $\delta^{18}O$ during these intervals.

Between 8.5-5.5 cal ka there is a re-appearance of endogenic carbonates indicating a weakening of the ISM precipitation with a slight decrease in Ti (Fig. 4.4), while the $\delta^{18}O$ does not show significant change indicating a stable period of relatively high lake levels.

For the interval C there is a gradual trend of isotopic enrichment in the carbonates, accompanied by decreasing Ti, increasing endogenic calcite (interval C1=5.5-3 cal ka), and the re-appearance of aragonite ca. 2.7 cal ka (interval C2=3-0 cal ka), and largely unchanged mean annual precipitation (MAP) (Leipe et al., 2014a). We interpret this interval to have a long term interval of progressively decreasing I/E caused by increasing evaporation.

4.5.4. Regional comparison and implications for atmospheric circulation reorganisation

The monsoon strengthening seen during intervals A and B has also been reported from other ISM (Sinha et al., 2005; Govil and Naidu, 2011) and EASM influenced regions indicating these to be common to the entire Asian monsoon realm. The succession of hydrological changes (wetter followed by drier, succeeded by early Holocene wettest period) coincides with the first strong intensification of the Asian monsoon circulation (Lister et al., 1991; Gasse et al., 1991; Wei and Gasse, 1999; Zhou et al., 1999; Sinha et al., 2005; Herzschuh, 2006; Zech et al., 2014*)*. During 11.2 to 8.5 cal ka, a major negative shift in $\delta^{18}O_{carb}$ (ca. 8‰) is observed. Increase in siliciclastic (Ti) input during this period, and almost negligible amount of endogenic carbonate (higher I/E) is consistent with the increase in solar insolation, which suggested the intensification of Holocene moisture input (Mishra et al., 2015). Millennial-scale coupling between the Asian monsoons and higher latitudes has previously been suggested for interglacials (e.g., Schulz et al., 1998; Wang et al., 2001; Yuan et al., 2004) and could be manifested through northward shifts in the mean position of the intertropical convergence zone (Chiang et al., 2003; Lea et al., 2003) leading to deeper ISM penetration in the Himalayan region (Sinha et al., 2005) during warmer intervals.

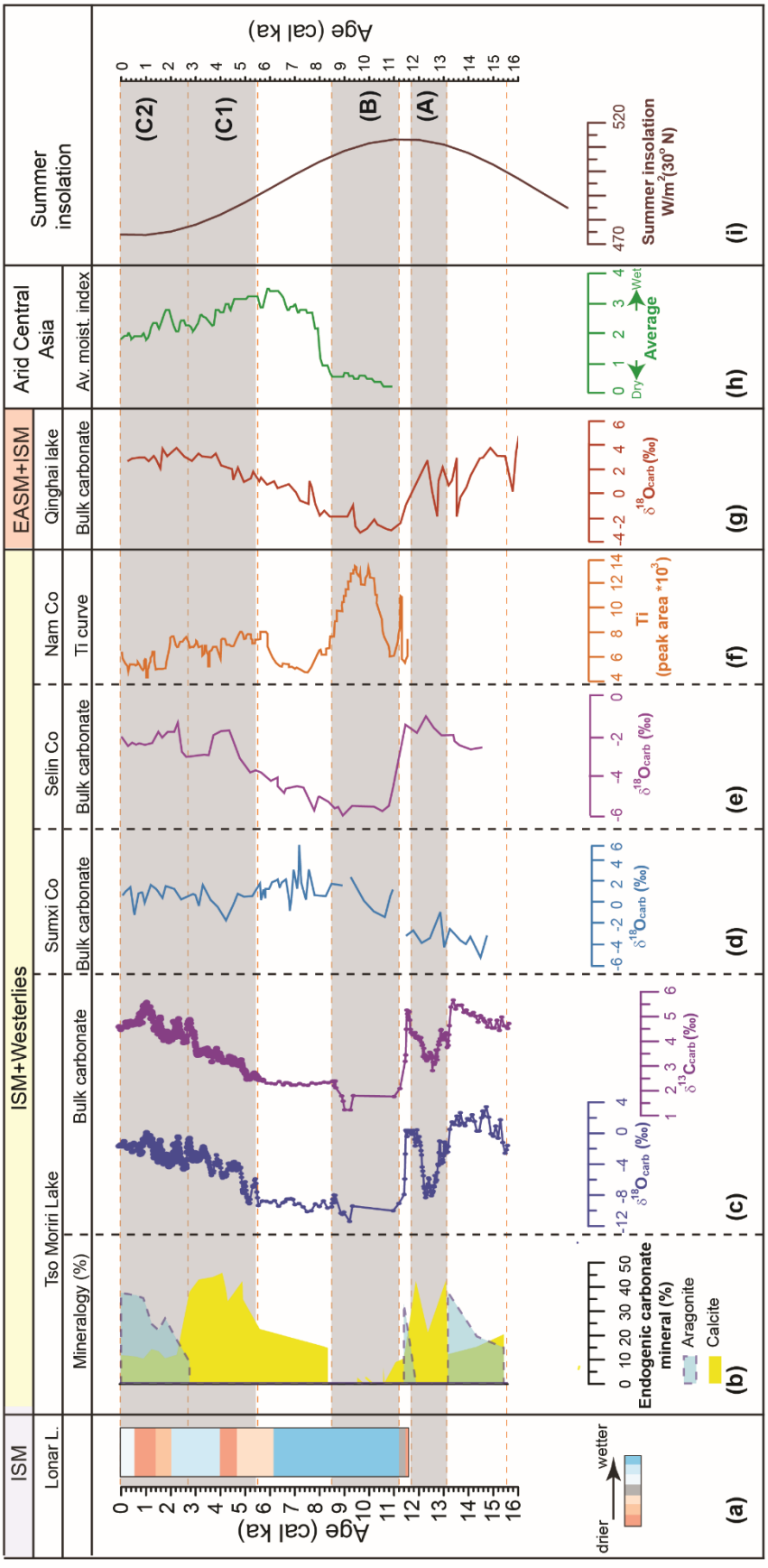

Fig. 4.5: Regional comparison of TsoMoriri data (panels b and c) with other sites fromthe ISM(Lonar Lake, panel a; Prasad et al., 2014), ISM+westerlies (panels b: TsoMoriri Lake, Mishra et al., 2015; c: this study; d: Sumxi Co, Fontes et al., 1993; e: Selin Co, Gasse et al., 1996; f: NamCo, Doberschütz et al., 2014), EASM+westerly (panel g: Qinghai Lake, Lister et al., 1991), and westerly (ACA, panel h: regional composite from Chen et al., 2008) influenced sites. Summer insolation at 30°N is shown in panel i (Berger and Loutre, 1991). Higher Ti (peak area) fromNam Co is indicative of higher erosion in response to increasedmoisture supply. The isotopic changes in Tso Moriri Lake, in selected intervals (grey bars) identified in this study, are compared with other regional records.

The period after 8.5 cal ka, was characterised by re-appearance of endogenic calcite, slight enrichment (average +1.2‰) in $\delta^{18}O_{carb}$, reduced surficial inflow (Ti), indicating a gradual weakening of ISM coincident with decreasing solar insolation and the southward movement of the intertropical convergence zone (Haug et al., 2001). This inference is also confirmed by lower MAP (Fig. 4.3) and is also seen in other monsoonal archives (Lister et al., 1991; Wei and Gasse, 1999; Demske et al., 2009; Chen et al., 2008). Interestingly, the post 8 cal ka intensified westerlies influence (Fig. 4.5) in arid central Asia (Chen et al., 2008) does not appear to have made a strong impact in the NW Himalayas as the Tso Moriri Lake shows decreasing I/E after 8.5 cal ka. The decreasing I/E trend intensifies after 2.7 cal ka is largely due to increasing evaporation as the MAP does not show any significant change after 5 cal ka (Leipe et al., 2014a).

Recent studies (Berkelhammer et al., 2012; Prasad et al., 2014; Dixit et al., 2014) have also discussed the role of ocean atmosphere teleconnections (El Niño-Southern Oscillation, Indian Ocean Dipole) in causing late Holocene ISM weakening in peninsular India. The intervals of prolonged ISM drought (4.6-3.9 cal ka and 2-0.6 cal ka) reported from central ISM regions (Anoop et al., 2013b; Prasad et al., 2014) at a first glance, do not appear to had made any impact in NW Himalayas, probably due to the buffering effect of glacial meltwater on the hydrological balance. We note that highest endogenic calcite values are reached between 5.5-2.7 cal ka and highest aragonite values are reached ca. 2.1 cal ka. However, the MAP (Leipe et al., 2014a) does not show any major change suggesting that the mineralogical changes could have been a result of an increase in evaporation rather than ISM variability.

4.6. Conclusions

The isotopic composition of endogenic carbonates in the Tso Moriri Lake provides insights into the changing hydrological (I/E) during the past ca. 15.5 cal ka. We provide evidence of (i) stepwise pattern of late glacial/Holocene transition caused by shifts in I/E balance in NW Himalaya. This pattern is characterised by abrupt fluctuations in ISM precipitation; (ii) the early (11.2-8.5 cal ka) Holocene warm period was characterised by the highest I/E during the past ca. 15.5 cal ka caused by increased ISM precipitation; (iii) The ISM began to weaken ca. 8.5 cal ka, with a stepwise intensification of the decreasing I/E trend at ca. 5.5 and 2.7 cal ka; (iv) the westerlies precipitation never attained the level of positive I/E balance as during the ISM intensification between 11.2-8.5 cal ka; (v) the

NW Himalayan region is less sensitive to droughts seen in peninsular India, probably due to the buffering effect of snow melt, and weaker late Holocene ISM in the NW Himalaya relative to the early Holocene.

4.7. Acknowledgements

This project is being funded by the DeutscheForschungsGemeinschaft under the coordinated programme “Himalaya: Modern and Past Climates” (HIMPAC, FOR 1380). The help extended by the Jammu & Kashmir Wildlife Department during the coring programme, especially by the Chief Wildlife Warden and Regional Wildlife Warden, Leh and their field staff at Tso Moriri Lake is gratefully acknowledged. The Tso Moriri coring and field expeditions have also received financial and logistic support from the Deutsches GFZ Potsdam, the Kashmir University, and the Indian Institute of Geomagnetism. We are grateful to S. Pinkerneil, B. Shehzad, C. Leipe, and B. Wünnemann for their help during the field work. The hard work invested by R. Niederreiter, D. Niederreiter and M. Köhler for raising the core is gratefully acknowledged. The authors confirm that they have no conflict of interest.

Chapter 5: Linking Holocene drying trends from Lonar Lake in monsoonal central India to North Atlantic cooling events

*Philip Menzel [a], Birgit Gaye [a], **Praveen K. Mishra** [b], Ambili Anoop [b], Nathani Basavaiah [c], Norbert Marwan [d], Birgit Plessen [b], Sushma Prasad [e], Nils Riedel [f], Martina Stebich [f], Martin G. Wiesner [a]*

[a] Institute of Geology, University of Hamburg, Bundesstr. 55, 20146 Hamburg, Germany
[b] Helmholtz-Centre Potsdam - German Research Centre for Geosciences (GFZ), Telegrafenberg, 14473 Potsdam, Germany
[c] Indian Institute of Geomagnetism, Plot 5, Sector 18, New Panvel, Navi Mumbai - 410218, India
[d] Potsdam-Institute for Climate Impact Research, Telegrafenberg A 51, 14412 Potsdam, Germany
[e] Institute of Earth- and Environmental Science, University of Potsdam, Karl-Liebknecht-Str. 24-25, 14476 Potsdam-Golm, Germany
[f] Senckenberg Research Station of Quaternary Palaeontology, Am Jakobskirchhof 4, 99423 Weimar, Germany

Manuscript status: Published in Palaeogeography, Palaeoclimatology, Palaeoecology. DOI: http://dx.doi.org/10.1016/j.palaeo.2014.05.044

Abstract

We present the results of biogeochemical and mineralogical analyses on a sediment core that covers the Holocene sedimentation history of the climatically sensitive, closed, saline, and alkaline Lonar Lake in the core monsoon zone in central India. We compare our results of C/N ratios, stable carbon and nitrogen isotopes, grain-size, as well as amino acid derived degradation proxies with climatically sensitive proxies of other records from South Asia and the North Atlantic region. The comparison reveals some more or less contemporaneous climate shifts. At Lonar Lake, a general long term climate transition from wet conditions during the early Holocene to drier conditions during the late Holocene, delineating the insolation curve, can be reconstructed. In addition to the previously identified periods of prolonged drought during 4.6 – 3.9 and 2.0 – 0.6 cal ka that have been attributed to temperature changes in the Indo Pacific Warm Pool, several additional phases of shorter term climate alteration superimposed upon the general climate trend can be identified. These correlate with cold phases in the North Atlantic region. The most pronounced climate deteriorations indicated by our data occurred during 6.2 to 5.2, 4.6 to 3.9, and 2.0 to 0.6 cal ka. The strong dry phase between 4.6 and 3.9 cal ka at Lonar Lake corroborates the hypothesis that severe climate deterioration contributed to the decline of the Indus Civilisation about 3.9 ka.

Keywords: Lake sediment; Indian Monsoon; Holocene; climate reconstruction; stable carbon isotope; amino acid

5.1. Introduction

The increasing demand for reliable climate projections due to the challenges related to global warming calls for enhanced investigation of the relationship between climate change and its effect on the environment. To assess future interaction between climate and environment, it is necessary to understand their interactions in the present and past. But, while modern observations are increasing rapidly and cover almost the whole world in high spatial and temporal resolution, the identification and investigation of suitable sites for palaeoclimate reconstruction is more difficult and requires great effort. Hence, several regions still lack a sufficient cover of investigated areas to help the scientific community in reconstructing the past climate and its influence on the former environment. One of these regions is India, which highly depends on the annual rainfall delivered by the Indian summer monsoon (ISM). This meteorological phenomenon affects a human population of more than one billion and is highly sensitive to climate change. In order to assess and to interpret potential future modifications of the Indian monsoon system, the knowledge of Holocene monsoon variability, its extremes, and their underlying causal mechanisms is crucial. And while terrestrial palaeo-records are available from the northern Indian subcontinent and the Himalayan region (Gasse et al., 1991; Gasse et al., 1996; Enzel et al., 1999; Denniston et al., 2000; Thompson et al., 2000; Bookhagen et al., 2005; Prasad and Enzel, 2006; Clift et al., 2008; Demske et al., 2009; Wünnemann et al., 2010; Alizai et al., 2012), the number and length of comparable records from central and south India are limited (Yadava and Ramesh, 2005; Caner et al., 2007; Sinha et al., 2007; Berkelhammer et al., 2010). To address this issue, we have investigated the Holocene sedimentation history of Lonar Lake from central India with a special focus on centennial scale palaeoclimate reconstruction.

Based on mineralogical, palynological, and biogeochemical investigations on the ca. 10 m long sediment core, the longest, well dated palaeoclimate archive from India's core monsoon zone, Prasad et al., (2014) reconstructed the broad, Holocene climatic development of the Lonar Lake region, identified two millennial scale dry phases, and discussed the stability of the ISM – El Niño Southern Oscillation (ENSO) links and the influence of shifts in the position of the Indo Pacific Warm Pool (IPWP) on the prolonged droughts in the ISM realm. Here we present stable carbon and nitrogen isotope data from Prasad et al., (2014) as well as new data from amino acid, sediment

composition, and grain-size analysis and interpret them with respect to centennial scale, Holocene climate variability and its tele-connections with the North Atlantic climate.

Bond et al., (2001) hypothesised a connection between North Atlantic cooling events and cosmogenic nuclide production rates, the latter indicating small changes in solar output. Additionally, they found virtually synchronous "quasi-periodic" ~ 1500 year cyclicity in both their palaeo-record and nuclide production rates. Thus, they postulated a reaction of climate to small changes in solar output, which would not be limited to the North Atlantic region but which would affect the global climate system (Bond et al., 2001). Correlations between the high and the mid-latitude climate, as reconstructed from Greenland ice cores (Johnsen et al., 2001; Stuiver and Grootes, 2000) and ice-rafted debris in North Atlantic deep sea records (Bond et al., 1997), and the low latitude tropical climate have been found in various climate reconstructions (Haug et al., 2001; Gupta et al., 2003; Hong et al., 2003; Dykoski et al., 2005; Wang et al., 2005; Fleitmann et al., 2007; Koutavas and Sachs, 2008) supporting the assumption that different climate systems react to the same cause, like solar output variation, (Bond et al., 2001; Soon et al., 2014) either independently or via tele-connections. However, since many palaeoclimate investigations concerning the correlations between tropical climate and North Atlantic climate were carried out in peripheral ISM regions (Hong et al., 2003; Fleitmann et al., 2007), these records could not indicate if the change in moisture availability was exclusively linked to an alteration in monsoonal summer rainfall rather than to altered winter westerly precipitation. Lonar Lake is one of the very few natural lakes located in the core monsoon zone in central India, and it is fed exclusively by precipitation of the Indian summer monsoon and stream inflow that is closely linked to monsoon rainfall (Anoop et al., 2013b). Additionally, available precipitation data from the region close to Lonar Lake indicate a good correlation with the all India rainfall record of the last century (1901 – 2002). Correlation between the all India rainfall record (ftp://www.tropmet.res.in/pub/data/rain/iitm-regionrf.txt) and the annual precipitation data of the meteorological stations in Buldhana, Jalna, Hingoli, and Washim (http://www.indiawaterportal.org/met_data/) varies between 0.62 and 0.69 ($p < 0.001$), making Lonar Lake a key site to investigate the connection between Indian monsoon strength and its connection to North Atlantic climate change.

5. 2. Study site

Lonar Lake is a closed basin lake situated at the floor of a meteorite impact crater that formed during the Pleistocene (~ 570 ± 47 ka) on the Deccan Plateau basalts (Jourdan et al., 2011). The lake is located at Buldhana District in Maharashtra, central India at 19.98° N and 76.51° E (Fig. 5.1). The meteorite crater has a diameter of ca. 1880 m, and the almost circular lake covers an area of about 1 km². The modern crater floor is located at ca. 470 m above sea level, which is around 140 m below the rim crest elevation. The inner rim wall is fairly steep with slopes of 15° – 18° in the east and up to ~ 30° in the west and south-west (Basavaiah et al., 2014).

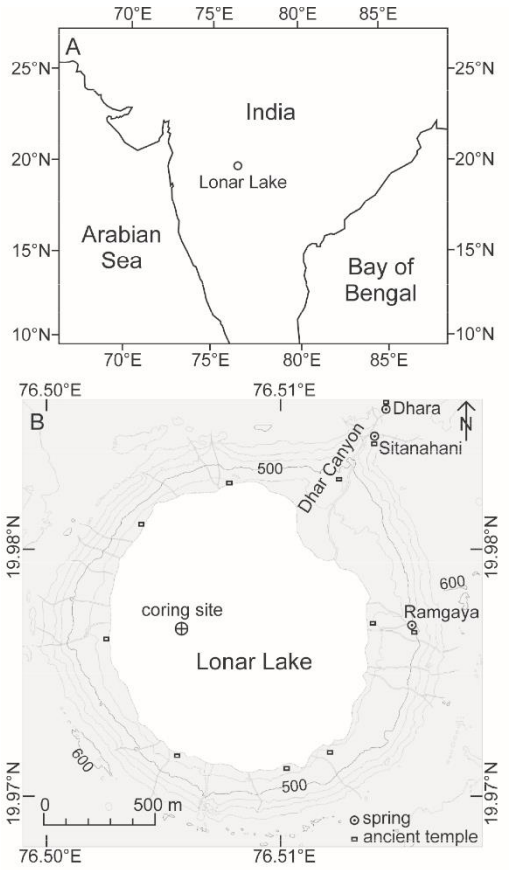

Fig. 5.1: A) Regional overview and location of Lonar Lake; B) Study area showing the coring site

Lonar Lake is located in the 'core monsoon zone' of the Indian summer monsoon (Gadgil, 2003). The south-west monsoon from June to end of September is characterised by strong winds and brings in average rainfall of ~ 700 mm. Precipitation during December to April occurs only in rare cases. The temperature can exceed 40°C before the onset of the monsoon and declines during the monsoon phase to an average of approximately 27°C. The post monsoon from October to February is characterised by

relatively low temperatures at an average of 23°C (http://indiawaterportal.org/met_data/). The lake is fed by surface runoff during the monsoon season and three perennial streams that are closely linked to monsoon rainfall as indicated by tritium dating (Anoop et al., 2013b). Two of them, the Dhara stream and the Sitanahani stream are entering the crater from the north-east. They have formed the Dhara Canyon, an erosive incision, and have built up an alluvial fan into the lake. Today this fan is used for agricultural plantation. The Ramgaya stream, the third stream feeding the lake, springs from the inner crater wall and enters the lake from the eastern shore. Nowadays the three streams are diverted towards the Dhara fan to irrigate the agricultural fields. Water discharge is only conducted by evapotranspiration; no outflowing stream is present and no loss due to seepage occurs as the lake level is below the local groundwater level (Nandy and Deo, 1961).

The modern lake is ca. 6 m deep, brackish, alkaline, and eutrophic with permanent bottom water anoxia (Basavaiah et al., 2014). The eutrophication promotes phytoplankton blooms especially during and subsequent to the monsoon when nutrients are washed into the lake. The algal assemblage is primarily made up of cyanophyceae (Badve et al., 1993). Thermophilic, halophilic, and alkalophilic bacteria in numbers of 10^2 to 10^4 viable cells/ml (Joshi et al., 2008) and methanogenic archaea (Surakasi et al., 2007) were reported from Lonar Lake. The lake lacks most zooplankton species and higher organisms. The zooplankton community within the lake consists of ciliates, culicid larvae, and rotifers (Mahajan, 2005). Only few exemplars of the ostracod *Cypris subglobosa* and the gastropod *Lymnea acuminate* have been observed in the lake (Badve et al., 1993).

The vegetation of the inner crater walls changes from the upper part near the rim crest to the bottom part close to the lake shore. The upper part of the inner crater walls is covered by drought tolerant grass and thorn shrub species, further down grows teak (*Tectona grandis*) dominated dry deciduous forest, and the bottom part of the inner crater walls is overgrown by semi evergreen forests. The alluvial fan, which has formed due to riverine erosion in the north-east of the lake, is used for crop plantation and cattle grazing. The fan is characterised by vegetation cover of grasses, sedges, and crop plants like banana (*Musa* x *paradisiaca*), millet (*Setaria italica*), corn (*Zea mays*), custard-apple (*Annona reticulata*), and papaya (*Carica papaya*) (Menzel et al., 2013).

5.3. Methods and material

5.3.1. Sampling

Two parallel ca. 10 m long cores were retrieved in May-June 2008 at 5.4 m water depth using a UWITEC sediment piston corer. The cores were opened in the laboratory; a composite core was constructed and sub-sampled in 0.5 cm resolution using L-channel sampling procedure. All samples despite those for grain-size analyses were freeze-dried and ground manually in an agate mortar.

5.3.2. Analytical methods

The total carbon (TC), total nitrogen (TN), and total organic carbon (TOC) contents and the $\delta^{15}N$ and $\delta^{13}C_{org}$ isotopic composition were determined using an elemental analyser (NC2500 Carlo Erba) coupled with a ConFlowIII interface on a DELTAplusXL mass spectrometer (ThermoFisher Scientific). The isotopic composition is given in the delta (δ) notation indicating the difference, in per mil (‰), between the isotopic ratios of the sample relative to an international standard: δ (‰) = $[(R_{sample} / R_{standard}) - 1] \times 1000$. The ratio and standard for carbon is $^{13}C/^{12}C$ and VPDB (Vienna PeeDee Belemnite) and for nitrogen $^{15}N/^{14}N$ and air N_2, respectively.

For TC, TN and $\delta^{15}N$ determination, around 20 mg of sample material was loaded in tin capsules and burned in the elemental analyser. The TC and TN contents were calibrated against acetanilide whereas for the nitrogen isotopic composition two ammonium sulphate standards (e.g. IAEA N-1 and N-2) were used. The results were proofed with an internal soil reference sample (Boden3). Replicate measurements resulted in a standard deviation better than 0.1% for N and 0.2‰ for $\delta^{15}N$.

The TOC contents and $\delta^{13}C_{org}$ values were determined on *in situ* decalcified samples. Around 3 mg of sample material was weighted into Ag-capsules, dropped with 20% HCl, heated for 3 h at 75°C, and finally wrapped into the Ag-capsules and measured as described above. The calibration was performed using elemental (Urea) and certified isotopic standards (USGS24, IAEA CH-7) and proofed with an internal soil reference sample (Boden3). The reproducibility for replicate analyses is 0.1% for TOC and 0.2‰ for $\delta^{13}C_{org}$.

Inorganic carbon (IC) was defined as the difference between TC and TOC. IC was converted to carbonate by multiplying with 8.33, since calcium carbonate was the only

carbonate phase detected in the sediments despite three distinct zones of the core where gaylussite crystals were found (1.58 to 4.22 m, 6.42 to 7.60 m, 9.10 to 9.25 m). These crystals were handpicked under microscope prior to analyses. The percentage of lithogenic material in the sediments was calculated using the formula:

$$Lith\ (\%) = 100\% - (total\ organic\ matter\ [\%] + carbonate\ [\%])$$

Analyses of AA and HA were carried out on a Biochrom 30 Amino Acid Analyser according to the method described by Lahajnar et al., (2007). Briefly, after hydrolysis of the samples with 6 mol L^{-1} HCl for 22h at 110°C under a pure argon atmosphere, HCl was removed from an aliquot by repeated evaporation using a vacuum rotating evaporator (Büchi 011) and subsequent dissolution of the residue in distilled water. After evaporating the aliquot three times, the residue was taken up in an acidic buffer (pH: 2.2) and injected into the analyser. The individual monomers were separated with a cation exchange resin and detected fluorometrically according to the procedure described by Roth and Hampaĭ, (1973). Duplicate analysis of a standard solution according to this method results in a relative error of 0.1 to 1.3% for the concentration of individual AA monomers. Duplicate measurement of a sediment sample revealed a relative error of < 1% for AA and HA concentrations, < 10% for molar contribution of low concentrated (< 1 mol%) AA monomers, and < 2.5% for higher concentrated (> 1 mol%) AA monomers.

Grain-size distribution of the core samples was determined using a Malvern Mastersizer 2000 analyser. The pre-treatment of sediments included the wet-oxidising of the organic matter and the chemical dissolution of carbonates at room temperature. Ca. 0.3 g freeze-dried sample aliquots were treated with 10 ml H_2O_2 (30%) which was added in two steps. The excess oxidising agent was removed by repeated washing with Millipore water (18.2 MΩcm), centrifugation (6000 rpm, 5 min), and suction of the supernatant. The carbonates of the solid residues were dissolved by the addition of 3.5 ml 1 M HCl overnight. The solid residues were repeatedly washed (see above) and suspended in 20 ml Millipore water. The de-acidified samples were kept in an ultrasonic vibrator for 15 min to disaggregate all grains. The instrument measured the grain-size of the suspended particles from 0.02 to 2000 µm for 100 grain-size classes. The content of coarse particles (> 200 µm) in the small aliquots exposed to measurement cannot be representative for the entire sample. Therefore, we re-calculated the volume-percentage

for the grain-size fraction 0.02 to 200 µm.

5.3.3. Statistical method

To assess the interrelation of climatic changes in central India and the North Atlantic region as well as the concurrence of climate changes in central India and the solar output we have calculated the major frequencies in our climate proxy data as well as the correlation between our proxy and the ^{14}C production rate. Before the spectral analysis, the long term climate trend was removed from the whole time series by applying a Gaussian kernel based filter with a kernel bandwidth of 500 years. The spectral analysis is then performed as the Fourier transform of the auto-correlation function. Since the sampling of the time series is irregular, the auto-correlation estimation is also based on a Gaussian kernel (bandwidth of 0.5 years), allowing us to directly apply this method without preceding interpolation (Rehfeld et al., 2011). A statistical test was performed to create a confidence interval for the found spectrum. For the test, we have fitted an auto-regressive process of first order (AR1) to the unfiltered original time series, created 10,000 realisations of this AR1 process, and applied the same kernel based high-pass filter as for the original time series. From these 10,000 realisations, we calculated the power spectra by Fourier transform of the auto-correlation function and estimated the 90% confidence interval (software NESToolbox for MATLAB used).

5.3.4. Chronology

The age model for the core is based on 19 AMS ^{14}C dated samples of wood, leaves, gaylussite crystals, and bulk organic matter (Table 5.1; Prasad et al., 2014). The oldest dated sample of the core shows an age of 11016 ± 161 cal a, suggesting that the core covers the complete Holocene sedimentation history of Lonar Lake. The radiocarbon dating was carried out at Poznan radiocarbon laboratory, Poland. Since the catchment geology comprises carbonate free basaltic rocks of the Deccan Traps, no correction for hard water effect was conducted. However, the elevated salinity and pH in combination with stratification of the water body led to an ageing of the bulk organic matter samples (Prasad et al., 2014). Calibration of the ^{14}C dates was carried out using the program OxCal, interpolating with the INTCAL04 and NH3 calibration curves (Bronk Ramsey, 2008).

5.3.5. Mineralogical and biogeochemical proxies

Our reconstruction of the climatic history of the Lonar Lake region and its comparison to the North Atlantic region is mainly based on lithogenic contribution to the sediments, grain-size, atomic organic carbon to total nitrogen ratio (C/N), $\delta^{13}C_{org}$, $\delta^{15}N$, and amino acid derived indices. The C/N, $\delta^{13}C_{org}$, and $\delta^{15}N$ data were reported and interpreted with respect to climate variability and climatic tele-connections of the Lonar Lake region with the Pacific by Prasad et al., (2014). Additionally, the occurrence of evaporitic gaylussite crystals in the sediments, as reported by Anoop et al., (2013b), was used for the climate reconstruction. The mechanisms driving the changes in the parameters are shortly summarised in the following sections.

a) Lithogenic contribution

The lithogenic contribution to lake sediments mostly depends on the erosion that takes place in the catchment area, transport energy, and shore line proximity (Koinig et al., 2003; Magny et al., 2012). The intensity of erosion at a lake, which is not affected by temperatures below the freezing point, is mostly driven by the amount of rainfall, the occurrence of heavy rainfall events, and the density of vegetation that prevents erosion (Kauppila and Salonen, 1997; Anoop et al., 2013a). Human interferences like deforestation, agricultural land use, and construction activity must be considered as potential causes of enhanced erosion especially in the younger past (Wilmshurst, 1997). Counterintuitive, phases of enhanced precipitation potentially triggering stronger erosion do not necessarily coincide with elevated lithogenic percentages in the lake sediments. This is due to the spreading of vegetation during climatically wet phases, but can also be controlled by changes in lake level. During wet phases, the lake level increases, which also increases the distance between a sampling site and the lake shore. Thus, high proportions of the eroded material from the catchment are deposited relatively close to the shore in shallow water and do not reach the deeper sampling site. These mechanisms seem to dominate at Lonar Lake, since time slices of the Lonar core that show strong evidence of dry climate coincide with high lithogenic contribution to the sediments.

Thus, the lithogenic contribution seems to be a good proxy for the climate reconstruction at Lonar Lake with high values indicating low lake level during drier climate and low values indicating high lake level during wetter climate.

b) Grain-size

The grain-size of lake sediments depends much on the source of the sediment load. But if the source of the sediments does not change, the grain-size can give information about changes in the hydrodynamics of inflowing streams, the amount of precipitation, the occurrence of heavy rainfall events, seasonality, shore line or sediment source (e.g., river mouth) proximity, changes in the internal hydrodynamics (e.g., currents), and external factors affecting the catchment erosion (McLaren and Bowles, 1985; Sun et al., 2002; Peng et al., 2005). The sorting of the sediments can be used to reconstruct the transport distance and the rate of deposition.

The grain-size data are particularly useful for the broad, Holocene climate reconstruction at Lonar Lake since they depend on changes in monsoon strength. However, for the reconstruction of smaller scale climate variability, the resolution of grain-size data might not be high enough, especially in the lower part of the core, where sedimentation rates are low.

c) C/N

The C/N ratio is often used to determine the source of organic matter (OM) in lake and coastal sediments (Meyers, 1997). Since aquatic OM is relatively enriched in nitrogen rich proteins, and vascular plant OM is relatively enriched in nitrogen depleted lignin and cellulose, the ratio of carbon to nitrogen is much lower in aquatic OM than in OM of terrestrial origin. C/N ratios of 4-10 indicate the origin of aquatic OM source, whereas C/N ratios of >20 typically indicate dominant contribution of terrestrial plants (Meyers and Ishiwatari, 1993). However, the use of C/N ratios as OM source indicator can be biased since C/N ratios can be altered during degradation. This can shift the C/N ratio to higher values if the degraded OM is enriched in labile nitrogen rich compounds like proteins, peptides, and free amino acids, which are most abundant in planktonic OM. On the other hand, OM of terrestrial origin tends to become relatively depleted in carbon during degradation, since nitrogen deficient components like carbohydrates and lipids are preferentially decomposed (Meyers and Lallier-Vergès, 1999). Nevertheless, these alterations are usually of minor magnitude; hence, the source information of the C/N ratio is mainly preserved.

At the modern Lonar Lake, soils show a tendency towards low C/N ratios (Menzel et al., 2013). This is related to the aforementioned preferential degradation of

nitrogen depleted components in combination with the immobilisation of re-mineralised nitrogen, which can be absorbed by clay minerals in the form of NH_4^+ (Mengel, 1996; Sollins et al., 1984). This effect has the strongest influence on sediments that show low TOC contents.

The C/N ratio does not provide much direct information for the climate reconstruction. It is particularly useful for determining the OM source, which is not much climate dependent. During wet conditions, more terrestrial OM might be washed into the lake due to denser vegetation and stronger rainfall, but this could also cause more nutrient in-wash into the lake promoting the production of aquatic OM. Thus, the C/N ratio cannot be used as a climate proxy but identifies changes in OM source and supports the interpretation of other palaeoclimate proxies that are affected by changes in OM source.

d) $\delta^{13}C_{org}$

$\delta^{13}C_{org}$ in lake sediments is influenced by the abundances of land plant OM and aquatic OM in the sediments. The $\delta^{13}C$ of terrestrial OM is mainly driven by the percentage of plants using the C_3 pathway and plants using the C_4 pathway of CO_2 assimilation. C_3 plants show $\delta^{13}C$ values of -23 to -35‰, whereas C_4 plants have $\delta^{13}C$ values of -10 to -16‰ (O'Leary, 1988). C_3 plants are more abundant during wet conditions whereas C_4 plants usually spread during phases of dry climate (Tieszen et al., 1979).

$\delta^{13}C$ of the aquatic OM depend on the $\delta^{13}C$ of dissolved inorganic carbon (DIC) and on the concentration of CO_2(aq.) in the photic zone. Lower pCO_2(aq.) leads to reduced fractionation during CO_2 uptake by phytoplankton, and thus to ^{13}C enrichment in aquatic OM (Lehmann et al., 2004). The factors controlling the isotopic composition of DIC in Lonar Lake are i) the aquatic productivity driven by nutrient supply to the lake, ii) redox conditions of surface sediments and lake water, determining the mechanisms and inorganic products of OM decomposition, iii) the pH of lake water, shifting the equilibrium of the three types of DIC (CO_2(aq.), HCO_3^-, and CO_3^{2-}), iv) the development and stability of lake stratification, affecting the exchange of DIC between the photic and aphotic zones, and v) CO_2 degassing caused by lake level decline during climatically dry phases. Generally, factors enriching the DIC in ^{13}C are linked to eutrophication, dryer climate, and lake stratification. In highly productive lakes, ^{13}C deficient OM is

transported into the sediments, leaving the DIC in the photic zone enriched in ^{13}C (Hodell and Schelske, 1998). This effect can be expedited by strong lake stratification, hampering the convection of lake water, and thus the transport of ^{13}C depleted CO_2, which is produced during OM degradation mostly in the aphotic zone, into the photic zone. Additionally, eutrophic conditions and lake stratification support the development of anoxia in deep waters. This causes the production of highly ^{13}C depleted methane during OM degradation, which can escape the lake system in gaseous state if it is not re-oxidised. Methanogenesis in anoxic sediments is accompanied by the release of ^{13}C enriched CO_2 at the expense of ^{13}C depleted methane. Thus, if methane is degassed from the lake water and not re-oxidised, anoxia leads to enriched $\delta^{13}C$ values of lake water DIC (Gu et al., 2004). In response to dryer climate, evaporation intensifies and the lake level lowers; this increases the salinity, and thus the alkalinity and pH of lake water. Under highly alkaline conditions, the equilibrium of the three types of DIC shifts towards HCO_3^- and CO_3^{2-}, which are enriched in ^{13}C compared to CO_2(aq.) (Zhang et al., 1995). Under these CO_2(aq.) depleted conditions, the growth of phytoplankton capable of using HCO_3^- as carbon source is promoted producing ^{13}C enriched aquatic OM (Stuiver, 1975). Additionally, exceeding evaporation can cause supersaturation of carbonate in the lake water, and consequently CO_2 degassing, which is accompanied by an increase in $\delta^{13}C$ of DIC (Lei et al., 2012).

Since $\delta^{13}C$ increases under dry conditions in both aquatic OM and terrestrial OM, it is a good climate proxy in our record. The only limitation is the influence of lake water anoxia, which more likely occurs in a deeper lake during wet conditions or as a consequence of eutrophication. The anoxia can cause a change in $\delta^{13}C$ of aquatic OM due to methane degassing or methane oxidation, factors that disappear in a shallow oxic lake.

e) $\delta^{15}N$

The introduction and cycling of nitrogen in lakes involves several dissolved inorganic nitrogen (DIN) species and transformation processes, associated with more or less strong isotopic fractionation. Thus, $\delta^{15}N$ of OM in lakes can exhibit highly diverse values, linked to several processes. Usually, plankton discriminates against ^{15}N during DIN uptake, with the exception of plankton that is capable of fixing molecular nitrogen (Talbot and Lærdal, 2000). Hence, phases of intense phytoplankton blooms are

associated with increased $\delta^{15}N$ values of DIN in the photic zone. Comparable to carbon uptake, low concentrations of DIN lead to reduced isotopic fractionation of plankton, amplifying the increase of $\delta^{15}N$ during phases of high aquatic productivity (Peterson and Fry, 1987). However, the most important processes in determining the $\delta^{15}N$ values of DIN, and thus in $\delta^{15}N$ of aquatic OM are the conversion processes of the different DIN species. The most prominent processes are nitrification, denitrification, and ammonia volatilisation, which are associated with strong fractionation factors. Nitrification occurs under oxic conditions and results in ^{15}N depleted nitrate and ^{15}N enriched ammonium, whereas denitrification, occurring under anoxic conditions, leads to ^{15}N enrichment of nitrate at the expense of ^{15}N depleted molecular nitrogen. The strongest fractionating process most probably affecting the DIN pool of Lonar Lake is ammonia volatilisation. This process becomes important in aquatic environments showing high pH values (>9). Under these conditions, the equilibrium between ammonium and ammonia shifts towards ammonia, which is significantly depleted in ^{15}N compared to ammonium (20-35‰) and can escape the water column in gaseous state (Casciotti et al., 2011). Thus, ammonia volatilisation leads to increasing $\delta^{15}N$ values of the remaining DIN in lake water.

Even though terrestrial OM does not contribute as much to the $\delta^{15}N$ variability in lake sediments as to $\delta^{13}C_{org}$ due to the fact that terrestrial OM has much lower nitrogen contents than aquatic OM, changes in $\delta^{15}N$ during phases of low aquatic productivity and high terrestrial OM contribution to the sediments can indicate shifts in the vascular plant and soil nitrogen isotopic composition. In general, $\delta^{15}N$ of soil and terrestrial plant OM increases with increasing temperature and decreasing precipitation (Amundson et al., 2003).

The use of $\delta^{15}N$ as a proxy for climate reconstruction at Lonar Lake is limited since $\delta^{15}N$ values of aquatic OM depend on the redox conditions of lake water with high values occurring under anoxic conditions but also increasing due to high pH. And whereas anoxic water is more likely accompanying high lake levels during wet conditions, the pH increases during dry conditions when ions become concentrated in the shrinking water body. Additionally, terrestrial OM shows a wide range of $\delta^{15}N$ values due to different nitrogen uptake mechanisms, making it difficult to interpret in terms of climate variability.

f) Amino acids

The monomeric distribution of the amino acids is commonly used to determine the state of OM degradation in sediments. For the assessment of the OM degradation state, we have calculated the Lonar degradation index (LI), which was first calculated for modern Lonar Lake sediments on the basis of the molar percentages of 19 amino acids (Menzel et al., 2013). The LI compares the amino acid assemblage of the core samples with the data set of Menzel et al., (2013), which includes fresh OM like plankton and vascular plants, moderately degraded sediment trap and surface sediment samples, and highly degraded soil samples from Lonar Lake and its catchment. The calculation of the LI follows the approach of the degradation index (DI) calculation developed by Dauwe and Middelburg (1998) and Dauwe et al., (1999):

$$LI = \sum_i \left[\frac{var_i - AVGvar_i}{STDvar_i} \right] \times fac.coef._i$$

where, var_i is the original mole percentage of each amino acid in the sample, $AVGvar_i$ and $STDvar_i$ are the arithmetic average and the standard deviation and $fac.coef._i$ is the factor coefficient of the first axis of a principle component analysis (PCA) of the individual amino acids in the data set of Menzel et al., (2013). Negative values indicate less degraded and positive values more degraded state of the OM compared to the average of the reference data set.

The second amino acid derived proxy we used is a ratio of individual amino acids that are relatively enriched during aerobic degradation and amino acids that are relatively enriched during anaerobic degradation, named Ox/Anox:

$$Ox/Anox = \frac{Asp + Glu + \beta\text{-}Ala + \gamma\text{-}Aba + Lys}{Ser + Met + Ile + Leu + Tyr + Phe}$$

This ratio has been applied to the modern Lonar Lake sediments (Menzel et al., 2013) to evaluate the redox conditions during OM degradation and is based on a study of Cowie et al., (1995).

The amino acid derived indices seem to be good proxies for climate reconstruction as they can be used to identify phases of aerobic degradation within the sediments. Especially during wet phases that induce a deep anoxic lake, elevated values

of theses indices identify relatively short-term, dry anomalies. Highest values are most probably related to subaerial degradation, and thus to phases of lake desiccation. In rare cases, the indices could be biased by input of eroded soils, which would cause elevated values. In addition, eutrophication causes low LI and Ox/Anox values due to strong aquatic production and the consequent development of lake water anoxia.

5.4. Results and discussion

The results of our investigation of the biogeochemical and lithological properties of the Holocene sediments from Lonar Lake are shown in Fig. 5.2. The percentages of the different grain-size classes indicate sediments dominated by clayey silt with few exceptions showing sandy silt (Fig. 5.3). The sandy silt samples are from 863 to 900 cm depth (10.5 to 7.8 cal ka). Based on the changes in biogeochemical properties, lithology, and sedimentation rate, Prasad et al., (2014) have identified the large scale climate development over the whole Holocene as well as two phases of prolonged drought. Here we present several shorter phases of climate changes superimposed on the large scale trend. The identified phases of drier and wetter climate can be correlated with other Asian palaeomonsoon records and palaeoclimate records from the North Atlantic region. A detailed description is given below (section 5.4.2) after a summary of the large scale climate development with additional remarks regarding the grain-size and amino acid data.

5.4.1. Large scale Holocene climate transition

The general long term palaeoclimate trend at the climatically sensitive Lonar Lake reconstructed by Prasad et al., (2014) starts with a drying period that probably coincides with the Younger Dryas at ~ 11.4 cal ka, which marks a dry period prior to the beginning of the Holocene in many geological records of India and adjacent regions (Overpeck et al., 1996; Bar-Matthews et al., 1997; Wei and Gasse, 1999; Gasse, 2000; Wang et al., 2001; Morrill et al., 2003; Sharma et al., 2004; Dykoski et al., 2005; Demske et al., 2009). Median grain-size of this section is low indicating low energy transport, which is probably due to dry conditions with reduced sediment input by run-off and precipitation fed streams and enhanced aeolian deposition. High LI values indicate strongly degraded OM in these sediments, and the high Ox/Anox ratios point to subaerial decomposition of the OM. Thus, the bottommost sediment section most likely represents a palaeosol.

The beginning of the Holocene is marked by a transition from dry to wet climate with an abrupt increase in monsoon strength after ~11.4 cal ka (Prasad et al., 2014). The phase of monsoon onset and strengthening is reflected in the sediments by high lithogenic input, which was eroded from the sparsely vegetated crater walls and transported to the dried out lake bed. The values of the biogeochemical parameters and the grain-sizes are comparable to those of the underlying soil, and thus indicate high contribution of eroded soil material to the sediments. On top of this section, few gaylussite crystals can be found, denoting a drier phase at ~ 11.1 cal ka.

Subsequently, the early Holocene between 11.1 and 6.2 cal ka is characterised by wet conditions (Fig. 5.4). The sediments of this section show low lithogenic contribution, and consequently low sedimentation rates. Thus, the section represents a deep lake with less eroded material reaching the sampling site. A deep lake developed quickly after 11.1 cal ka as is obvious from seasonally laminated sediments (Prasad et al., 2014). The median grain-size values indicate a shift to medium silt, and thus to slightly coarser material. This might be due to higher energy transport during strong rainfall events. The aquatic productivity was low during this phase, as shown by the high C/N ratios (mean = 30.1), which denote dominant contribution of terrestrial OM. Since 9.9 cal ka the $\delta^{13}C_{org}$ values stabilised on a relatively low level (mean = -20.9‰) indicating a C_3 dominated vegetation in the catchment of the lake. The predominantly low LI and Ox/Anox values of the section and the increasing $\delta^{15}N$ values between 9.1 and 6.2 cal ka point to extended anoxia in the water column and the sediments.

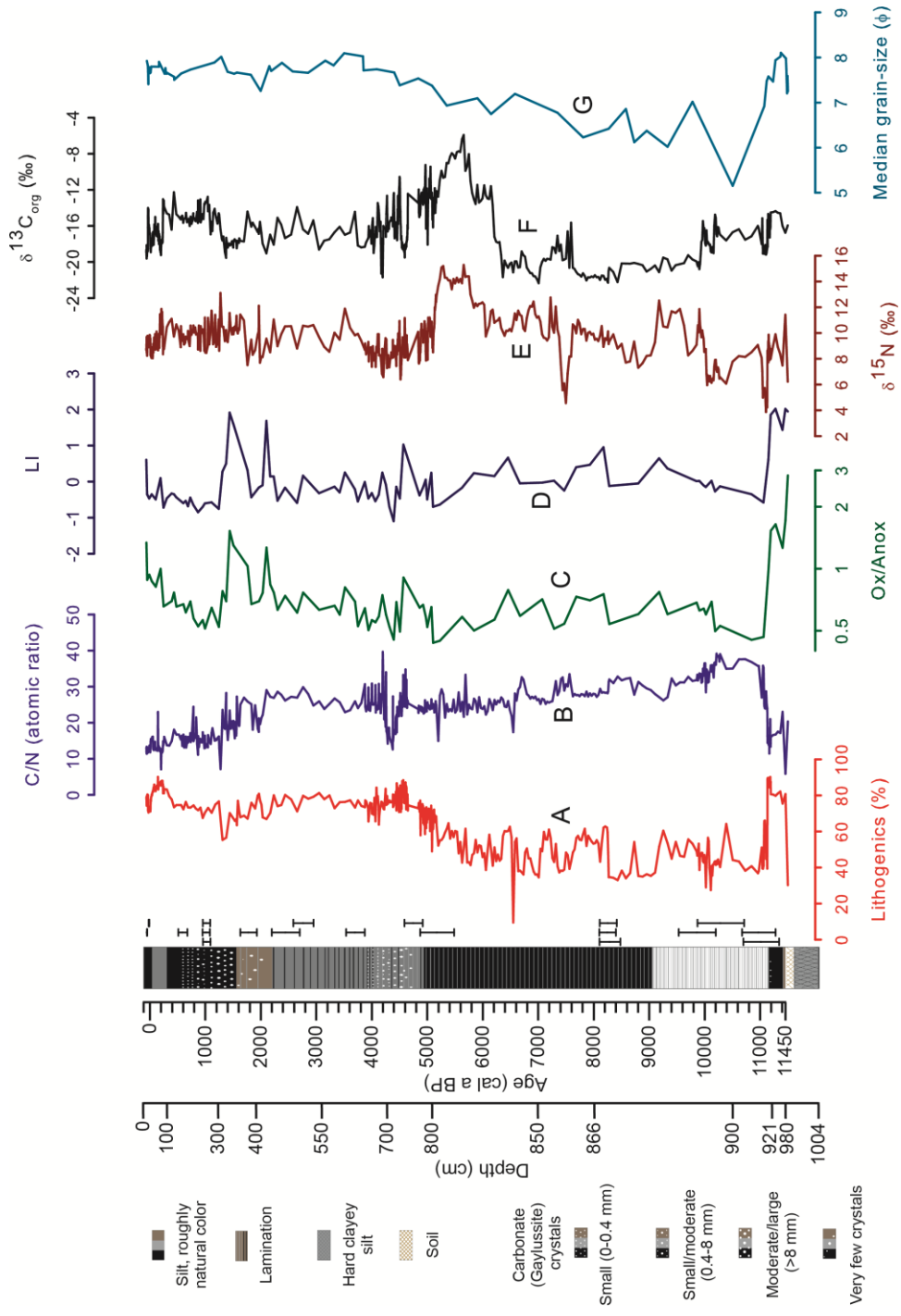

Fig. 5.2: Summary of the analytical results: A) Schematic lithology of the Lonar Lake core and down-core variation in lithogenic contribution; B) C/N ratio; amino acid derived indices C) Ox/Anox and D) LI; E) stable nitrogen; and F) carbon isotopic ratios of bulk organic matter; and G) median grain-size. C/N, $\delta^{13}C_{org}$, and $\delta^{15}N$ were reported by Prasad et al., (2014); gaylussite crystal occurrence was reported by Anoop et al., (2013b). Error bars indicate the standard deviation range (2σ) of calibrated radiocarbon dates.

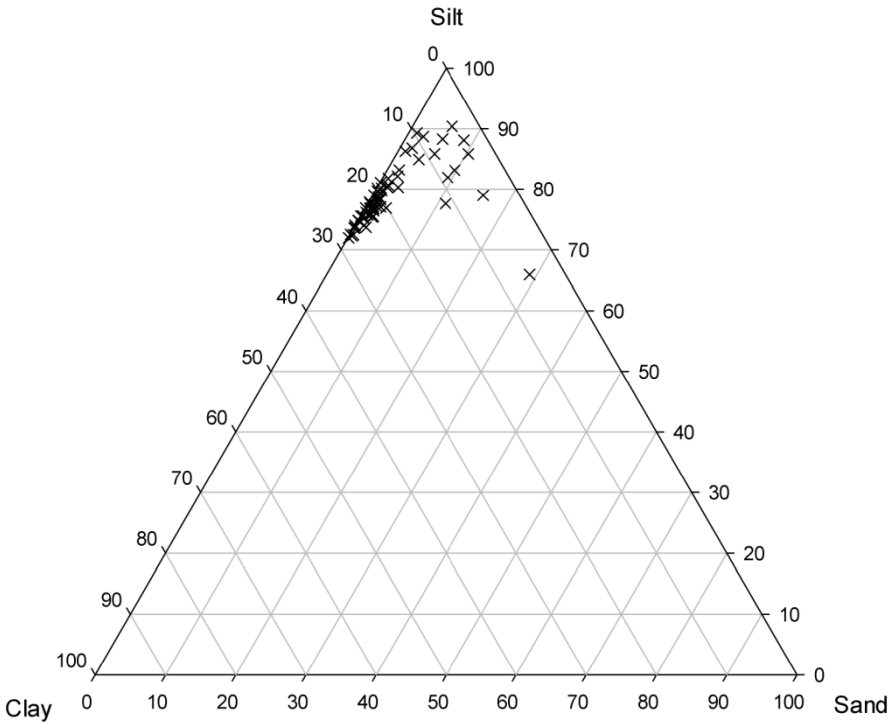

Fig. 5.3: Ternary diagram showing the percentages of the different grain-size classes (clay, silt, sand) of the analysed sediment samples of the Lonar Lake core sediment.

The time slice between 6.2 and 3.9 cal ka is regarded as being a transitional phase between wet climate during the early Holocene and dry climate during the late Holocene. This time slice shows two drying phases accompanied by strong water body reduction between 6.2 and 5.2 cal ka and between 4.6 and 3.9 cal ka, respectively. The former drying phase is most obvious from high $\delta^{13}C_{org}$ and $\delta^{15}N$ values, whereas the latter shows elevated lithogenic contribution and gaylussite crystal precipitation (Fig. 5.4), which indicates strongest lake level decline.

Following the climate transition between 6.2 and 3.9 cal ka, evidence of relatively dry climate persists until today. Elevated $\delta^{13}C_{org}$ values, lithogenic contribution, Ox/Anox ratios, and finer median grain-sizes indicate drier conditions compared to the early Holocene. The lithogenic contribution and the Ox/Anox ratios denote a shallow lake, and the $\delta^{13}C_{org}$ values imply a dominance of C_4 catchment vegetation. The grain-size data indicate weaker monsoon rains causing lower transport energy. Additionally, the alluvial fan in the north-east of the lake might have been exposed due to the lower lake level, possibly reducing the velocity of the streams that enter the lake from the north-east and east. Probably, this effect has also reduced the distance between the sampling site and the source of fine sediment (alluvial fan/stream mouth) causing a shift to finer grain-sizes and increasing the sedimentation rate. A phase of exceedingly dry conditions is indicated by the reoccurrence of evaporitic gaylussite crystals between 2.0 and 0.6 cal ka (Anoop et al., 2013b; Prasad et al., 2014). The climate

information of the younger part of the core might be mirrored to some extent due to anthropogenic interferences, as for example eutrophication and deforestation. A persistent decrease in C/N ratio since 1.3 cal ka indicates permanently elevated nutrient supply to the lake, which cannot be observed in the older parts of the core. Thus, a natural source of these additional nutrients seems unlikely. Since ca. 0.8 cal ka strong anthropogenic interference is evident from several near shore temples that have been built during the Yadavan rule approximately in the 12th century (Malu et al., 2005).

In general, the impact of long term Holocene climate change on palaeolimnology becomes notably obvious from the $\delta^{13}C_{org}$, lithogenic contribution, and grain-size values in our record and quite well delineates the insolation curve since the end of the Younger Dryas (Fig. 5.4), which additionally seems to drive the position of the summer Inter-Tropical Convergence Zone (ITCZ), and thus the strength and northwards extent of the summer monsoon rainfall (Fleitmann et al., 2007). One point that might be questioned is the characteristic of the climate deterioration at 6.2 cal ka, which is reflected in the Lonar Lake record by a sharp increase in $\delta^{13}C_{org}$, and thus points to an abrupt change, which was also reported from other records (Morrill et al., 2003). Nevertheless, we believe that this abrupt change is related to short-term climate variability and that the sudden increase in $\delta^{13}C_{org}$ at 6.2 cal ka most likely represents the transgression of a threshold in annual precipitation that led to the decline in terrestrial C_3 plant vegetation and the increase in C_4 plant contribution. Also, the changes in lake level as displayed by the lithogenic content in the sediments show a relatively smooth transition from a deep to a shallow lake. Additionally, the relatively short-term of the interval of drying between 6.2 and 3.9 cal ka is obvious from the subsequent change to wetter conditions indicated by subaquatic sedimentation and the disappearance of the gaylussite minerals. Thus, the transition from generally wet to drier climate after the Holocene climate optimum seems to occur gradually, and abrupt changes in the biogeochemical parameters are due to relatively short-term climate anomalies as postulated by Fleitmann et al., (2007) and reported from several regions (Hodell et al., 1999; Gupta et al., 2003; Hong et al., 2003; Gupta et al., 2005; Demske et al., 2009; Wünnemann et al., 2010).

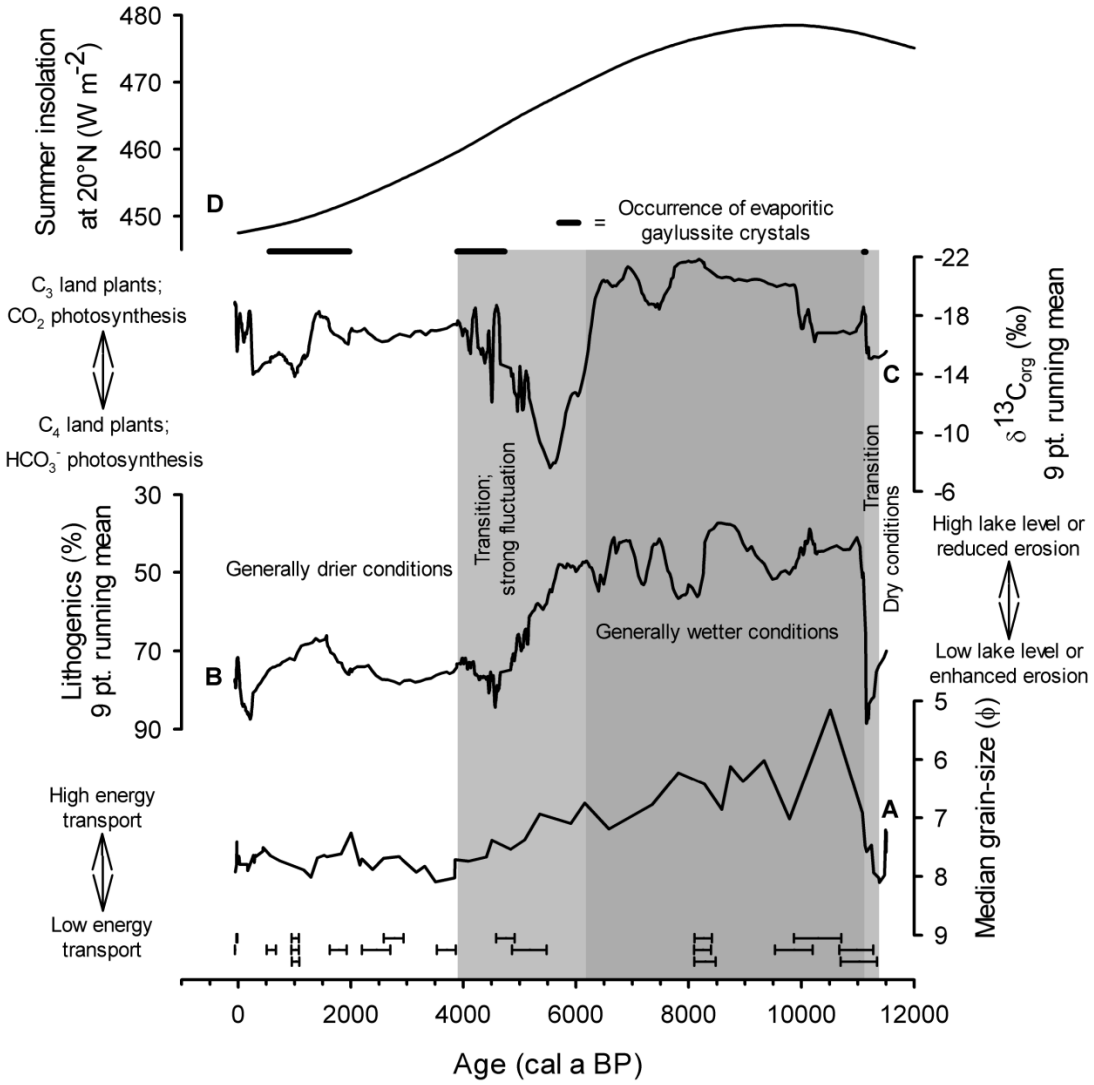

Fig. 5.4: Long term Holocene climate trend at Lonar Lake as interpreted from our data: Comparison of median grain-size (A); lithogenic contribution (B); $\delta^{13}C_{org}$ values (C) (Prasad et al., 2014); and summer (JJA) insolation at 20° N (D) (Berger and Loutre, 1991). Error bars indicate the standard deviation range (2σ) of calibrated radiocarbon dates.

5.4.2. Centennial scale Holocene climate variability

Besides the large scale millennial climate trend, several smaller centennial scale climate variations can be reconstructed from the Lonar Lake bioclastic record. While the role of ENSO and shifts in the position of the Indo Pacific Warm Pool (IPWP) in causing the prolonged droughts during 4.6 to 3.9 and 2.0 to 0.6 cal ka have been discussed by Prasad et al., (2014), the short-term climate variability identified in our new dataset cannot be explained by the same mechanism necessitating the search for alternative causal mechanisms. Several studies have identified links between Asian monsoon and North Atlantic palaeoclimate with cold events in the North Atlantic region, as identified by ice-rafted debris in deep sea cores (Bond et al., 1997 and 2001), being linked to decreases in monsoon strength over Asia (Gupta et al., 2003; Hong et al., 2003; Dykoski et al., 2005; Fleitmann et al., 2007; Wang et al.,

2005). Nearly all Bond events are isochronally reflected by indications of short-term changes in monsoon strength in the proxies from Lonar Lake sediment core (Fig. 5.5). Since the centennial scale climate variations at Lonar Lake are reflected in different proxies and not all proxies show every phase of climate change, we calculated a Bioclastic Climate Index (BCI) that combines the Holocene course of the independent and climatically sensitive $\delta^{13}C_{org}$, lithogenic contribution, and combined amino acid proxy values. Since the variations in $\delta^{15}N$ and C/N values within the Lonar Lake record seem not to be predominantly driven by climate change or at least are considerably biased by other processes (see sections 5.3.5. (c) and (e)), we did not include them into the BCI calculation. The BCI shows the deviation from the mean values given in percent of the maximum variation of the respective proxy in the data set according to the formula:

$$\mathrm{BCI}\,(\%) = \frac{\Delta^{13}\mathrm{C}_{\mathrm{org}}\,(\%) + \Delta\mathrm{lith}\,(\%) + 0.5\,\mathrm{x}\,[\Delta\mathrm{LI}\,(\%) + \Delta\mathrm{Ox/Anox}\,(\%)]}{3}$$

with high values indicating drier and low values indicating wetter conditions. We used half of the sum of the LI and Ox/Anox values to not overstate the variability in amino acid data as both values are calculated from the same data set, and thus are not fully independent. Further, linearly interpolated values for the amino acid derived proxies were used as these proxies were measured in a lower resolution than $\delta^{13}C_{org}$ and lithogenic contribution. Since the BCI also shows the long term palaeoclimate trend, a detrended curve was calculated to emphasise the centennial scale palaeoclimate variations (Fig. 5.6). The applicability of the BCI in reconstructing changes in precipitation is corroborated by its negative correlation (-0.55; $p < 0.01$), despite human interferences at Lonar Lake in modern times, with the all India rainfall record (ftp://www.tropmet.res.in/pub/data/rain/iitm-regionrf.txt) by applying a low-pass filter to the rainfall data and the Gaussian kernel based correlation analysis (NESToolbox for MATLAB used; Rehfeld et al., 2011). In addition to the BCI, the occurrence of evaporitic gaylussite crystals (Anoop et al., 2013b) was used to interpret the climatic changes at Lonar Lake since the gaylussite crystals exclusively indicate changes in Lonar Lake hydrology related to reduced available effective moisture.

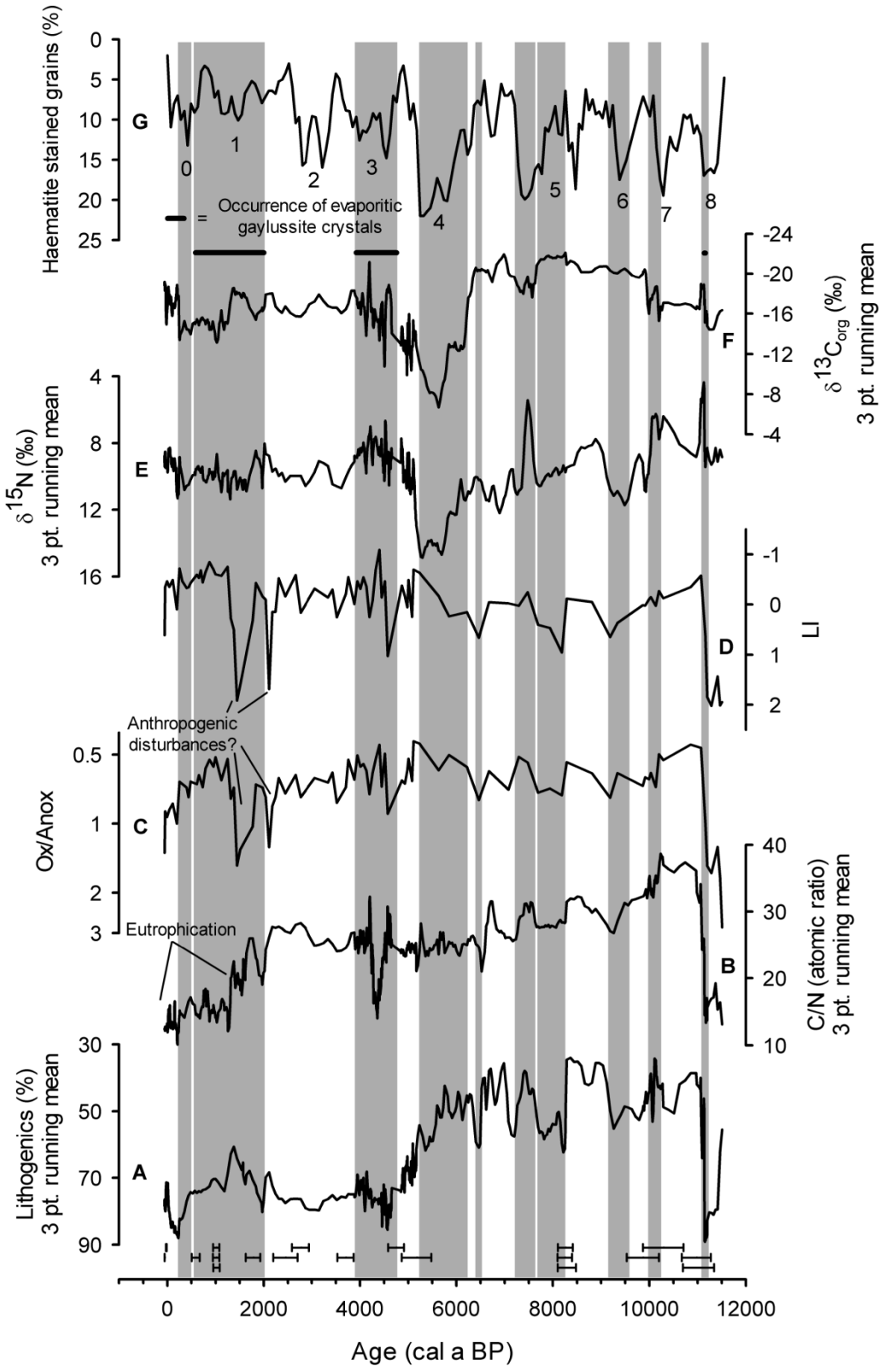

Fig. 5.5: Comparison of our data of lithogenic contribution (A), C/N ratio (B), Ox/Anox ratio (C), LI (D), $\delta^{15}N$ (E), and $\delta^{13}C_{org}$ (F) to the percentage of haematite stained grains (G) in core MC52, a climate record from the North Atlantic region (Bond et al., 2001). C/N, $\delta^{13}C_{org}$, and $\delta^{15}N$ were reported by Prasad et al., (2014); gaylussite crystal occurrence was reported by Anoop et al., (2013b). Numbers 0 – 8 designate cold events in the North Atlantic region (Bond events). Grey shaded intervals denote periods that are interpreted to be phases of climate deterioration at Lonar Lake. Error bars indicate the standard deviation range (2σ) of calibrated radiocarbon dates.

Largely, the changes in the de-trended BCI are coincident with the intervals of increased ice rafted debris in the North Atlantic (Bond et al., 2001). The oldest of the Holocene cooling events in the North Atlantic region, the Bond event 8, can be correlated with the occurrence of gaylussite crystals in the Lonar Lake core on top of the section that represents the phase of climate transition and monsoon onset after the soil formation (Fig. 5.5). The Bond event 7 is concurrently correlated to a double-peaked increase in $\delta^{13}C_{org}$ and to an increase in lithogenic contribution. The $\delta^{13}C_{org}$ increases are interpreted as changes in terrestrial vegetation to more C_4 plant abundance, indicating drier conditions. The subsequent decrease in $\delta^{13}C_{org}$ denotes the transition to C_3 plant domination, and thus wetter conditions during the early Holocene. A concurrent climate variation to Bond event 6 is indicated by elevated LI and Ox/Anox values as well as high $\delta^{15}N$ values (Fig. 5.5). The amino acid based indices reveal an increase in oxygen supply to the sediments at 9.15 cal ka, and the pollen record points to a dry phase, during which the whole sediment section of this subunit became exposed to oxic or even subaerial conditions, since only few pollen that are resistant to aerobic decomposition are preserved in the sediments older than 9.2 cal ka (Riedel & Stebich, in preparation). Enhanced oxygen supply could also be responsible for the elevated $\delta^{15}N$ values, since an increase in $\delta^{15}N$ during aerobic degradation was reported from in vitro (Lehmann et al., 2002) as well as from in vivo (Freudenthal et al., 2001) investigations. A drying trend in the Asian tropical region during this so called 9.2 ka event was reported before and also related to a cooling trend in the North Atlantic region (Dykoski et al., 2005; Fleitmann et al., 2008). Elevated LI, Ox/Anox, and lithogenic contribution values in the Lonar Lake core comparable to the values at 9.2 cal ka can be found during 8.2 – 7.7 cal ka (Fig. 5.5). This phase correlates within dating uncertainties with a cool phase in the North Atlantic situated at the early stage of Bond event 5. The relatively short cool phase during the early stage of Bond event 5 is also known as the 8.2 ka event. Similar to the 9.2 ka event, a cooling trend in the North Atlantic region was accompanied by a drying trend in monsoon-influenced Asia (Alley et al., 1997; Wang et al., 2005). It is widely accepted that the cooling during the 8.2 ka event was caused by a pulse of freshwater that burst out of the Lakes Agassiz and Ojibway through the Hudson Straight, which weakened the thermohaline Atlantic meridional overturning circulation, thus leading to the climate anomaly (Barber et al., 1999; Teller et al., 2002; Kendall et al., 2008). The peak at the later stage of Bond event 5 is correlated with elevated $\delta^{13}C_{org}$ values and an increase in lithogenic contribution (Fig. 5.5). Elevated LI, Ox/Anox, and lithogenic contribution at 6.45 cal ka correlate within dating uncertainties with

a cool phase at the beginning of Bond event 4. The following intensification of the North Atlantic cold spell (Bond event 4) and the Bond event 3 are reflected by the most obvious centennial scale climate changes shown by our data. These two phases constitute the climate transition from generally wet to generally drier conditions during the mid-Holocene (see section 5.4.1) at 6.2 – 5.2 cal ka and 4.6 – 3.9 cal ka, respectively, which is consistent with reports of southward migration of the ITCZ, monsoon weakening, and related drying trends from various locations of the Asian monsoon realm (Enyel et al., 1999; Morrill et al., 2003; Parker et al., 2004; Prasad and Enzel, 2006; Staubwasser and Weiss, 2006; Fleitmann et al., 2007; Demske et al., 2009; V. Prasad et al., 2014). The older phase, concordant with Bond event 4, is characterised by a strong increase in $\delta^{13}C_{org}$ with two sudden shifts, the first by ~ 8‰ at about 6.2 cal ka and the second by ~ 4‰ at about 5.7 cal ka. The second shift in $\delta^{13}C_{org}$ is accompanied by an increase in $\delta^{15}N$ of ~ 2‰. The increase in $\delta^{13}C_{org}$ is most likely linked to two major factors. A shift in terrestrial vegetation from C_3 dominance to more C_4 contribution seems to explain the increase in $\delta^{13}C_{org}$ at 6.2 cal ka since S. Sarkar (in preparation) found an increase in $\delta^{13}C$ of long chain n-alkanes. The second increase in $\delta^{13}C_{org}$ at 5.8 cal ka results in $\delta^{13}C_{org}$ values that even exceed the values of C_4 land plants, and thus the second shift cannot be explained by a further change in the terrestrial fraction of the OM alone. Hence, the elevated $\delta^{13}C_{org}$ values seem to be related to a change in the aquatic system. A reasonable explanation is an increase in pH, as a result of an increased salt concentration in the water during lake level decline in response to relatively dry conditions, and a related shift in the dominant photosynthetic inorganic carbon source from CO_2 to HCO_3^- (Prasad et al., 2014). The assumption that elevated pH is responsible for the $\delta^{13}C_{org}$ increase is corroborated by the concurrent increase in $\delta^{15}N$. In anoxic waters, which most probably were present during the related time as indicated by the low Ox/Anox ratios, high pH causes ammonia volatilisation that leads to a $\delta^{15}N$ increase of aquatic OM (Casciotti et al., 2011). After 5.2 cal ka, the $\delta^{13}C_{org}$ and $\delta^{15}N$ values gradually decrease, which could indicate a slightly wetter period from 5.2 to 4.6 cal ka but which could also be due to the disappearance of the anoxic water layer as a response to further lake level decline. Subsequently, the dry phase between 4.6 and 3.9 cal ka, which has been correlated with an expansion of the IPWP (Prasad et al., 2014) but also partly correlates with Bond event 3, does not show as elevated $\delta^{13}C_{org}$ and $\delta^{15}N$ values as the previous dry episode. This seems to be related to the disappearance of the anoxic water layer, and hence the lack of ammonia volatilisation, producing ^{15}N enriched ammonium, and the lack of methanogenesis, producing ^{13}C enriched CO_2. The strongest indications for dry climate during this period are the occurrence of evaporitic gaylussite

crystals throughout this zone (Anoop et al., 2013b) and the elevated lithogenic content in the sediments indicating low lake level. However, the decreased $\delta^{13}C_{org}$ values are responsible for the lower BCI values during this time slice even though the occurrence of gaylussite crystals indicates drier conditions compared to the time slice 6.2 to 5.2 cal ka (Fig. 5.6). Subsequently, the only Bond event that does not show a marked complement in the Lonar Lake record is Bond event 2 between ca. 3.5 and 2.7 cal ka. This might be due to the fact that generally drier conditions had been established after the very dry period correlated with Bond events 4 and 3. Thus, the wetter period during ca. 3.9 to 3.5 cal ka did not provide enough excess in precipitation over evaporation to establish a high lake level with strong anoxic hypolimnion and vegetation dominated by C_3 plants. Hence, if the period between 3.5 and 2.7 cal ka was drier at Lonar Lake compared to the period 3.9 to 3.5 cal ka, no significant changes in our proxies could be expected as long as the lake does not desiccate. Nevertheless, two minor positive shifts in $\delta^{13}C_{org}$ and contemporaneous increases in the amino acid derived indices result in two BCI peaks that possibly indicate drier conditions at Lonar Lake corresponding to the double-peaked North Atlantic cooling event during Bond event 2 (Fig. 5.6). The following period of strong evidence of climate deterioration at Lonar Lake is again marked by evaporitic gaylussite crystals and was dated at an age of 2.0 – 0.6 cal a (Anoop et al., 2013b; Prasad et al., 2014). Thus, it can be correlated with Bond event 1 but exceeds the time span of the Bond event by about 500 years, which is in accordance with the report of decadal scale famines in India during the 14^{th} and 15^{th} century (Sinha et al., 2007). However, this strong drying event is also coincident with an increase in ENSO like conditions (Moy et al., 2002; Rein et al., 2005) in the Pacific (Prasad et al., 2014) suggesting complex links to the North Atlantic and to the Pacific forcings. The dry climate of this period, as indicated by the gaylussite precipitation, is not well reflected in the BCI. This is due to the eutrophication, which causes the development of lake water anoxia and a related descent of the amino acid derived proxy values. The BCI indicates an abrupt transition to wet climate at 1.3 cal ka (Fig. 5.6), which is due to the biased amino acid indices. Thus, the BCI values during the phase of strongest anoxia between 1.3 and 0.3 cal ka, as indicated by the Ox/Anox ratio, are shifted to lower values, hence indicating wetter climate than actually prevailed. Finally, Bond event 0 is concurrently correlated to increased $\delta^{13}C_{org}$ and lithogenic contribution values between 440 and 240 cal a (Fig. 5.5). Again, anthropogenic interference cannot be ruled out here in the younger part of the core. But, since the two-step increase in $\delta^{13}C_{org}$ at 440 and 260 – 245 cal a and the subsequent decrease in $\delta^{13}C_{org}$ correlate with two minima in solar activity, the Spörer Minimum and the Maunder Minimum, and a subsequent increase in solar activity, it seems

likely that these changes are driven by monsoon strength weakening during the 'Little Ice Age' (Bond event 0) and the subsequent climate amelioration (Anderson et al., 2002; Agnihotri et al., 2008).

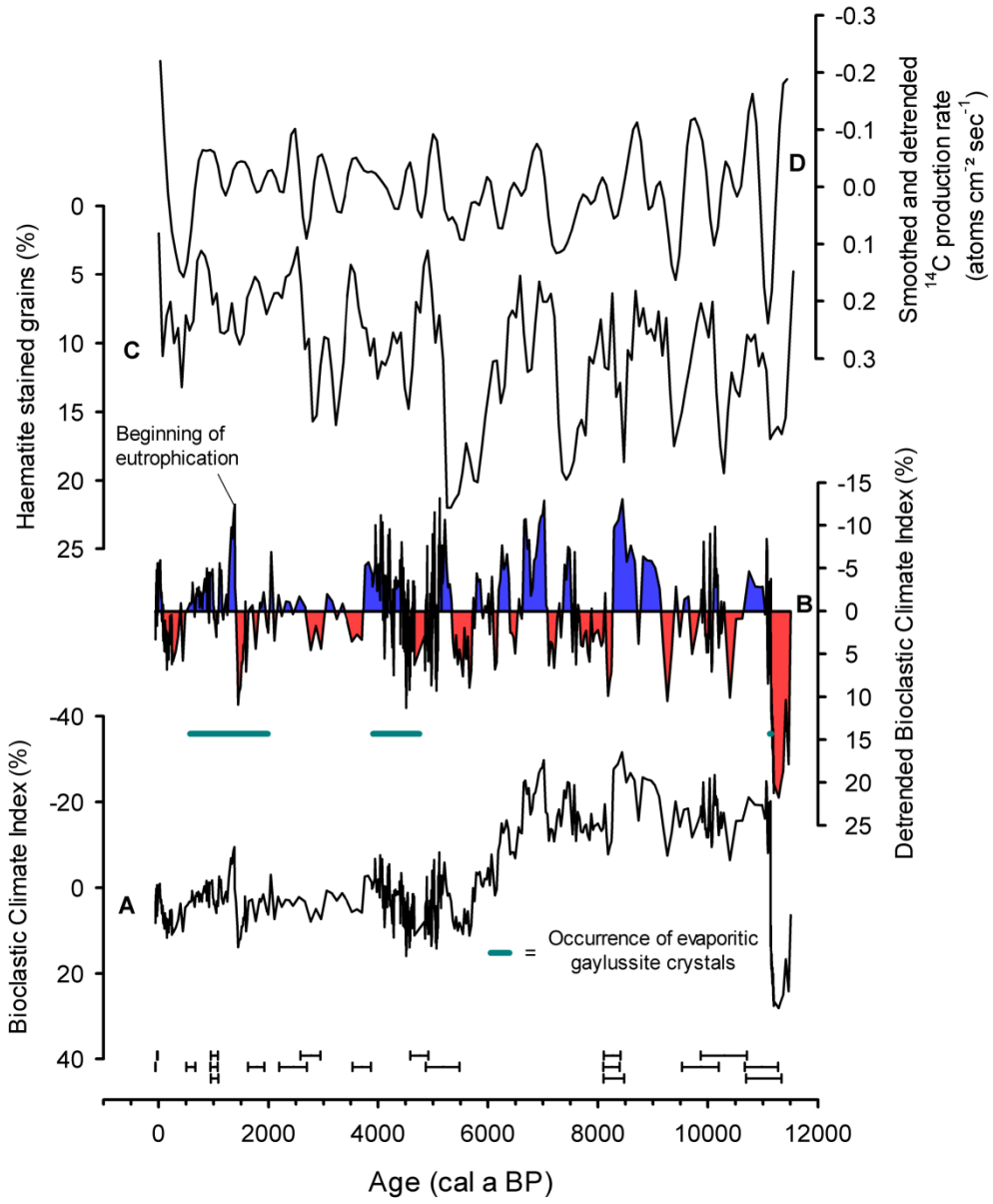

Fig. 5.6: Comparison between the Bioclastic Climate Index (BCI) (A), the detrended BCI (B), the climate record from the North Atlantic Region (C), and the detrended and smoothed ^{14}C production rate (D) (Bond et al., 2001). Detrending of the BCI was performed by applying a Gaussian kernel based filter with a kernel bandwidth of 500 years to the values of the time slice <11.14 cal ka The values of the time slice ≥ 11.14 cal ka were adjusted by subtracting the lowest value of this time slice from the data since a rapid shift in BCI values at 11.14 cal ka occurs. Red and blue colour fills indicate relatively dry and wet phases, respectively. Error bars indicate the standard deviation range (2σ) of calibrated radiocarbon dates.

Multiple proxies (Prasad et al., 2014; this study) indicate that there are both tropical and high latitude influences on the ISM that can be finally linked to solar variability. The fact that all phases of climate cooling in the North Atlantic region identified by Bond et al., (2001) are largely contemporaneously (within dating uncertainties) accompanied by climate

deteriorations at Lonar Lake, as inferred from changes in BCI and evaporative gaylussite crystal precipitation, indicates that the North Atlantic and the Indian monsoon climate systems were linked during the Holocene. Evidence for contemporaneous climate variability in the Asian tropics and the North Atlantic region during the Holocene has also been reported from annually laminated, precisely dated stalagmites (Liu et al., 2013). A reasonable explanation for such a concurrent linkage is an atmospheric tele-connection, which has the potential to connect the two systems without substantial delay. Coupled ocean-atmosphere climate simulations could show that cooling of the northern hemisphere results in reduced summer monsoon rainfall over India (Broccoli et al., 2006; Pausata et al., 2011). This is due to the development of an asymmetric Hadley cell accompanied by a southwards shift of the ITCZ, which causes an enhanced net energy (heat) transport from the tropics to the cooled northern hemisphere (Broccoli et al., 2006). Such a southwards shift of the ITCZ would lead to weaker-than-normal Asian summer monsoon, and thus might be the mechanism responsible for the Asian-North Atlantic climate connection indicated by our data. Another mechanism that might have contributed to the connection could be the effect of northern hemisphere cooling on Eurasian snow cover if the cold phases recorded in the North Atlantic region have caused enhanced snow accumulation over Eurasia. Modern observations and model calculations show that extent and duration of Eurasian snow cover affect the Asian monsoon system (Bamett et al., 1989; Bamzai and Shukla, 1999). Prolonged Eurasian snow cover during spring cools the overlying air since energy is used to melt the snow and to evaporate the melt water instead of warming the land surface, thus having a downwind effect on South Asian landmasses and weakening the thermal gradients between land and ocean, which causes a weaker-than-normal summer monsoon (Barnett et al., 1989).

The reason for the North Atlantic cooling events might be reduction in insolation triggered by reduced solar output. This was postulated by Bond et al., (2001) who found that the North Atlantic cooling events correlate with smoothed and detrended ^{14}C and ^{10}Be production rates (^{14}C shown in Fig. 5.6), which are inversely correlated with solar output (Beer, 2000). They also found a ca. 1500 year periodicity of the palaeoclimate variation in their record, which is in agreement with palaeoclimate variations reconstructed from other records (see Mayewski et al., 2004) and the link between periodicities in climate archives and solar activity (Soon et al., 2014). To compare these findings with our data, we have calculated the major frequencies in our climate proxy data as well as the correlation between the BCI and the ^{14}C production rate. Before the spectral analysis, the long term climate trend was removed from the whole time series by applying a Gaussian kernel based filter with a kernel

bandwidth of 500 years. The correlation between the detrended ^{14}C production rate (Bond et al., 2001) and the detrended BCI is relatively high (0.63), thus supporting the hypothesis that climate variability in India is influenced by changes in solar irradiance (Gupta et al., 2005). The power spectral analysis revealed a 1519 year periodicity besides 120 year, 274 year, 435 year, and 822 year periodicities in our data set (Fig. 5.7). Thus, a periodicity in climate variability similar to the "1500-year cycle" observed by Bond et al., (2001) is present in our record and corroborates the connection of the North Atlantic and the Indian monsoon palaeoclimates. The other periodicities seem to be related to solar cycles. The periodicities of 120 and 435 years equal eccentricity periodicities (122 and 432 years), whereas the 822 year cycle might be related to precession and obliquity cycles of 840 years (Loutre et al., 1992). Due to the difference, it is questionable if the 274 year cycle in our data set is related to the 245 year cycle of eccentricity, obliquity, and precession (Loutre et al., 1992), but the possibility should not be excluded. In summary, we conclude that while IPWP forcings are important in causing millennial scale periods of prolonged dryness during the mid and late Holocene in central India (Prasad et al., 2014), the subtle short-term changes identified by the BCI indicate the presence of North Atlantic forcings as well.

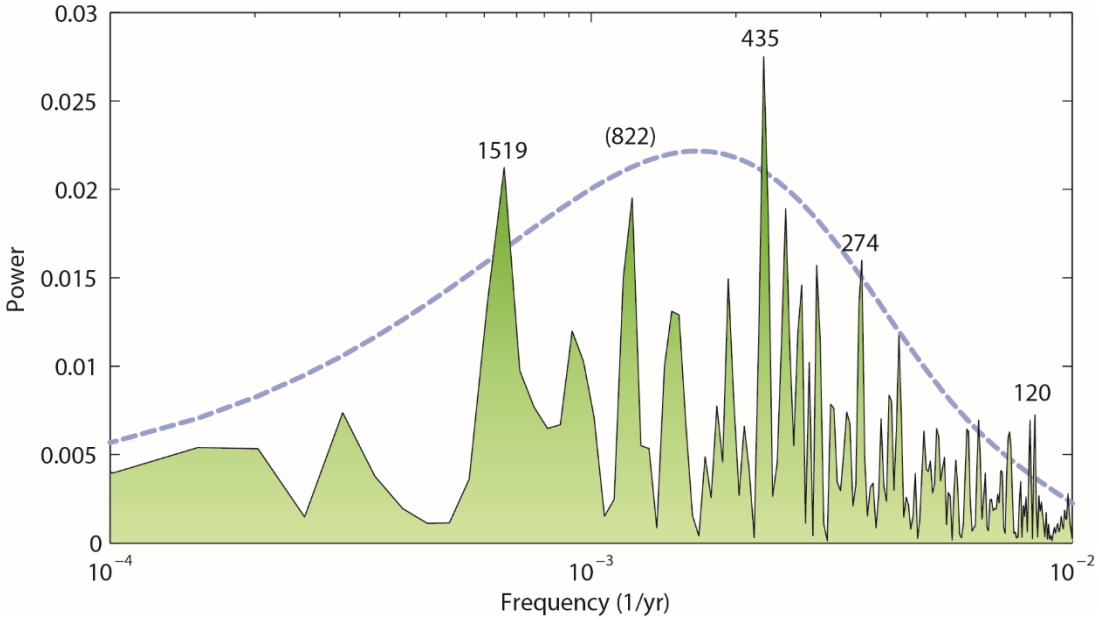

Fig. 5.7: Powerspectrum indicating the most prominent periodicities within the Bioclastic Climate Index data set. The blue line represents the 90% confidence level of statistical significance.

5.4.3. Implication for the archaeological history

Our palaeoclimate reconstruction from Lonar Lake gives some clues according to the ongoing discussion about the role of mid-Holocene climate change on the de-urbanisation and abandonment of most Mature Harappan cities in the Indus valley region and the dislocation of settlements during the Late Harappan phase after 3.9 cal ka especially to the western Ganga

Plains (Possehl, 1997). Singh, (1971) postulated that the development and expansion of the Harappan Civilisation was strongly related to favourable climate conditions and to severe climate deterioration during its decline. However, Possehl, (1997) and Enzel et al., (1999) proposed that the influence of climate to the fate of the Harappan Civilisation was minimal or absent. But, since the capture of rivers that contributed to the water supply of the Harappan cities caused by tectonic activity during the time of Harappan decline could not be confirmed (Clift et al., 2012) and since almost all of these rivers were monsoon fed (Tripathi et al., 2004; Giosan et al., 2012) vulnerability of the urban Harappan sites to weakened monsoon seems likely. And while Staubwasser and Weiss (2006) argue for a direct link between the decline of the Harappan Civilisation and the relatively short dry episode at about 4.2 cal ka, others hypothesise that the gradual climatic decline between ~ 5 and 4 cal ka caused an adaption of the cultivation methods to reduced summer monsoon rainfall (Gupta et al., 2006; Madella and Fuller, 2006; MacDonald, 2011) and related diminution in seasonal flooding (Giosan et al., 2012).

Our data support the view that the rise of the Harappan Civilisation did not occur during a phase of wettest climate (Enzel et al., 1999) but that the development of the huge cultural centres was more likely linked to the climate deterioration during the transition from the wetter early Holocene towards the drier late Holocene. A similar development was reconstructed for the rise and fall of the Mayan cities in Central America where the spread of urban centres coincided with a phase of declining humidity between 1.3 and 1.15 ka and the abandonment started subsequently at ~ 1.15 ka probably due to persistent dry conditions (Kennett et al., 2012). The development of highly populated centres in the Indus Valley was possibly due to the reduction of annual rainfall and the concentration of cultivable acreage along the rivers that provided enough water for agriculture in the form of seasonal flooding to supply the resident population. The fact that diminished available effective moisture at Lonar Lake between 4.6 and 3.9 cal ka correlates well with other records from the Asian monsoon realm (Hong et al., 2003; Gupta et al., 2005; Demske et al., 2009; Wünnemann et al., 2010) displays the supra-regional character of this drying trend and corroborates the assumption that the climatically sensitive sites especially in the relatively dry regions of the western Harappan territories were forced to adapt to severe shortages in water supply as for example to rivers that became ephemeral. A consequent change in agricultural strategy towards cultivation of crops that called for a more extensive land use and could not support the highly populated centres seems to be a reasonable explanation for the gradual decline of the Harappan Civilisation.

5.5. Conclusions

The analyses of the C/N, $\delta^{13}C_{org}$, $\delta^{15}N$, lithogenic contribution, grain-size, and amino acid degradation indices LI and Ox/Anox ratio values in combination with the evaporitic gaylussite crystals from the sediment core samples of the climatically sensitive Lonar Lake revealed several environmental and hydrological changes during the Holocene that can be related to climate shifts.

The long term Holocene climate development at Lonar Lake shows three phases. The first phase is characterised by dry conditions at about 11.4 cal ka followed by a transition to wetter conditions during the time of monsoon onset and strengthening (~ 11.4 – 11.1 cal ka). The second phase comprises the early Holocene and shows wet conditions with high lake level and C_3 dominated catchment vegetation. A subsequent transition to drier conditions occurs between ca. 6.2 and 3.9 cal ka. The late Holocene represents the third phase, which is characterised by relatively dry conditions as indicated by lower lake level and terrestrial vegetation with high C_4 plant contribution. Comparison of these findings with other climate records from South Asia and the North Atlantic region displays a strong similarity, with strong monsoon phases in Asia correlating with warm periods in the North Atlantic region and weak monsoon correlating with colder climate in the North Atlantic region (Johnsen et al., 2001). These climatic conditions seem to be closely related to the northern hemisphere insolation, which additionally seems to drive the position of the ITCZ, and thus the northwards extent of the summer monsoon rainfall (Fleitmann et al., 2007).

The long term climate trend is superimposed by several shorter term climate fluctuations. Some of these fluctuations have also been observed in other high-resolution climate records from Asia, and they can be correlated with the North Atlantic Bond events (Bond et al., 1997 and 2001). The correlation is the same as observed for the long term trend with cold periods in the North Atlantic correlating with dry periods over South Asia and vice versa. All the 9 Bond events during the Holocene are isochronally (within dating uncertainties) reflected in the Lonar Lake record. This point to a connection between the two climate systems or to an identical trigger of climate variability. The fact that the Bioclastic Climate Index (BCI) quite well delineates the solar output proxy ^{14}C production rate (Bond et al., 2001) corroborates the assumption that variations in solar activity triggered centennial scale variability of the Indian monsoon climate during the Holocene. However, the amplitude of the BCI not solely depends on the centennial climate variability but is also influenced by the long term Holocene climate variability, other tele-connections (e.g., Pacific climate;

Prasad et al., 2014), local climate phenomena, changes in environmental conditions, and anthropogenic interferences. Thus, the amplitude of the BCI curve does not always reliably display the absolute strength of climate variability.

With respect to the archaeological record from India and Pakistan, our results support the hypothesis that the rise of the Harappan Civilisation was linked to the climate deterioration during the transition from wetter climate of the early Holocene to drier climate of the late Holocene. We believe that the decline of the urban centres especially in the western Harappan territories might best be explained by a gradual reduction of summer monsoon between ~ 4.6 and 3.9 cal ka and a consequent adoption of new agricultural practices and crops that demanded a social adjustment.

5.6. Acknowledgements

The authors like to thank R. Niederreiter of UWITEC in Mondsee, Austria and K. Deenadayalan and Md. Arif of the IIG in Mumbai for their support during field work, F. Langenberg and N. Lahajnar of the IfGeo in Hamburg and U. Kegel of the GFZ for their assistance during laboratory analyses. Special thanks go to S. Pinkerneil of the GFZ for sample preparation and elemental and stable isotope measurements. We thank two anonymous reviewers, who provided very informative comments, and thus helped to improve the quality of the article. We gratefully acknowledge the cooperation by the Forest and Wildlife Department of Maharashtra State, India. Funding was provided by the German Research Foundation (Grants: GA 755/7-1; PR 755/7-2) within the framework of the project "Himalaya: Modern and Past Climates" (HIMPAC; FOR 1380).

Table

Table 5.1: Radiocarbon ages from the Lonar Lake core; first published by Prasad et al., (2014). Calibration of the ^{14}C dates was carried out using the program OxCal, interpolating with the INTCAL04 and NH3 calibration curves (Bronk Ramsey, 2008).

Lab No.	Material	Composite Depth (cm)	^{14}C date (2σ) (^{14}C yr)	Calendar age range (2σ) (cal yr)
Poz 44133	Bulk	0	116.79 ± 0.84	-55 to -59
Poz 44142	Wood	20	143.51 ± 0.0086	-16 to -28
Poz 44143	Bulk		107.88 ± 0.76	
Poz 27189	Wood	163.5	564 ± 60	669 to 505
Poz 41602	Bulk		760 ± 360	
Poz 41605	Gaylussite crystal	266	1105 ± 60	1076 to 944
Poz 27190	Wood	266.5	1105 ± 60	1079 to 947
Poz 41603	Bulk		1075 ± 60	
Poz 41604	Wood	267.5	1100 ± 60	1086 to 950
Poz 41607	Wood	383.5	1840 ± 70	1924 to 1624
Poz 27236	Wood	482	2315 ± 70	2696 to 2192
Poz 44141	Bulk	511.5	2680 ± 70	2944 to 2580
Poz 44226	Bulk	612	3470 ± 70	3867 to 3531
Poz 27237	Wood	778	4185 ± 70	4911 to 4583
Poz 27191	Wood	820	4600 ± 120	5479 to 4867
Poz 41611	Wood	870	7420 ± 80	8396 to 8096
Poz 27193	Wood	870.5	7460 ± 180	8412 to 8104
Poz 27194	Wood	872	7410 ± 200	8476 to 8100
Poz 27373	Wood	882.5	8880 ± 120	10197 to 9529
Poz 27253	Wood	899	8990 ± 160	10707 to 9867
Poz 27238	Leaf	902	9740 ± 100	11274 to 10670
Poz 27192	Wood	904	9570 ± 200	11338 to 10694

Chapter 6: Conclusions and Future Perspectives

6.1. Conclusions

My thesis is a compilation of four separate manuscripts, dealing with the monsoon variability during the late Quaternary period. The primary aim was to identify climate sensitive proxies, and apply them to reconstruct palaeo-environment/climate for developing a better understanding of the monsoon-westerlies dynamics in the ISM realm. Specifically, the following objectives were addressed:

1. Establishing a link between modern lake sediment properties and environmental conditions to identify climate sensitive proxies.

My study dealt with the geochemical, organic, mineralogical and sedimentological investigations of the catchment and the lake surface sediments from the Tso Moriri Lake, (NW Himalayas), and evaluated the potential of measured parameters for palaeoenvironmental reconstruction i.e. proxy identification. Additionally, hydrochemical analysis of the lake and feeder stream waters and investigation of surface sediments was undertaken to obtain information on the present limnological status and factors controlling the modern sedimentation processes within the lake. The Tso Moriri Lake basin showed a distinct thermal stratification and an oxygenated bottom, which could be linked to the mixing of the lake waters. Hydrochemistry of feeder springs showed that the lithology of the catchment area controls the water ionic composition, whereas evaporation processes control the lake water chemistry. The influence of evaporation is evident from the presence of authigenic aragonite in lake surface sediments, and enrichment of stable isotopes (δD and $\delta^{18}O$) in the lake waters when compared to the inflow streams and precipitation. Based on our investigations, several independent proxies have been developed for the palaeoenvironmental reconstruction.

- The authigenic carbonates and Sr/Ca ratio can be used to infer changes in salinity.
- Distinction between authigenic and allochthonous organic matter based solely on C/N values is difficult in this oligotrophic lake, limiting the application of organic isotopes for palaeoenvironmental reconstruction.
- Grain size variability within the lake basin reflects the energy and mode of transport and can also be used as an indicator of shoreline proximity during shallow lake phases.
- Due to dynamic transport processes within the lake and the variation in the grain size of the sediments, Si/Al and CPA (Chemical Proxy of Alteration) were selected as useful weathering indices.

2. Using the identified proxies to reconstruct ISM and westerlies variability on millennial to decadal timescales.

My results provided a high-resolution palaeoclimate reconstruction from the Tso Moriri Lake, NW Himalaya. The geochemical, mineralogical and sedimentological investigations on the core sediments revealed the climate forced hydrological variability *i.e.* ([Precipitation+Melt water=I]/[Evaporation=E]) (I/E) and lake level changes since glacial period (~26 cal ka). Based on, autochthonous and allochthonous mineralogy, abundances of macrophytes and grain size variability, multiple hydrological stages were identified in the Tso Moriri Lake (Chapter 3).

My work indicated that the early Holocene intensification was visible in both NW Himalaya and central India though the wettest phase ended earlier in the former (ca. 8.5 cal ka) as compared to the latter (ca. 6 cal ka). The central Indian Lonar Lake record showed evidence of multiple abrupt events throughout the Holocene, as well as two periods of extended drought (4.6-3.9 cal ka and 2.0-0.6 cal ka) during the late Holocene. These "extremes" do not appear to be recorded in the high altitude Tso Moriri Lake, probably due to the buffering effect of snowmelt, stronger westerlies, and/or weaker ISM influence in the NW Himalaya during the late Holocene.

3. Identifying the impact of seasonal precipitation and meltwater to the local hydrological balance.

The selection of two lakes from climatically different regimes enabled an interesting comparison. The lake level in Tso Moriri is controlled by meltwater and limited seasonal precipitation. The Lonar Lake lies in the core monsoon zone, and the lake level is primarily governed by ISM and limited groundwater inflow. As discussed above, while the early Holocene ISM intensification could be seen in both the lakes, the meltwater plays a prominent role in governing the hydrological balance in the high altitude Tso Moriri Lake. Even during the early Holocene wet phase when the ISM impact was strongest in the Himalayan region, the reconstructed mean annual precipitation of ca. 600-700 mm (Leipe et al., 2014a) is not sufficient to sustain a deepwater lake in this region.

Regional comparison of reconstructed hydrological changes from Tso Moriri Lake with other archives from the Asian summer monsoon and westerlies domain shows that the intensified westerly influence that resulted in higher lake levels (after 8 cal ka) in central Asia was not strongly felt in NW Himalaya. Additionally, during the late Holocene, the droughts

and events observed in monsoon dominated region are not unambiguously visible in the NW, Himalaya.

6.2. Future Prospects

Identifying the regional impact of past climate change, inferring their causal mechanisms, with a view to prediction in a global warming scenario, is one of the key challenges of the 21st century, with serious implications for future economic development, societies, and the environment. An extensive database of well dated, long term climate record is essential to reduce uncertainty in climate predictions by testing and refining climate models. My work on two lakes has highlighted several additional points to be pursued in future:

- Increasing the spatial coverage of the palaeo-data in the ISM realm for obtaining a better understanding of the past climate variability. These, in turn, should be compared to the database from the East Asian monsoon realm to understand overall Asian monsoon variability.
- Marine-terrestrial comparison to understand the role of teleconnections in causing extreme events.
- Monitoring: Quantification of palaeo-data using modern monitoring (sediment traps and hydro-meteorological data).
- Palaeoclimate simulations of different duration and different time slices are needed to understand the typical circulation anomalies responsible for the occurrence of extremes (floods and droughts) and identify the physical causal mechanisms.

References

Achyuthan, H., Nagasundaram, M., Gourlan, A. T., Eastoe, C., Ahmad, S. M., Padmakumari, V. M., 2014. Mid-Holocene Indian Summer Monsoon variability off the Andaman Islands, Bay of Bengal. Quaternary International 349, 232-244.

Adhikari, D. P., 2011. Paleolimnology of Lake Yamanaka as reflected on particle-size distribution. Bulletin of the Department of Geology 14, 35-42.

Agnihotri, R., Dutta, K., Bhushan, R., Somayajulu, B. L. K., 2002. Evidence for solar forcing on the Indian monsoon during the last millennium. Earth and Planetary Science Letters 198, 521-527.

Agnihotri, R., Kurian, S., Fernandes, M., Reshma, K., D'Souza, W., Naqvi, S.W.A., 2008. Variability of subsurface denitrification and surface productivity in the coastal eastern Arabian Sea over the past seven centuries. The Holocene 18, 755-764.

Alizai, A., Hillier, S., Clift, P.D., Giosan, L., Hurst, A., VanLaningham, S., Macklin, M., 2012. Clay mineral variations in Holocene terrestrial sediments from the Indus Basin. Quaternary Research 77, 368-381.

Alley, R.B., Mayewski, P.A., Sowers, T., Stuiver, M., Taylor, K.C., Clark, P.U., 1997. Holocene climatic instability: A prominent, widespread event 8200 yr ago. Geology 25, 483-486.

Amundson, R., Austin, A.T., Schuur, E.A.G., Yoo, K., Matzek, V., Kendall, C., Uebersax, A., Brenner, D., Baisden, W.T., 2003. Global patterns of the isotopic composition of soil and plant nitrogen. Global Biogeochemical Cycles 17, 1031.

An, Z., Kukla, G.J., Porter, S.C., Xiao, J., 1991. Magnetic susceptibility evidence of monsoon variation of the Loess Plateau of Central China during the last 130,000 years. Quaternary Research 36, 29‑36.

An, Z., Clemens, S. C., Shen, J., Qiang, X., Jin, Z., Sun, Y., Prell, W. L., Luo, J., Wang, S., Xu, H., Cai, Y., Zhou, W., Liu, X., Liu, W., Shi, Z., Yan, L., Xiao, X., Chang, W., Wu, F., Ai, L., Lu, F., 2011. Glacial-interglacial Indian summer monsoon dynamics. Science 333, 719-723.

Anderson, T.F., Arthur, M.A., 1983. Stable isotopes of oxygen and carbon and their application to sedimentological and palaeoenvironmental problems, in: Arthur, M.A., Anderson, T.F., Kaplan, I.R., Veizer, J., Land, L.S. (Eds.), Stable Isotopes in Sedimentary Geochemistry. Society of Economic Palaeontologists and Mineralogists Short course 10, 1‑151.

Anderson, D.M., Overpeck, J.T., Gupta, A.K., 2002. Increase in the Asian southwest monsoon during the past four centuries. Science 297, 596-599.

Anoop, A., Prasad, S., Krishnan, R., Naumann, R., Dulski, P., 2013a. Intensified monsoon and spatiotemporal changes in precipitation patterns in the NW Himalaya during the early-mid Holocene. Quaternary International 313-314, 74-84.

Anoop, A., Prasad, S., Plessen, B., Naumann, R., Menzel, P., Basavaiah, N., Weise, S., Gaye, B., Brauer, A., 2013b. Palaeoenvironmental implications of evaporative Gaylussite crystals from Lonar lake, Central India. Journal of Quaternary Science 28, 349–359.

Ashok, K., Guan, Z. and Yamagata, T., 2001. Impact of the Indian Ocean dipole on the relationship between the Indian monsoon rainfall. Geophys. Res. Lett. 28, 4499-4502.

Badve, R.M., Kumaran, K.P.N., Rajshekhar, C., 1993. Eutrophication of Lonar Lake, Maharashtra. Current Science 65, 347-351.

Bamzai, A. S., Shukla J., 1999 Relation between Eurasian Snow Cover, Snow Depth, and the Indian Summer Monsoon: An Observational Study. J. Climate 12, 3117-3132.

Barber, D.C., Dyke, A., Hillaire-Marcel, C., Jennings, A.E., Andrews, J.T., Kerwin, M.W., Bilodeau, G., McNeely, R., Southon, J., Morehead, M.D., Gagnon, J.M., 1999. Forcing of the cold event of 8,200 years ago by catastrophic drainage of Laurentide lakes. Nature 400, 344-348.

Bar-Matthews, M., Ayalon, A., Kaufman, A., 1997. Late Quaternary paleoclimate in the eastern Mediterranean region from stable isotope analysis of speleothems at Soreq Cave, Israel. Quaternary Research 47, 155-168.

Barnett, T.P., Dümenil, L., Schlese, U., Roeckner, E., Latif, M., 1989. The effect of Eurasian snow cover on regional and global climate variations. Journal of the Atmospheric Sciences 46, 661-685.

Basavaiah, N., Wiesner, M., Anoop, A., Menzel, P., Riedel, N., Gaye, B., Brauer, A., Stebich, M., Prasad S., 2014. Environmental implications of surface sediments from the monsoonal Lonar Lake, Central India. Fundamental and Applied Limnology 184, 51-68.

Beer, J., 2000. Long-term indirect indices of solar variability. Space Science Reviews 94, 53-66.

Beer, J., Mende, W., Stellmacher, R., 2000. The role of the sun in climate forcing. Quaternary Science Reviews 19, 403-415.

Benn, D.I., Owen, L. A., 1998. The role of the Indian summer monsoon and the mid-latitude westerlies in Himalayan glaciation: review and speculative discussion. Journal of the Geological Society, London 155, 353-363.

Berger, A., Loutre, M.F., 1991. Insolation values for the climate of the last 10 million years. Quaternary Science Reviews 10, 297-317.

Bergmann, J., Friedel, P., Kleeberg, R., 1998. BGMN-a new fundamental parameters based Rietveld program for laboratory X-ray sources, its use in quantitative analysis and structure investigations. CPD Newsletter 20, 5–8.

Berkelhammer, M., Sinha, A., Mudelsee, M., Cheng, H., Edwards, R.L., Cannariato, K., 2010. Persistent multidecadal power of the Indian Summer Monsoon. Earth and Planetary Science Letters 290, 166-172.

Berkelhammer, M., Sinha, A., Stott, L., Cheng, H., Pausata, F. S. R., Yoshimura, K., 2012. An abrupt shift in the Indian monsoon 4000 years ago. Climates, Landscapes, and Civilizations, 75-88.

Berthelsen, A., 1953. On the geology of the Rupshu District, N.W. Himalaya: A contribution to the Problem of the Central Gneisses. Meddelelser fra Dansk Geologisk Forening 12, 350-415.

Bhattacharyya, A., 1991. Ethnobotanical observations in the Ladakh region of Northern Jammu and Kashmir state, India. Economic Botany 45, 305-308.

Björck, S., Wohlfarth, B., 2001. ^{14}C chronostratigraphic techniques in palaeolimnology. In: Last, W.M., Smol, J.P. (Eds), Tracking environmental change using lake sediments, vol 1: basin analysis, coring, and chronological techniques. Kluwer, Dordrecht, pp 205–245.

Blanford H.F., 1886. Rainfall of India.Mem. India Meteorol. Dep. 2, 217–448.

Bond, G., Showers, W., Cheseby, M., Lotti, R., Almasi, P., deMenocal, P., Priore, P., Cullen, H., Hajdas, I., Bonani, G., 1997. A pervasive millennial-scale cycle in North Atlantic Holocene and glacial climates. Science 278, 1257-1266.

Bond, G., Kromer, B., Beer, J., Muscheler, R., Evans, M.N., Showers, W., Hoffmann, S., Lotti-Bond, R., Hajdas, I., Bonani, G., 2001. Persistent solar influence on North Atlantic climate during the Holocene. Science 294, 2130-2136.

Bookhagen, B., Thiede, R.C., Strecker, M.R., 2005. Late Quaternary intensified monsoon phases control landscape evolution in the northwest Himalaya. Geology 33, 149-152.

Bookhagen, B., Burbank, D.W., 2010. Towards a complete Himalayan hydrological budget: the spatiotemporal distribution of snowmelt and rainfall and their impact on river discharge. Journal of Geophysical Research-Earth Surface 115, 2003-2012.

Borgaonkar, H.P., Pant, G.B., Rupa Kumar, K., 1996. Ring-width variations in Cedrusdeodara and its climatic response over the western Himalaya. Int. J. Climatol. 16, 1409–1422.

Broccoli, A.J., Dahl, K.A., Stouffer, R.J., 2006. Response of the ITCZ to Northern Hemisphere cooling. Geophysical Research Letters 33, L01702.

Bronk Ramsey, C., 2008. Deposition models for chronological records. Quaternary Science Reviews 27, 42-60.

Buggle, B., Glaser, B., Hambach, U., Gerasimenko, N., Marković, S., 2011. An evaluation of geochemical weathering indices in loess–paleosol studies. Quaternary International 240, 12-21.

Cane, M. A., Molner, P., 2001. Closing of the indonesian seaway as a precursor to east African aridification around 304 million years ago. Nature 411, 157–162.

Caner, L., Lo Seen, D., Gunnell, Y., Ramesh, B.R., Bourgeon, G., 2007. Spatial heterogeneity of land cover response to climatic change in the Nilgiri highlands (Southern India) since the last glacial maximum. The Holocene 17, 195-205.

Casciotti, K.L., Buchwald, C., Santoro, A.E., Frame, C., 2011. Assessment of nitrogen and oxygen isotopic fractionation during nitrification and its expression in the marine environment, in: Klotz, M.G. (Ed.), Methods in Enzymology: Research on nitrification and related processes, Vol 486, Part A. Elsevier Academic Press Inc, San Diego, pp. 253-280.

Champion, H. G., Seth, S. K., 1968. A Revised Survey of the Forest Types of India. Government of India, New Delhi.

Chandan, P., Gautam, P., Chatterjee, A., 2006. Nesting sites and breeding success of black-necked crane *Grus nigricollis* in Ladakh, India. In: Boere, G.C., Galbraith, C.A., Stroud, D.A. (Ed.), Waterbirds around the World. Edinburgh, UK, pp. 311–314.

Chandan, P., Chatterjee, A., Gautam, P., 2008. Manadement Planning of Himalayan high altitude wetlands. A case study of Tso Moriri and Tso Kar wetlands in Ladakh, India. In Sengupta, M., Dalwani, R., (Eds.), Proceedings of Taal 2007: The 12th World Lake Conference, pp-1446-1452.

Charney JG. 1969. The intertropical convergence zone and the hadley circulation of the atmosphere. Proc. WMO/IUCG Symp. Numer.Weather Predict. Jpn. Meteorol. Agency III:73–79

Chen, F., Yu, Z., Yanag, M., Ito, E., Wang, S., Madsen, D.B., Huang, X., Zhao, Y., Sato, T., Birks, J.B., Boomen, I., Chen, J., An, C., Wünnemann, B., 2008. Holocene moisture evolution in arid central Asia and its out-of-phase relationship with Asian monsoon history. Quaternary Sciences Reviews 27, 351-364

Chiang, J.C.H., Biasutti, M., Battisti, D.S., 2003. Sensitivity of the Atlantic ITCZ to Last Glacial Maximum boundary conditions. Paleoceanography 18, 1094–1112.

Clift, P.D., Giosan, L., Blusztajn, J., Campbell, I.H., Allen, C., Pringle, M., Tabrez, A.R., Danish, M., Rabbani, M.M., Alizai, A., Carter, A., Lückge, A., 2008. Holocene erosion of the Lesser Himalaya triggered by intensified summer monsoon. Geology 36, 79-82.

Clift, P.D., Carter, A., Giosan, L., Durcan, J., Duller, G.A.T., Macklin, M.G., Alizai, A., Tabrez, A.R., Danish, M., VanLaningham, S., Fuller, D.Q., 2012. U-Pb zircon dating evidence for a Pleistocene Sarasvati River and capture of the Yamuna River. Geology 40, 211-214.

Cohen, J., and Entekhabi, D., 2001. The Influence of Snow Cover on Northern Hemisphere Climate Variability. Atmosphere-Ocean 39, 35 – 53.

Cowie, G.L., Hedges, J.I., Prahl, F.G., de Lange, G.J., 1995. Elemental and major biochemical changes across an oxidation front in a relict turbidite: An oxygen effect. Geochimica et Cosmochimica Acta 59, 33-46.

Cuven, S., Francus, P., Lamoureux, S. F., 2010. Estimation of grain size variability with micro X-ray fluorescence in laminated lacustrine sediments, Cape Bounty, Canadian High Arctic. Journal of Paleolimnology 44, 803-817.

Dasch, E. J., 1969. Strontium isotopes in weathering profiles, deep-sea sediments and sedimentary 5 rocks. Geochim. Cosmochim. Acta. 33, 1521–1552.

Dauwe, B., Middelburg, J.J., 1998. Amino acids and hexosamines as indicators of organic matter degradation state in North Sea sediments. Limnology and Oceanography 43, 782-798.

Dauwe, B., Middelburg, J.J., Herman, P.M.J., Heip, C.H.R., 1999. Linking diagenetic alteration of amino acids and bulk organic matter reactivity. Limnology and Oceanography 44, 1809-1814.

Dayem, K. E., Molnar, P., Battisti, D. S., Roe, G. H., 2010. Lessons learned from oxygen isotopes in modern precipitation applied to interpretation of speleothem records of paleoclimate from eastern Asia. Earth and Planetary Science Letters 295, 219-230.

De Choudens-Sanchez, V., Gonzalez, L. A., 2009. Calcite and aragonite precipitation under controlled instantaneous supersaturation: elucidating the role of CaCO3 saturation state and Mg/Ca ratio on calcium carbonate polymorphism. Journal of Sedimentary Research 79, 363-376.

de Sigoyer, J., Guillot, S., Dick, P., 2004. Exhumation of the ultrahigh pressure Tso Morari unit in eastern Ladakh (NW Himalaya): A case study. Tectonics 23, TC3003.

de Terra, H., Hutohinson, G. E., 1934. Evidence of Recent Climatic Changes. Shown by Tibetan Highland Lakes. Geogr. Jour. LXXXIV, 311-320.

Demske, D., Tarasov, P.E., Wünnemann, B., Riedel, F., 2009. Late glacial and Holocene vegetation, Indian monsoon and westerly circulation in the Trans-Himalaya recorded in the lacustrine pollen sequence from Tso Kar, Ladakh, NW India. Palaeogeography, Palaeoclimatology, Palaeoecology 279, 172-185.

Denniston, R.F., González, L.A., Asmerom, Y., Sharma, R.H., Reagan, M.K., 2000. Speleothem evidence for changes in Indian summer monsoon precipitation over the last ~2300 years. Quaternary Research 53, 196-202.

Deotare, B.C., 2006. Late Holocene Climatic Change: Archaeological Evidence from the Purna Basin, Maharashtra. Journal Geological Society of India 68, 517-526.

Dickson R.R., 1984. Eurasian snow cover and India monsoon rainfall-an extension of the Hahn-Shukla results. J. Climate Appl. Meteor. 23, 171–173.

Dietze, E., Wünnemann, B., Hartmann, K., Diekmann, B., Jin, H., Stauch, G., Yang, S., Lehmkuhl, F., 2013. Early to mid-Holocene lake high-stand sediments at Lake Donggi Cona, northeastern Tibetan Plateau, China. Quaternary Research 79, 325-336.

Dixit, Y., Hodell, D.A., Petrie, C.A., 2014. Abrupt weakening of the summer monsoon in northwest India ~4100 ago. Geology 42, 339-342.

Döberschütz, S., Frenzel, P., Haberzettl, T., Kasper, T., Wang, J., Zhu, L., Daut, G., Schwalb, A., Mäusbacher, R., 2014. Monsoonal forcing of Holocene paleoenvironmental change on the central Tibetan Plateau inferred using a sediment record from Lake Nam Co (Xizang, China). Journal of Paleolimnology 51, 253-266.

Dreybrodt, W., 1999. Chemical kinetics, speleothem growth and climate. Boreas 28, 347-356.

Dubay, C. I., Simmons, G. M., 1979. The contribution of macrophytes to the metalimnetic oxygen maximum in a montane, oligotrophic lake. American Midland Naturalist 101, 108-117.

Dykoski, C.A., Edwards, R.L., Cheng, H., Yuan, D.X., Cai, Y.J., Zhang, M.L., Lin, Y.S., Qing, J.M., An, Z.S., Revenaugh, J., 2005. A high-resolution, absolute-dated Holocene and deglacial Asian monsoon record from Dongge Cave, China. Earth and Planetary Science Letters 233, 71-86.

Dvorský, M., Doležal, J., de Bello, F., Klimešová, J., Klimeš, L., 2011. Vegetation types of East Ladakh: species and growth form composition along main environmental gradients. Applied Vegetation Science 14, 132-147.

Enzel, Y., Ely, L.L., Mishra, S., Ramesh, R., Amit, R., Lazar, B., Rajaguru, S.N., Baker, V.R., Sandler, A., 1999. High-resolution Holocene environmental changes in the Thar Desert, northwestern India. Science 284, 125-128.

Epard, J.-L., Steck, A., 2008. Structural development of the Tso Morari ultra-high pressure nappe of the Ladakh Himalaya. Tectonophysics 451, 242–264.

Epstein, S., Buchsbaum, R., Lowenstam, H.A., Urey, H.C., 1953. Revised carbonate-water temperature scale. Bulletin of the Geological Society of America 64, 1315–1326.

Esper J, Cook, E. R., Schweingruber, F. H., 2002. Low frequency signals in long tree-ring chronologies for reconstructing past temperature variability. Science 295, 2250–2253.

Eugster, H.P., Hardie, L.A., 1978. Saline lakes. In: Lerman, A. (Ed.), Lakes: Chemistry, Geology, Physics, Saline lakes. Springer, New York, pp. 237–293.

Feng, S., Hu, Q., 2008. How the North Atlantic Multidecadal Oscillation may have influenced the Indian summer monsoon during the past two millennia, Geophys. Res. Lett. 35, L01707.

Fleitmann, D., Burns, S.J., Mudelsee, M., Neff, U., Kramers, J., Mangini, A., Matter, A., 2003. Holocene forcing of the Indian monsoon recorded in a stalagmite from southern Oman. Science 300, 1737–1739.

Fleitmann, D., Burns, S.J., Mangini, A., Mudelsee, M., Kramers, J., Villa, I., Neff, U., Al-Subbary, A.A., Buettner, A., Hippler, D., Matter, A., 2007. Holocene ITCZ and Indian monsoon dynamics recorded in stalagmites from Oman and Yemen (Socotra). Quaternary Science Reviews 26, 170-188.

Fleitmann, D., Mudelsee, M., Burns, S.J., Bradley, R.S., Kramers, J., Matter, A., 2008. Evidence for a widespread climatic anomaly at around 9.2 ka before present. Paleoceanography 23.

Fontes, J. Ch., Melieres, F., Gibert, E., Liu, Q., Gasse, F., 1993. Stable isotope and radiocarbon balances of two Tibetan lakes (Sumxi Co, Longmu Co) from 13,000 yr BP. Quaternary Science Reviews 12, 875 – 887.

Fontes, J.-C., Gasse, F., Gibert, E., 1996. Holocene environmental changes in Lake Bangong basin (Western Tibet). Part 1: Chronology and stable isotopes of carbonates of a Holocene lacustrine core. Palaeogeography, Palaeoclimatology, Palaeoecology 120, 25-47.

Freudenthal, T., Wagner, T., Wenzhöfer, F., Zabel, M., Wefer, G., 2001. Early diagenesis of organic matter from sediments of the eastern subtropical Atlantic: Evidence from stable nitrogen and carbon isotopes. Geochimica et Cosmochimica Acta 65, 1795-1808.

Fuchs, G., Linner, M., 1996. On the geology of the Suture Zone and Tso Morari Dome in Eastern Ladakh (Himalaya). Jahrbuch der Geologischen Bundesanstalt 139, 191 – 207.

Gadgil S., 2007. The Indian Monsoon: Physics of the monsoon. Resonance, 12, 4–20.

Gadgil, S., 2003. The Indian monsoon and its variability. Annual Review of Earth and Planetary Sciences 31, 429-467.

Gadgil, S., 2014. El Niño and the summer monsoon of 2014. Current science 106, 1335-1336.

Gasse, F., Arnold, M., Fontes, J.C., Fort, M., Gilbert, E., Huc, A., Li, B., Li, Y., Liu, Q., Melieres, F., Van Campo, E., Wang, F., Zhang, Q., 1991. A 13,000-year climate record from western Tibet. Nature 353, 742-745.

Gasse, F., Fontes, J.-C., Van Campo, E., Wei, K., 1996. Holocene environmental changes in Bangong Co basin (Western Tibet). Part 4: Discussion and conclusions. Palaeogeography, Palaeoclimatology, Palaeoecology 120, 79-92.

Gasse, F., 2000. Hydrological changes in the African tropics since the Last Glacial Maximum. Quaternary Science Reviews 19, 189-211.

Ghosh, S., Das, D., Kao, S.C., Ganguly, A.R., 2011. Lack of uniform trends but increasing spatial variability in observed Indian rainfall extremes. Nature Climate Change 2, 86-91.

Gibbs, R. J., 1970. Mechanisms controlling world water chemistry. Science 170, 1088-1090.

Giosan, L., Clift, P.D., Macklin, M.G., Fuller, D.Q., Constantinescu, S., Durcan, J.A., Stevens, T., Duller, G.A.T., Tabrez, A.R., Gangal, K., Adhikari, R., Alizai, A., Filip, F., VanLaningham, S., Syvitski, J.P.M., 2012. Fluvial landscapes of the Harappan civilization. Proceedings of the National Academy of Sciences 109, E1688-E1694.

Gong, D.Y., Ho, C.H., 2002. The Siberian high and climate change over middle to high latitude Asia. Theoretical and Applied Climatology 72, 1-9.

Goswami, B. N., 2005. South Asian Summer Monsoon: An overview: in the global monsoon System: Research and Forecast Edited by C.-P. Chang, Bin Wang, Ngar-Cheung Gabriel Lau, Chapter 5, pp 47

Goswami, B. N., Venugopal, V., Sengupta, D., Madhusoodanan, M. S., Xavier, P. K., 2006. Increasing trend of extreme rain events over India in a warming environment. Science 314, 1442-1445.

Govil, P., Naidu, P.D., 2011. Variations of Indian monsoon precipitation during the last 32 kyr reflected in the surface hydrography of the Western Bay of Bengal, Quaternary Science Reviews 30, 3871-3879.

Gu, B.H., Schelske, C.L., Hodell, D.A., 2004. Extreme 13C enrichments in a shallow hypereutrophic lake: Implications for carbon cycling. Limnology and Oceanography 49, 1152-1159.

Guillot, S., de Sigoyer, J., Lardeaux, J. M., Mascle, G., 1997. Eclogitic metasediments from the TsoMorari area (Ladakh, Himalaya): evidence for continental subduction during India-Asia convergence. Contributions to Mineralogy and Petrology 128, 197–212.

Gujja, B., Chatterjee, A., Gautam, P., Chandan, P., 2003.Wetlands and lakes at the top of the World. Mountain Research and Development 23 (3), 219-221.

Gupta, A.K., Anderson, D.M., Overpeck, J.T., 2003. Abrupt changes in the Asian southwest monsoon during the Holocene and their links to the North Atlantic Ocean. Nature 421, 354–357.

Gupta, A.K., Das, M., Anderson, D.M., 2005. Solar influence on the Indian summer monsoon during the Holocene. Geophysical Research Letters 32, L17703.

Gupta, A.K., Anderson, D.M., Pandey, D.N., Singhvi, A.K., 2006. Adaptation and human migration, and evidence of agriculture coincident with changes in the Indian summer monsoon during the Holocene. Current Science 90, 1082-1090.

Gupta, S. M., 2010. Indian monsoon cycles through the last twelve million years. e-Journal Earth Science, India

Haberzettl, T., Fey, M., Lücke, A., Maidana, N., Mayr, C., Ohlendorf, C., Schäbitz, F., Schleser, G.H., Wille, M., Zolitschka, B., 2005. Climatically induced lake level changes during the last two millennia as reflected in sediments of Laguna Potrok Aike, southern Patagonia (Santa Cruz, Argentina). Journal of Paleolimnology 33, 283-302.

Haberzettl, T., Corbella, H., Fey, M., Janssen, S., Lücke, A., Mayr, C., Ohlendorf, C., Schäbitz, F., Schleser, G.H., Wille, M., Wulf, S., Zolitschka B., 2007. Lateglacial and Holocene wet—dry cycles in southern Patagonia: chronology, sedimentology and geochemistry of a lacustrine record from Laguna Potrok Aike, Argentina. The Holocene 17, 297-310.

Halley E., 1686. An historical account of the trade winds and monsoons, observable in the seas between and near the tropics with an attempt to assign the physical cause of the said winds. Philosophical Transactions, Royal Society, London 16,153-168.

Hartmann, H., 1999. Studien zur Flora und Vegetation im östlichen Transhimalaya von Ladakh (Indien). Candollea 54, 171-230 (in English with German abstract).

Haug, G. H., Hughen, K. A., Sigman, D. M., Peterson, L. C., Röhl, U., 2001. Southward migration of the Intertropical Convergence Zone through the Holocene. Science 293, 1304-1308.

Hedrick, K.A., Seong, Y.B., Owen, L.A., Caffee M.W., Dietsch C., 2011. Towards defining the transition in style and timing of Quaternary glaciation between the monsoon-influenced greater Himalaya and the semi-arid Transhimalaya of Northern India. Quaternary International 236, 21–33.

Herzschuh, U., 2006. Palaeo-moisture evolution in monsoonal Central Asia during the last 50,000 years. Quaternary Science Reviews 25, 163-178.

Herzschuh, U., Winter, K., Wünnemann, B., Li, S., 2006. A general cooling trend on the central Tibetan Plateau throughout the Holocene recorded by the Lake Zigetang pollen spectra. Quaternary International 154-156, 113-121.

Herzschuh, U., Kramer, A., Mischke, S., Zhang, C., 2009. Quantitative climate and vegetation trends since the late glacial on the northeastern Tibetan Plateau deduced from Koucha Lake pollen spectra. Quaternary Research 71, 162-171.

Hiremath, K. M., Manjunath, H., Soon, W., 2014. Indian summer monsoon rainfall: Dancing with the tunes of the sun. New Astronomy 35, 8-19.

Hodell, D.A., Schelske, C.L., 1998. Production, sedimentation, and isotopic composition of organic matter in Lake Ontario. Limnology and Oceanography 43, 200-214.

Hodell, D.A., Brenner, M., Kanfoush, S.L., Curtis, J.H., Stoner, J.S., Song, X.L., Wu, Y., Whitmore, T.J., 1999. Paleoclimate of Southwestern China for the past 50,000 yr inferred from lake sediment records. Quaternary Research 52, 369-380.

Hong, Y.T., Hong, B., Lin, Q.H., Zhu, Y.X., Shibata, Y., Hirota, M., Uchida, M., Leng, X.T., Jiang, H.B., Xu, H., Wang, H., Yi, L., 2003. Correlation between Indian Ocean summer monsoon and North Atlantic climate during the Holocene. Earth and Planetary Science Letters 211, 371-380.

Hou, J., D'Andrea, W.J., Liu, Z., 2012. The influence of ^{14}C reservoir age on interpretation of paleolimnological records from the Tibetan Plateau. Quaternary Science Reviews 48, 67-79.

Hren, M.T., Bookhagen, B., Blisniuk, P.M., Booth, A.L., Chamberlain, C.P., 2009. $\delta^{18}O$ and δD of streamwaters across the Himalaya and Tibetan Plateau: implications for moisture sources and paleoelevation reconstructions. Earth and Planetary Science Letters 288**,** 20–32.

Hutchinson, G.E., 1937. Limnological studies in Indian Tibet. International Review of Hydrobiology 35, 134-177.

Johnsen, S.J., Dahl-Jensen, D., Gundestrup, N., Steffensen, J.P., Clausen, H.B., Miller, H., Masson-Delmotte, V., Sveinbjörnsdottir, A.E., White, J., 2001. Oxygen isotope and palaeotemperature records from six Greenland ice-core stations: Camp Century, Dye-3, GRIP, GISP2, Renland and NorthGRIP. Journal of Quaternary Science 16, 299-307.

Joshi, A.A., Kanekar, P.P., Kelkar, A.S., Shouche, Y.S., Vani, A.A., Borgave, S.B., Sarnaik, S.S., 2008. Cultivable bacterial diversity of alkaline Lonar Lake, India. Microbial Ecology 55, 163-172.

Joswiak, D.R., Yao, T.D., Wu, G.J., Zheng, W., 2010. A 70-yr record of accumulation and oxygen-18 variability in the Tanggula Mountains, central Tibetan Plateau. Climate of the Past 6, 219-227.

Jourdan, F., Moynier, F., Koeberl, C., Eroglu, S., 2011. 40Ar/39Ar age of the Lonar crater and consequence for the geochronology of planetary impacts. Geology 39, 671-674.

Juyal, N., Chamyal, L. S., Bhandari, S., Bhushan, R., Singhvi, A. K., 2006. Continental record of the southwest monsoon during the last 130ka: evidence from the southern margin of the Thar Desert, India. Quaternary Science Reviews 25, 2632-2650.

Kantrud, H.A., 1990. Sago pondweed (*Potamogeton pectinatus* L.): a literature review. Fish and Wildlife Resource Publication 176, 89.

Kar, R., Ranhotra, P.S., Bhattacharyya, A., Sekar, B., 2002. Vegetation vis-à-vis climate and glacial fluctuations of the Gangotri glacier since the last 2000 years. Current Science 82, 347–351.

Kauppila, T., Salonen, V.-P., 1997. The effect of Holocene treeline fluctuations on the sediment chemistry of Lake Kilpisjärvi, Finland. Journal of Paleolimnology 18, 145-163.

Kelkar, R. R., 2009. Monsoon prediction. B.S. Publications Hyderabad, India.

Kendall, R.A., Mitrovica, J.X., Milne, G.A., Törnqvist, T.E., Li, Y.X., 2008. The sea-level fingerprint of the 8.2 ka climate event. Geology 36, 423-426.

Kennett, D.J., Breitenbach, S.F.M., Aquino, V.V., Asmerom, Y., Awe, J., Baldini, J.U.L., Bartlein, P., Culleton, B.J., Ebert, C., Jazwa, C., Macri, M.J., Marwan, N., Polyak, V., Prufer, K.M., Ridley, H.E., Sodemann, H., Winterhalder, B., Haug, G.H., 2012. Development and Disintegration of Maya Political Systems in Response to Climate Change. Science 338, 788-791.

Kiel, A., Berking, J., Mügler, I., Schütt, B., Schwalb, A., Steeb, P., 2010. Hydrological and geomorphological basin and catchment characteristics of Lake Nam Co, South-Central Tibet. Quaternary International 218, 118-130.

Konig, K. A., Shotyk, W., Lotter, A. F., Ohlendorf, C., Sturm, M., 2003. 9000 years of geochemical evolution of lithogenic major and trace elements in the sediment of an alpine lake- the role of climate vegetation and land/use history. Journal of Paleolimnology 30, 307-320.

Kotlia, B. S., Singh, A. K., Joshi, L. M., Dhaila, B. S., 2014. Precipitation variability in the Indian Central Himalaya during last ca. 4,000 years inferred from a speleothem record: Impact of Indian Summer Monsoon (ISM) and Westerlies. Quaternary International (in press).

Koutavas, A., Sachs, J.P., 2008. Northern timing of deglaciation in the eastern equatorial Pacific from alkenone paleothermometry. Paleoceanography 23, PA4205.

Krishnamurti, T.N., Bhalme, H.N., 1976. Oscillation of a monsoon system, Part I: observational aspects. J.Atmos. Sci. 33, 1937-1954.

Krishnan, R., Sundaram, S., Swapna, P., Kumar, V., Ayantika, D.C., Mujumdar, M., 2011. The crucial role of ocean-atmosphere coupling on the Indian monsoon anomalous response during dipole events. Climate Dynamics 37, 1-17

Krishnan, R., Vinay Kumar, V., Sugi M., Yoshimura J., 2009. Internal feedbacks from monsoon-midlatitude interactions during droughts in the Indian summer monsoon. Journal of Atmospheric Sciences 66, 553-578.

Krishnaswamy, J., Vaidyanathan, S., Rajagopalan, B., Bonell, M., Sankaran, M., Bhalla, R. S., Badiger, S., 2014. Non-stationary and non-linear influence of ENSO and Indian Ocean Dipole on the variability of Indian monsoon rainfall and extreme rain events. Climate Dynamics. DOI 10.1007/s00382-014-2288-0.

Kutzbach, J.E., Guetter, P.J., 1986. The influence of changing orbital parameters and surface boundary-conditions on climate simulations for the past 18,000 years. Journal of the Atmospheric Sciences 43, 1726–1759.

Kutzbach, J. E., Prell, W. L., Ruddiman W. F., 1993. Sensitivity of eurasian climate to surface uplift of the tibetan plateau. J. of Geol. 101, 177–190.

Lahajnar, N., Wiesner, M.G., Gaye, B., 2007. Fluxes of amino acids and hexosamines to the deep South China Sea. Deep-Sea Research Part I: Oceanographic Research Papers 54, 2120-2144.

Land, L.S., 1980. The isotopic and trace element geochemistry of dolomite: the state of the art, in: Zenger, D.H. (Eds.), Concepts and Models of Dolomitisation. SEPM Special Publication 28, 87–110.

Lauterbach, S., Witt, R., Plessen, B., Dulski, P., Prasad, S., Mingram, J., Gleixner, G., Hettler-Riedel, S., Stebich, M., Schnetger, B., Schwalb, A., Schwarz, A., 2014. Climatic imprint of the mid-latitude Westerlies in the Central Tian Shan of Kyrgyzstan and teleconnections to North Atlantic climate variability during the last 6000 years. The Holocene. DOI: 10.1177/0959683614534741.

Lea, D.W., Pak, D.K., Peterson, L.C., Hughen, K.A., 2003. Synchroneity of tropical and high-latitude Atlantic temperatures over the last glacial termination. Science 301, 1361–1364

Lehmann, M.F., Bernasconi, S.M., Barbieri, A., McKenzie, J.A., 2002. Preservation of organic matter and alteration of its carbon and nitrogen isotope composition during simulated and in situ early sedimentary diagenesis. Geochimica et Cosmochimica Acta 66, 3573-3584.

Lehmann, M.F., Bernasconi, S.M., McKenzie, J.A., Barbieri, A., Simona, M., Veronesi, M., 2004. Seasonal variation of the δ13C and δ15N of particulate and dissolved carbon and nitrogen in Lake Lugano: Constraints on biogeochemical cycling in a eutrophic lake. Limnology and Oceanography 49, 415-429.

Lei, Y.B., Yao, T.D., Sheng, Y.W., Zhang, E.L., Wang, W.C., Li, J.L., 2012. Characteristics of δ13CDIC in lakes on the Tibetan Plateau and its implications for the carbon cycle. Hydrological Processes 26, 535-543.

Leipe, C., Demske D., Tarasov P., 2014a. A Holocene pollen record from the northwestern Himalayan lake Tso Moriri: Implications for palaeoclimatic and archaeological research. Quaternary International 348, 93-112.

Leipe, C., Demske, D., Tarasov, P. E., Wünnemann, B., Riedel, F., 2014b. Potential of pollen and non-pollen palynomorph records from Tso Moriri (Trans-Himalaya, NW India) for reconstructing Holocene limnology and human-environmental interactions. Quaternary International 348, 113-129.

Leng, M., J., Marshall, J. D., 2004. Palaeoclimate interpretation of stable isotope data from lake sediment archives. Quaternary Science Reviews 23, 811-831.

Leng, M. J., Jones, M. D., Frogley, M. R., Eastwood, W. J., Kendrick, C. P., Roberts, C. N., 2010. Detrital carbonate influences on bulk oxygen and carbon isotope composition of lacustrine sediments from the Mediterranean. Global and Planetary Change 71, 175-182.

Lesher, S.R., 2011. Climate change impacts to a high altitude lake in the Indian Himalaya. Dissertation Thesis, San Diego State University.

Li, J.B., Cook, E.R., Chen, F.H., Davi, N., D'Arrigo, R., Gou, X.H., Wright, W.E., Fang, K.Y., Jin, L.Y., Shi, J.F., Yang, T., 2009. Summer monsoon moisture variability over China and Mongolia during the past four centuries. Geophysical Research Letters 36, L22705.

Limmer, D. R., Böning, P., Giosan, L., Ponton, C., Köhler, C. M., Cooper, M. J., Tabrez, A. R., Clift, P.D., 2012. Geochemical record of Holocene to Recent sedimentation on the Western Indus continental shelf, Arabian Sea. Geochemistry, Geophysics, Geosystems 13, Q01008.

Lippmann, F., 1973. Sedimentary Carbonate Minerals. New York, Springer-Verlag, pp. 228.

Lister, G.S., Kelts, K., Chen Ke, Z., Yu, J.-Q., Niessen, F., 1991. Lake Qinghai, China: closed basin lake levels and the oxygen isotope record for Ostracoda since the latest Pleistocene. Palaeogeography, Palaeoclimatology, Palaeoecology 84, 141–162.

Liu, Y.H., Henderson, G.M., Hu, C.Y., Mason, A.J., Charnley, N., Johnson, K.R., Xie, S.C., 2013. Links between the East Asian monsoon and North Atlantic climate during the 8,200-year event. Nature Geoscience 6, 117-120.

Lockwood, J.G., 1974. World Climatology. The English language book society and Edward Arnold, London, 330 pp.

Lopez, P., Navarro, E., Marce, R., Ordoñez, J., Caputo, L., Armengol, J., 2006. Elemental ratios in sediments as indicators of ecological processes in Spanish reservoirs. Limentica 25, 499-512.

Lotter, A. F., 2014. Multi-Proxy climatic reconstructions. In: Birks, J., Battarbee, R., & Mackay, A. (Eds.) Global change in the Holocene. Routledge.

Loutre, M.F., Berger, A., Bretagnon, P., Blanca, P.L., 1992. Astronomical frequencies for climate research at the decadal to century time scale. Climate Dynamics 7, 181-194.

MacDonald, G., 2011. Potential influence of the Pacific Ocean on the Indian summer monsoon and Harappan decline. Quaternary International 229, 140-148.

Madella, M., Fuller, D.Q., 2006. Palaeoecology and the Harappan Civilisation of South Asia: A reconsideration. Quaternary Science Reviews 25, 1283-1301.

Magny, M., 2004. Holocene climate variability as reflected by mid-European lake-level fluctuations and its probable impact on prehistoric human settlements. Quaternary International 113, 65-79.

Magny, M., Joannin, S., Galop, D., Vannière, B., Haas, J. N., Bassetti, M., Bellintani, P., Scandolarf, R., Desmet, M., 2012. Holocene palaeohydrological changes in the northern Mediterranean borderlands as reflected by the lake-level record of Lake Ledro, northeastern Italy. Quaternary Research 77, 382-396.

Mahajan, A.D., 2005. Preliminary survey of planktonic diversity in Lonar lake water, in: Banmeru, P.K., Banmeru, S.K., Mishra, V.R. (Eds.), Biodiversity of Lonar crater. Anamaya Publishers, New Delhi, India, pp. 58-62.

Maloof, A. C., Stewart, S. T., Soule, S. A., Weiss, B. P., Swanson-Hysell, N. L., Louzada, K. L., Garrick-Bethell, I., Poussart, P. M., 2009. Geology of Lonar Crater, India. Geological Society of America Bulletin 122, 109 –126.

Malu, R.A., Kulkarni, K.M., Kodarkar, M.S., 2005. Conservation and management of biotic environment in Lonar crater lake: An ecological wonder of India, in: Banmeru, P.K., Banmeru, S.K., Mishra, V.R. (Eds.), Biodiversity of Lonar crater. Anamaya Publishers, New Delhi, pp. 39-46.

Marzin, C., Kallel, N., Kageyama, M., Duplessy, J. C., Braconnot, P., 2013. Glacial fluctuations of the Indian monsoon and their relationship with North Atlantic climate: new data and modelling experiments. Clima. Past. 9, 2135-2151.

MATLAB and Statistics Toolbox Release 2010. The MathWorks, Incorporated. Natick, Massachusetts, United States of America.

Mayewski, P.A., Rohling, E.E., Stager, J.C., Karlén, W., Maasch, K.A., Meeker, L.D., Meyerson, E.A., Gasse, F., van Kreveld, S., Holmgren, K., Lee-Thorp, J., Rosqvist, G., Rack, F., Staubwasser, M., Schneider, R.R., Steig, E.J., 2004. Holocene climate variability. Quaternary Research 62, 243-255.

McLaren, P., Bowles, D., 1985. The effects of sediment transport on grain-size distributions. Journal of Sedimentary Research 55, 457-470.

Mengel, K., 1996. Turnover of organic nitrogen in soils and its availability to crops. Plant and Soil 181, 83-93.

Menzel, P., Gaye, B., Wiesner, M.G., Prasad, S., Stebich, M., Das, B.K., Anoop, A., Riedel, N., Basavaiah, N., 2013. Influence of bottom water anoxia on nitrogen isotopic ratios and amino acid contributions of recent sediments from small eutrophic Lonar Lake, central India. Limnology and Oceanography 58, 1061-1074.

Menzel, P., Gaye, B., Mishra, P. K., Anoop, A., Basavaiah, N., Marwan, N., Plessen, B., Prasad, S., Riedel, N., Stebich, M., Wiesner, M. G., 2014. Linking Holocene drying trends from Lonar Lake in monsoonal central India to North Atlantic

cooling events. Palaeogeography, Palaeoclimatology, Palaeoecology 410, 164-178.

Meyers, P. A., Ishiwatari, R., 1993. Lacustrine organic geochemistry—an overview of indicators of organic matter sources and diagenesis in lake sediments. Organic geochemistry 20, 867-900.

Meyers, P.A., 1997. Organic geochemical proxies of paleoceanographic, paleolimnologic, and paleoclimatic processes. Organic Geochemistry 27, 213-250.

Meyers, P.A., Lallier-Vergès, E., 1999. Lacustrine sedimentary organic matter records of Late Quaternary paleoclimates. Journal of Paleolimnology 21, 345-372.

Milankovitch, M., 1930. Mathematische Klimalehre und astronomische Theorie der Klimaschwankungen. In W. Köppen, R. Geiger (Eds.), Handbuch der Klimatologie, Bornträger, Berlin.

Minyuk, P. S., Borkhodoev, V. Y., Wennrich, V., 2013. Inorganic data from El'gygytgyn Lake sediments: stages 6-11. Climate of the Past Discussions 9, 393-433.

Mischke, S., Zhang, C., 2010. Holocene cold events on the Tibetan Plateau. Global and Planetary Change 72, 155-163.

Mischke, S., Weynell, M., Zhang, C., Wiechert, U., 2013. Spatial variability of ^{14}C reservoir effects in Tibetan Plateau lakes. Quaternary International 313-314, 147-155.

Mishra, C., Humbert-Droz, B., 1998. Avifaunal survey of Tsomoriri Lake and adjoining Nuro Sumdo Wetland in Ladakh, Indian trans-Himalaya. Forktail 14, 65-67.

Mishra, P. K., Anoop, A., Jehangir, A., Prasad, S., Menzel, P., Schettler, G., Naumann, R., Weise, S., Anderson, N., Yousuf, A. R., Gaye, B., 2014. Limnology and modern sedimentation patterns in high altitude Tso Moriri Lake, NW Himalaya – implications for proxy development. Fundamental of Applied Limnology 185, 325-348.

Mishra, P. K., Anoop, A., Schettler, G., Prasad, S., Jehangir, A., Menzel, P., Naumann, R., Yousuf, A.R., Basavaiah, A.R., Deenadayalan, K., Wiesner, M.G., Gaye, B., 2015. Reconstructed late Quaternary hydrological changes from Tso Moriri Lake, NW Himalaya. Quaternary International 371, 76-86.

Möller, P., Kubanek, B., 1976. Role of magnesium in nucleation processes of calcite, aragonite and dolomite. Neues Jahrbuch für Mineralogie, Abhandlungen 126, 199–220.

Morrill, C., Overpeck, J.T., Cole, J.E., 2003. A synthesis of abrupt changes in the Asian summer monsoon since the last deglaciation. The Holocene 13, 465-476.

Morrill, C., Overpeck, J.T., Cole, J.E., Liu, K.B., Shen, C., Tang, L. 2006. Holocene variations in the Asian monsoon inferred from the geochemistry of lake sediments in central Tibet. Quaternary Research 65, 232-243.

Morse, J.W., Wang, Q., Tsio, M.Y., 1997. Influences of temperature and Mg:Ca ratio on $CaCO_3$ precipitates from seawater. Geology 25, 85–87.

Moy, C.M., Seltzer, G.O., Rodbell, D.T., Anderson, D.M., 2002. Variability of El Nino/Southern Oscillation activity at millennial timescales during the Holocene epoch. Nature 420, 162-165.

Mucci, A., Morse, J.W., 1983. The incorporation of Mg^{2+} and Sr^{2+} into calcite overgrowths: influences of growth rate and solution composition. Geochimica et Cosmochimica Acta 47, 217-233.

Müller, G., 1967. Methods in Sedimentary Petrology. Hafner Publishing Company, New York.

Müller, P. J., Suess, E., Ungerer, C. A., 1986. Amino acids and sugars of surface particulate and sediment trap material from waters of the Scotia Sea. Deep Sea Research 33, 819 – 838.

Muscheler, R., Adolphi, F. and Svensson, A., 2014. Challenges in 14C dating towards the limit of the method inferred from anchoring a floating tree ring radiocarbon chronology to ice core records around the Laschamp geomagnetic field minimum. Earth and Planetary Science Letters 394, 209-215.

Nandy, N.C., Deo, V.B., 1961. Origin of the Lonar Lake and its alkalinity. Technical Journal of the Tata Iron and Steel Company 8, 144 - 155.

Neff, U., Burns, S.J., Mangini, A., Mudelsee, M., Fleitmann, D., Matter, A., 2001. Strong coherence between solar variability and the monsoon in Oman between 9 and 6 ka ago. Nature 411, 290–293

Nesbitt, H. W., Markovics, G., 1980. Chemical processes affecting alkalis and alkaline earths during continental weathering. Geochimica et Cosmochimica Acta 44, 1659-1666.

New, M., Lister, D., Hulme, M., Makin, I., 2002. A high-resolution data set of surface climate over global land areas. Climate Research 21, 1-25.

Officer, C.B., Drake, C.L., 1983. The Cretaceous-Tertiary transition. Science 219, 1383-1390.

O'Leary, M.H., 1988. Carbon isotopes in photosynthesis. Bioscience 38, 328-336.

Overpeck, J.T., Anderson, D.M., Trumbore, S., Prell, W.L., 1996. The southwest Indian Monsoon over the last 18000 years. Climate Dynamics 12, 213-225.

Pang, H., Hou, S., Kaspari, S., Mayewski, P. A., 2014. Influence of regional precipitation patterns on stable isotopes in ice cores from the central Himalayas. The Cryosphere 8, 289-301.

Panigrahy, S., Patel, J.G., Parihar, J.S., 2012. National Wetland Atlas: High Altitude Lakes of India. Space Applications Centre, ISRO, Ahmedabad, India.

Pant, G. B., K. Rupa Kumar, 1997. Climates of South Asia. John Wiley and Sons, Chichester, UK.

Parker, A.G., Eckersley, L., Smith, M.M., Goudie, A.S., Stokes, S., Ward, S., White, K., Hodson, M.J., 2004. Holocene vegetation dynamics in the northeastern Rub' al-Khali desert, Arabian Peninsula: A phytolith, pollen and carbon isotope study. J. Quat. Sci. 19, 665-676.

Pausata, F.S.R., Battisti, D.S., Nisancioglu, K.H., Bitz, C.M., 2011. Chinese stalagmite δ18O controlled by changes in the Indian monsoon during a simulated Heinrich event. Nature Geoscience 4, 474-480.

Peng, Y., Xiao, J., Nakamura, T., Liu, B., Inouchi, Y., 2005. Holocene East Asian monsoonal precipitation pattern revealed by grain-size distribution of core sediments of Daihai Lake in Inner Mongolia of north-central China. Earth and Planetary Science Letters 233, 467-479.

Peterson, B.J., Fry, B., 1987. Stable isotopes in ecosystem studies. Annual Review of Ecology and Systematics 18, 293-320.

Phadtare, N. R., 2000. Sharp Decrease in Summer Monsoon Strength 4000–3500 cal yr B.P. in the Central Higher Himalaya of India Based on Pollen Evidence from Alpine Peat. Quaternary Research 53, 122-129.

Pickering, K.T., Owen, L.A., 1994. An introduction to global environmental issues. Routledge, London, 390pp.

Ponton, C., Giosan, L., Eglinton, T. I., Fuller, D. Q., Johnson, J. E., Kumar, P., Collett, T. S., 2012. Holocene aridification of India. Geophysical Research Letters 39, L03704.

Possehl, G.L., 1997. The transformation of the Indus Civilization. Journal of World Prehistory 11, 425-472.

Prasad, S., Kusumgar, S., Gupta, S.K., 1997. A mid–late Holocene record of palaeoclimatic changes from Nal Sarovar—A palaeodesert margin lake in western India. Journal of Quaternary Science 12, 153–159.

Prasad, S., Enzel, Y., 2006. Holocene palaeoclimates of India. Quaternary Research 66, 442-453.

Prasad, S., Anoop, A., Riedel, N., Sarkar, S., Menzel, P., Basavaiah, N., Krishnan, R., Fuller, D., Plessen, B., Gaye, B., Röhl, U., Wilkes, H., Sachse, D., Sawant, R., Wiesner, M.G., Stebich, M., 2014. Prolonged monsoon droughts and links to indo-Pacific warm pool: A Holocene record from Lonar Lake, central India. Earth and Planetary Science Letters 391, 171-182.

Prasad, V., Farooqui, A., Sharma, A., Phartiyal, B., Chakraborty, S., Bhandari, S., Raj, R., Singh, A., 2014. Mid–late Holocene monsoonal variations from mainland Gujarat, India: A multi-proxy study for evaluating climate culture relationship. Palaeogeography, Palaeoclimatology, Palaeoecology 397, 38-51.

Prell, W. L., Kutzbach, J. E., 1992. Sensitivity of the Indian monsoon to forcing parameters and implications for its evolution. Nature 360, 647–653.

Rajeevan M., Gadgil S., Bhate J., 2010. Active and Break spells of the Indian summer monsoon. J.Earth Syst. Sci. 119, 229-247.

Rajendran, K., Kitoh, A., 2008. Indian summer monsoon in future climate projection by a super high resolution global model. Current Science 95, 1560-1569.

Rashid, H., England, E., Thompson, L., Polyak, L., 2011. Late glacial to Holocene Indian summer monsoon variability based upon sediment. Terrestrial, Atmospheric and Oceanic Sciences 22, 215-228.

Raymo, M.E., Ruddiman, W.F., 1992. Tectonic forcing of late Cenozoic climate. Nature 359, 117-122.

Rehfeld, K., Marwan, N., Heitzig, J., Kurths, J., 2011. Comparison of correlation analysis techniques for irregularly sampled time series. Nonlinear Processes in Geophysics 18, 389-404.

Reimer, P.J., Bard, E., Bayliss, A., Beck, J.W., Blackwell, P.G., Ramsey, C.B., Buck, C.E., Cheng, H., Edwards, R.L., Friedrich, M., Grootes, P.M., Guilderson, T.M., Haflidason, H., Hajdas, I., Hatté, C., Heaton, T.J., Hoffmann, D.L., Hogg, A.G., Hughen K.A., Kaiser, K.F., Kromer, B., Manning, S.W., Niu, M., Reimer, R.W., Richards, D.A., Scott, E.M., Southon, J.R., Staff, R.A., Turney, C.S.M., van der Plicht J., 2013. IntCal13 and Marine13 radiocarbon age calibration curves 0–50,000 years cal BP. Radiocarbon 55, 1869-1887.

Rein, B., Lückge, A., Reinhardt, L., Sirocko, F., Wolf, A., Dullo, W.C., 2005. El Niño variability off Peru during the last 20,000 years. Paleoceanography 20.

Roth, M., Hampaĭ, A., 1973. Column chromatography of amino acids with fluorescence detection. Journal of Chromatography A 83, 353-356.

Rowley, D. B., 1996. Age of initiation of collision between India and Asia: A review of stratigraphic data. Earth and Planetary Science Letters 145, 1-13.

Rozanski, K., Araguás-Araguás, L., Gonfiantini, R. 1993. Isotopic patterns in modern global precipitation. Geophysical Monograph Series 78, 1-36.

Ruddiman, W.F., Kutzbach, J.E., 1989. Forcing of late Cenozoic northern hemisphere climates by plateau uplift in southeast Asia and the American southwest. J. Geophys. Res. 94, 18409-18427.

Saji, N.H., Goswami, B.N., Vinayachandran, P.N., Yamagata, T., 1999. A dipole mode in the tropical Indian Ocean. Nature 401, 360-363.

Satyanaraya, S., Chaudhari, P. R., 2007. Lonar Lake: A unique ecosystem rich in salinity tolerant phytoplankton community. 12th World Lake Conference, Oct 28 – Nov 2, 2007: Jaipur, Abstract No. SG 5.

Schoell, M., 1978. Oxygen Isotope Analyses on Authigenic Carbonates from Lake Van Sediments and Their Possible Bearing on the Climate of the Past 10,000 Years. In The Geology of Lake Van, edited by E.T. Degens and F. Kurtman, 92–7. Ankara: The Mineral Research and Exploration Institute of Turkey

Schulz, H., von Rad, U., Erlenkeuser, H., 1998. Correlation between Arabian Sea and Greenland climate oscillations of the past 110,000 years. Nature 393, 54-57.

Sharma, S., Joachimski, M., Sharma, M., Tobschall, H.J., Singh, I.B., Sharma, C., Chauhan, M.S., Morgenroth, G., 2004. Lateglacial and Holocene environmental changes in Ganga plain, Northern India. Quaternary Science Reviews 23, 145-159.

Shukla J., 1987. Interannual variability of monsoons, in Monsoons, edited by J.S. Fein and P.L. Stephens, 399-464, John Willey and Sons.

Sikka, D. R., 1980. Some aspects of the large-scale fluctuations of summer monsoon rainfall over India in relation to fluctuations in the planetary and regional scale circulation parameters. Proc. Indian Acad. Sci. (Earth, Planet, Sci.) 89, 179.

Simpson, G., 1921. The South-West Monsoon. Quarterly Journal of the Royal Meteorological Society 47, 151-171.

Singh, G., 1971. The Indus Valley culture: Seen in the context of post-glacial climatic and ecological studies in north-west India. Archaeology & Physical Anthropology in Oceania 6, 177-189.

Singh, P., Saikia, A., Pant, N.C., Verma, P.K., 2013. Insights into the P–T evolution path of Tso Morari eclogites of the north-western Himalayas: Constraints on the geodynamic evolution of the region. Journal of Earth System Science 122, 677-698.

Singh, D., Tsiang, M., Rajaratnam, B., Diffenbaugh, N. S., 2014. Observed changes in extreme wet and dry spells during the South Asian summer monsoon season. Nature Climate Change. DOI: 10.1038/NCLIMATE2208.

Sinha, A., Cannariato, K. G., Stott, L. D., Li, H. C., You, C. F., Cheng, H., Edwards R.L., Singh, I. B., 2005. Variability of Southwest Indian summer monsoon precipitation during the Bølling-Ållerød. Geology 33, 813-816.

Sinha, A., Cannariato, K. G., Stott, L. D., Cheng, H., Edwards, R. L., Yadava, M. G., Ramesh, R., Singh, I. B., 2007. A 900-year (600 to 1500 AD) record of the Indian summer monsoon precipitation from the core monsoon zone of India. Geophysical Research Letters 34, L16707.

Sirocko, F., Sarnthein, M., Erlenkeuser, H., Lange, H., Arnold, M., Duplessy, J. C., 1993. Century-scale events in monsoonal climate over the past 24,000 years. Nature 364, 322-324.

Sollins, P., Spycher, G., Glassman, C.A., 1984. Net nitrogen mineralization from light- and heavy-fraction forest soil organic matter. Soil Biology and Biochemistry 16, 31-37.

Soon, W., Velasco Herrera, V.M., Selvaraj, K., Traversi, R., Usoskin, I., Chen, C.-T.A., Lou, J.-Y., Kao, S.-J., Carter, R.M., Pipin, V., Severi, M., Becagli, S., 2014. A review of Holocene solar-linked climatic variation on centennial to millennial timescales: Physical processes, interpretative frameworks and a new multiple cross-wavelet transform algorithm. Earth-Science Reviews 134, 1-15.

Spötl C., Vennemann, T. W., 2003. Continuous flow isotope ratio mass spectrometric analysis of carbonate minerals. Rapid communications in mass spectrometry 17, 1004-1006.

Sridhar, A., Laskar, A., Prasad, V., Sharma, A., Tripathi, J., Balaji, D., Maurya, D. M., Chamyal, L. S., 2014. Late Holocene flooding history of a tropical river in western India in response to southwest monsoon fluctuations: A multi proxy study from lower Narmada valley. Quaternary International (in press).

Srivastava, P., Bhambri, R., Kawishwar, P. & Dobhal, D. P., 2013: Water level changes of high altitude lakes in Himalaya-Karakoram from ICESataltimetry. Journal of Earth System Science 122, 1533-1543.

Staubwasser, M., Weiss, H., 2006. Holocene climate and cultural evolution in late prehistoric–early historic West Asia. Quaternary Research 66, 372-387.

Steck, A., Epard, J.-L., Vannay, J.-C., Hunziker, J., Girard, M., Morard, A., Robyr, M., 1998. Geological transect across the Tso Morari and Spiti areas-the nappe structures of the Tethys Himalaya. Eclogae Geologicae Helvetiae 91, 103–121.

Steck, A., 2003. Geology of the NW Indian Himalaya. Eclogae Geologicae Helvetiae 98, 147–196.

Stein, M., Starinsky, A., Katz, A., Goldstein, L.S., Machlus, M., Schramm, A., 1997. Strontium isotopic, chemical, and sedimentological evidence for the evolution of lake Lisan and Dead Sea. Geochimica et Cosmochimica Acta 61, 3975–3992.

Stiller, M., Rounick, J. S., Shasha, S., 1985. Extreme carbon isotope enrichments in evaporating brines. Nature 316, 434 – 435.

Stocker, T. F., Qin, D., Plattner, G. K., Tignor, M., Allen, S. K., Boschung, J., Nauels, A., Xia, Y., Bex, V., Midgley, P. M., 2013. Climate change 2013: The physical science basis." Intergovernmental Panel on Climate Change, Working Group I Contribution to the IPCC Fifth Assessment Report (AR5) (Cambridge Univ Press, New York).

Stuiver, M., 1975. Climate versus changes in 13 C content of the organic component of lake sediments during the Quaternary. Quaternary Research 5, 251‐262.

Stuiver, M., Grootes, P.M., 2000. GISP2 oxygen isotope ratios. Quaternary Research 53, 277-284.

Stumm, W., Morgan, J.J., 1981. Aquatic Chemistry. John Wiley and Sons, New York.

Sun, D., Bloemendal, J., Rea, D.K., Vandenberghe, J., Jiang, F., An, Z., Su, R., 2002. Grain-size distribution functions of polymodal sediments in hydraulic and aeolian environments, and numerical partitioning of the sedimentary components. Sedimentary Geology 152, 263-277.

Surakasi, V.P., Wani, A.A., Shouche, Y.S., Ranade, D.R., 2007. Phylogenetic analysis of methanogenic enrichment cultures obtained from Lonar Lake in India: Isolation of Methanocalculus sp. and Methanoculleus sp. Microbial Ecology 54, 697-704.

Swain, A.M., Kutzbach, J.E., Hastenrath, S., 1983. Estimates of Holocene precipitation for Rajasthan, India, based on pollen and lake level data. Quaternary Research 19, 1–17

Talbot, M. R., 1990. A review of the palaeohydrological interpretation of carbon and oxygen isotopic ratios in primary lacustrine carbonates. Chemical Geology: Isotope Geoscience Section 80, 261-279.

Talbot, M.R., Lærdal, T., 2000. The Late Pleistocene-Holocene palaeolimnology of Lake Victoria, East Africa, based upon elemental and isotopic analyses of sedimentary organic matter. Journal of Paleolimnology 23, 141-164.

Teller, J.T., Leverington, D.W., Mann, J.D., 2002. Freshwater outbursts to the oceans from glacial Lake Agassiz and their role in climate change during the last deglaciation. Quaternary Science Reviews 21, 879-887.

Thakur, V. C., 1990. Indus Tsangpo suture zone in Ladakh-its tectonostratigraphy and tectonics. Proc. Indian Acad. Sci. (Earth Planet. Sci.) 99, 169-185.

Thompson, L.G., Yao, T., Davis, M.E., Henderson, K.A., Thompson, E.M., Lin, P.N., Beer, J., Synal, H.A., Dai, J.C., Bolzan, J.F., 1997. Tropical climate instability: The last glacial cycle from a Qinghai-Tibetan ice core. Science 276, 1821-1825.

Thompson, L.G., Yao, T., Mosley-Thompson, E., Davis, M.E., Henderson, K.A., Lin, P.-N., 2000. A high-resolution millennial record of the South Asian Monsoon from Himalayan ice cores. Science 289, 1916-1919.

Tieszen, L.L., Senyimba, M.M., Imbamba, S.K., Troughton, J.H., 1979. The distribution of C3 and C4 grasses and carbon isotope discrimination along an altitudinal and moisture gradient in Kenya. Oecologia 37, 337-350.

Tiwari, M., Managave, S., Yadava, M. G., Ramesh, R., 2009. Spatial and temporal coherence of paleomonsoon records from marine and land proxies in the indian region during the past 30 ka. In (Ed) N. Mukunda, Platinum Jubilee Special Publication of the Indian Academy of Sciences pp. 517–535 Bangaluru, India, 2009.

Tiwari, M., Singh, A. K., Ramesh, R., 2011. High-resolution monsoon records since last glacial maximum: a comparison of marine and terrestrial paleoarchives from South Asia. Journal of Geological Research 2011, 1-12.

Tripathi, J.K., Bock, B., Rajamani, V., Eisenhauer, A., 2004. Is River Ghaggar, Saraswati? Geochemical constraints. Current Science 87, 1141-1145.

Valero-Garcés, B. L., Delgado-Huertas, A., Ratto, N., Navas, A., 1999. Large ^{13}C enrichment in primary carbonates from Andean Altiplano lakes, northwest Argentina. Earth and Planetary Science Letters 171, 236–266.

Van Campo, E., Gasse, F., 1993. Pollen-and diatom-inferred climatic and hydrological changes in Sumxi Co Basin (Western Tibet) since 13,000 yr BP. Quaternary Research 39, 300-313.

Van Campo, E., Cour, P., Sixuan, H., 1996. Holocene environmental changes in Bangong Co basin (Western Tibet). Part 2: the pollen record. Palaeogeography, Palaeoclimatology, Palaeoecology 120, 49-63.

Van der Straaten, C.M., Mook, W.G., 1983. Stable isotope composition of precipitation and climatic variability, in Paleoclimate and Paleowaters. Collection of Environmental Isotope Studies, Int. At. Energy Agency, Vienna, pp. 53-64.

Van Zeist, W., Woldring, H., 1978. A postglacial pollen diagram from Lake Van in East Anatolia. Review of Palaeobo. Palynol. 26, 249-276.

Vinayachandran, P. N., Kurian, J., Neema, C. P., 2007. Indian Ocean response to anomalous conditions in 2006. Geophysical Research Letters 34.

Vogel, H., Wessels, M., Albrecht, C., Stich, H.-B., Wagner, B., 2010. Spatial variability of recent sedimentation in Lake Ohrid (Albania/Macedonia). Biogeosciences 7, 3333–3342.

Walker, M. J. C., Berkelhammer, M., Björck, S., Cwynar, L. C., Fisher, D. A., Long, A. J., Lowe, J. J., Newnham, R. M., Rasmussen, S. O., Weiss, H., 2012. Formal subdivision of the Holocene Series/Epoch: a Discussion Paper by a Working Group of INTIMATE (Integration of ice-core, marine and terrestrial records) and the Subcommission on Quaternary Stratigraphy (International Commission on Stratigraphy). Journal of Quaternary Science 27, 649-659.

Wang, Y.T., Cheng, H., Edwards, R.L., An, Z.S., Wu, J.Y., Shen, C.C., Dorale, J.A., 2001. A high-resolution absolute-dated late Pleistocene monsoon record from Hulu Cave, China. Science 294, 2345-2348.

Wang, P., Clemens, S., Beaufort, L., Braconnot, P., Ganssen, G., Jian, Z., Kershaw, P., Sarnthein, M., 2005. Evolution and variability of the asian monsoon system: state of the art and outstanding issues. Quaternary Science Reviews 24, 592–629.

Wang, Y.J., Cheng, H., Edwards, R.L., He, Y.Q., Kong, X.G., An, Z.S., Wu, J.Y., Kelly, M.J., Dykoski, C.A., Li, X.D., 2005. The Holocene Asian monsoon: Links to solar changes and North Atlantic climate. Science 308, 854-857.

Wang, Y., Liu, X., Herzschuh, U., 2010. Asynchronous evolution of the Indian and East Asian Summer Monsoon indicated by Holocene moisture patterns in monsoonal central Asia. Earth-Science Reviews 103, 135-153.

Wanner, H., Beer, J., Buetikofer, J., Crowley, T. J., Cubasch, U., Flueckiger, J., Goosse, H., Grosjean, M., Joos, F., Kaplan, J. O., Küttel, M., Müller, S. A., Prentice, I. C., Solomina, O., Stocker, T. F., Tarasov, P., Wagner, M., Widmann, M., 2008. Mid- to Late Holocene climate change: an overview. Quaternary Science Reviews 27, 1791-1828.

Wasson, R.J., Smith, G.I., Agrawal, D.P., 1984. Late Quaternary sediments, minerals, and inferred geochemical history of Didwana lake, Thar desert India. Palaeogeography, Palaeoclimatology, Palaeoecology 46, 345–372

Wei, K., Gasse, F., 1999. Oxygen isotopes in lacustrine carbonates of west China revisited: implications for post glacial changes in summer monsoon circulation. Quaternary Science Reviews 18, 1315–1334.

Wennrich, V., Francke, A., Dehnert, A., Juschus, O., Leipe, T., Vogt, C., Brigham-Grette, J., Minyuk, P. S., Melles, M., El'gygytgyn Science Party, 2013. Modern sedimentation patterns in Lake El'gygytgyn, NE Russia, derived from surface sediment and inlet streams samples. Climate of the Past 9, 135-148.

Wetzel, R., 2001. Limnology, Lake and River Ecosystems. Third Edition, Academic press.

White, W.M., 2013. Geochemistry. John Wiley and Sons, New York.

Whiticar, M.J., Faber, E., Schoell, M., 1986. Biogenic methane formation in marine and freshwater environments: CO2 reduction vs. acetate fermentation—isotope evidence. Geochimica et Cosmochimica Acta 50, 693–709.

Whitlock, C., Dean, W.E., Fritz, S.C., Stevens, L.R., Stone, J.R., Power, M.J., Rosenbaum J.R., Pierce K.L., Bracht-Flyr, B.B., 2012. Holocene seasonal variability inferred from multiple proxy records from Crevice Lake, Yellowstone National Park, USA. Palaeogeography, Palaeoclimatology, Palaeoecology 331, 90-103.

Wilmshurst, J.M., 1997. The impact of human settlement on vegetation and soil stability in Hawke's Bay, New Zealand. New Zealand Journal of Botany 35, 97-111.

Wu, Y., Li, S., Lücke, A., Wünnemann, B., Zhou, L., Reimer, P., Wang, S., 2010. Lacustrine radiocarbon reservoir ages in Co Ngoin and Zigê Tangco, central Tibetan Plateau. Quaternary International 212, 21-25.

Wulf, H., Bookhagen, B., Scherler, D., 2010. Seasonal precipitation gradients and their impact on fluvial sediment flux in the Northwest Himalaya. Geomorphology 118**,** 13-21.

Wünnemann, B., Demske, D., Tarasov, P., Kotlia, B.S., Reinhardt, C., Bloemendal, J., Diekmann, B., Hartmann, K., Krois, J., Riedel, F., Arya, N., 2010. Hydrological evolution during the last 15kyr in the Tso Kar lake basin (Ladakh, India), derived from geomorphological, sedimentological and palynological records. Quaternary Science Reviews 29, 1138-1155.

Yadava, M.G., Ramesh, R., 2005. Monsoon reconstruction from radiocarbon dated tropical Indian speleothems. The Holocene 15, 48-59.

Yao, T., Thompson, L. G., Shi, Y., Qin, D., Jiao, K., Yang, Z., Lide, T., Thompson, E. M., 1997. Climate variation since the last interglaciation recorded in the Guliya ice core. Science in China Series D: Earth Sciences 40, 662-668.

Yu, Z., McAndrews, J.H., Eicher, U., 1997. Middle Holocene dry climate caused by changes in atmospheric circulation patterns: Evidence from lake levels and stable isotopes. Geology 25, 251–254.

Yuan, D., Cheng, H., Edwards, R. L., Dykoski, C. A., Kelly, M. J., Zhang, M., Qing, J., Yushi, L., Wang, Y., Wu, J., Dorale, J. A., An, Z., Cai, Y., 2004. Timing, duration, and transitions of the last interglacial Asian monsoon. Science 304, 575-578.

Zech, M., Tuthorn, M., Zech, R., Schlütz, F., Zech, W., Glaser, B., 2014. A 16-ka $\delta^{18}O$ record of lacustrine sugar biomarkers from the High Himalaya reflects Indian Summer Monsoon variability. Journal of Paleolimnology 51, 241-251

Zhang, C., Mischke, S., 2009. A Late glacial and Holocene lake record from the Nianbaoyeze Mountains and inferences of lake, glacier and climate evolution on the eastern Tibetan Plateau. Quaternary Science Reviews 28, 1970-1983.

Zhang, J., Quay, P.D., Wilbur, D.O., 1995. Carbon isotope fractionation during gas-water exchange and dissolution of CO2. Geochimica et Cosmochimica Acta 59, 107-114.

Zhou, W., Head, M.J., Lu, X., An, Z., Jull, A.J.T., Donahue, D., 1999. Teleconnection of climatic events between East Asia and polar, high latitude areas during the last glaciation. Palaeogeography, Palaeoclimatology, Palaeoecology 152, 163‑172.

Appendix

Table S2.1: ^{137}Cs activity from sediment core TM-10 (see Fig. 2.1a for sample location)

Depth_top (cm)	Depth_base (cm)	^{137}Cs activity (Bq/kg)	±^{137}Cs error (Bq/kg)	Sample weight (g)	Measurement time (days)
0	1	4.8	1.6	1.05	35
1	2	20.5	1.7	0.84	28.9
2	3	9.8	3.1	0.52	25
3	4	4.2	1.9	0.53	74.9
4	5	-0.1	3.2	0.36	49.1
9	10	1.3	3.7	0.6	13
14	15	-0.7	2.3	0.51	49
19	20	3.3	5.7	0.69	3.9

Table S2.2: $CaCO_3$ free-based data was calculated from the raw data presented in main text (Chapter 2)

(a) Mineralogy of catchment samples (CaCO3-free based)

Sample	Quartz	Muscovite	Chlorite	Orthoclase	Plagioclase	Musovite/Chlorite
L-35	57.7	10.1	4.1	3.7	24.4	2.5
L-21	64.8	9.4	3.5	5.4	16.9	2.7
L-36	66.0	9.9	3.5	4.8	15.8	2.8
TMS-7	61.8	6.9	1.7	9.1	20.6	4.0
TMS-9	54.9	19.0	0.0	6.8	19.3	--
L-23	51.5	18.8	7.3	5.2	15.3	2.6
L-24	72.0	0.0	7.2	3.9	16.9	0.0
L-26	59.8	20.1	6.2	3.8	10.1	3.2
TMS-21	47.0	23.1	9.6	9.0	11.2	2.4
L-31	55.5	12.8	5.2	7.3	19.2	2.5
TMS-14	51.5	26.6	7.5	0.0	14.4	3.6
L-33	56.7	16.5	7.2	5.0	10.2	2.3
L-41	55.5	20.7	6.5	3.9	13.3	3.2
L-38	61.0	13.9	4.9	4.9	15.3	2.8
L-17	50.6	20.6	6.6	4.0	18.2	3.1
L-8	50.7	8.2	4.3	7.0	29.7	1.9
L-13b	50.9	5.2	4.8	4.0	35.1	1.1
L-13c	42.2	13.5	6.3	5.8	30.3	2.1
TMS-3	46.3	12.0	14.4	3.9	20.2	0.8
TMS-29	57.9	16.0	4.8	7.1	14.2	3.3
L-44	57.7	18.6	6.2	7.6	9.9	3.0
Average	**55.8**	**14.4**	**5.8**	**5.3**	**18.1**	**2.5**
RSD (%)	**12.4**	**44.6**	**48.7**	**38.4**	**37.0**	**37.5**

(b) Mineralogy of Lake sediment ($CaCO_3$-free based)

	Quartz	Muscovite	Chlorite	Plagioclase	Mus/Chl	Water depth (m)
TM-05	23.1	48.8	15.4	12.6	3.2	72
TM-6	32.3	32.3	35.5	0.0	0.9	40
TM-08	25.0	52.1	12.5	10.4	4.2	75
TM-9	23.5	49.0	27.5	0.0	1.8	62
TM-10	21.6	51.1	19.6	7.7	2.6	105
TM-11	22.0	50.8	18.6	8.5	2.7	90
TM-12	23.4	54.7	14.1	7.8	3.9	84
TM-13a	22.4	48.3	20.7	8.6	2.3	77
TM-14a	26.9	46.3	17.9	9.0	2.6	50
Average	**24.5**	**48.2**	**20.2**	**7.2**	**2.7**	
RSD (%)	**12.8**	**12.6**	**33.6**	**57.0**	**35.1**	

(c) Lake sediment (CaCO3 free) normalised with catchment sediments (CaCO3 free)

	Quartz	Muscovite	Chlorite	Plagioclase
TM-05	0.4	3.4	2.7	0.7
TM-6	0.6	2.2	6.1	0.0
TM-08	0.4	3.6	2.2	0.6
TM-9	0.4	3.4	4.7	0.0
TM-10	0.4	3.6	3.4	0.4
TM-11	0.4	3.5	3.2	0.5
TM-12	0.4	3.8	2.4	0.4
TM-13a	0.4	3.4	3.6	0.5
TM-14a	0.5	3.2	3.1	0.5
Average	0.4	3.3	3.5	0.4

List of Publications

Peer reviewed

- **Mishra, Praveen, K**., Prasad, S., Anoop, A., Plessen, B., Jehangir, A., Gaye, B., Menzel, P., Weise, S. M., Yousuf, A. R., 2015. Carbonate isotopes from high altitude Tso Moriri Lake (NW Himalayas) provide clues to late glacial and Holocene moisture variability and atmospheric circulation changes. Palaeogeography, Palaeoclimatology, Palaeoecology 425, 76-83.
- **Mishra, Praveen, K**., Anoop, A., Schettler, G., Prasad, S., Jehangir, A., Menzel, P., Naumann, R., Yousuf, A.R., Basavaiah, N., Deenadayalan, K., Wiesner, M.G., B. Gaye, B., 2015. Reconstructed late Quaternary hydrological changes from Tso Moriri Lake, NW Himalaya. Quaternary International 371, 76-86.
- Menzel, P., Gaye, B., **Mishra, Praveen, K.**, Anoop, A., Basavaiah, N., Marwan, N., Plessen, B., Prasad, S., Riedel, N., Stebich, M. Wiesner, M.G., 2014. Linking Holocene drying trends from Lonar Lake in central India to North Atlantic cooling events. Paleoclimatology Paleoecology Paleogeography. doi: 10.1016/j.palaeo.2014.05.044
- **Mishra, Praveen, K.**, Anoop, A., Jehangir, A., Prasad, S., Menzel, P., Schettler, G., Naumann, R., Weise, S., Anderson, N., Yousuf, A. R., Gaye, B., 2014. Limnology and modern sedimentation patterns in high altitude Tso Moriri Lake, NW Himalaya – implications for proxy development. Fundamental of Applied Limnology 185, 325-348.

Conference proceedings

- **Mishra, Praveen K**., Prasad, S., Anoop, A., Menzel, P., Jehangir, A., Plessen, B., Naumann, R., Gaye, B., Yousuf, A.R.. Mineralogical and isotopic data provide clues to climate change during the late Quaternary – a case study from Tso Moriri Lake, NW Himalaya (India). General Assembly European Geosciences Union (Vienna, Austria 2014).
- **Mishra, Praveen K**., Dietze, E., Schettler, G., Anoop, A., Menzel, P., Gaye, B., Jehnagir, A., Prasad, S. Multiproxy Investigations on Tso Moriri Lake, Indian

Himalayas provide clues to climate controlled lake level changes. Fall Meeting, AGU, San Francisco, Calif., American Geophysical Union (AGU)-2013.

- **Mishra, Praveen, K**., Dietze, E., Schettler, G., Plessen, B., Anoop, A., Menzel, P., Gaye, B., Jehangir, A., Wiesner, S., Prasad, S. Multiproxy Investigations on Tso Moriri Lake, Indian Himalayas – regional climate or a global signal ? 28th Himalayan Karakorum Tibet workshop & International Symposium on Tibetan Plateau (Tübingen, 2013).
- **Mishra, Praveen K**., Anoop, A., Menzel, P., Gaye, B., Basavaiah, N., Jehangir, A., Prasad, S., 2013. Holocene Climatic Variability in the Indian Monsoon Domain. General Assembly European Geosciences Union (Vienna, Austria 2013).
- **Mishra Praveen, K.,** Anoop, A., Menzel, P., Basavaiah, N., Gaye, B., Wiesner, M. G., Riedel, N., Stebich, M., Brauer, A., Prasad, S. Holocene climate variability in the Indian Subcontinent. GV & Sediment Meeting, Hambug, Germany (23-28, Sep, 2012).